Development of new anticorrosion coatings based on the combination of suitable waterborne polymeric binders and corrosion inhibitors

Diulia Caroline Quites Rodrigues

University of the Basque Country UPV/EHU, Donostia-San Sebastián - Spain

Deakin University, Melbourne - Australia

(2022)

Contents

Chapter 1

Introduction and thesis outline

Chapter 2

Incorporation of a coumarate based corrosion inhibitor in waterborne polymeric binders for corrosion protection applications

Chapter 3

Comparison of corrosion inhibition ability of different coumarate based compounds incorporated into waterborne binders

Chapter 4

Development of waterborne anticorrosive coatings by the incorporation of coumarate based corrosion inhibitors and phosphate functionalization

Chapter 5

Corrosion protection of mild steel in acidic environment by cetrimonium cinnamate cationic surfactants

Chapter 6

Conclusions

Appendix I

Chapter 1

Introduction and thesis outline

1.1 Overview

Steel is the most important engineering material of the present era, and it has the prospect of remaining dominant for the foreseeable future[1]. The development of modern civilization would not have been possible without it[1]. Steel is used in a wide range of sectors, such as construction, machinery, energy, utensil, rail, shipbuilding, and transportation[1,2] due to its relatively low cost and good mechanical properties, including ductility, toughness, high machinability, and weldability[2,3]. However, steel is particularly susceptible to corrosion, which makes its protection a challenge for our days.

A recent report from NACE (National Association of Corrosion Engineers) International points out how broad and expensive are the problems associated with the premature corrosion of steel, and estimates its global cost to be around $ US 2.5 trillion, corresponding to 3.4 % of the global GDP (gross domestic product) in 2013[4]. Besides the economic loss, premature corrosion is frequently associated with structural failures that could result in accidents of catastrophic proportions, injury/loss of human lives, and environmental impacts[5,6], making the study and improvement of techniques to mitigate corrosion critically relevant. Indeed, there has been a strong emphasis on the development of techniques for the mitigation of metallic corrosion, such as new corrosion inhibitors and advanced, smart and functional paints[7,8].

In this introduction chapter, the undesireable phenomena of steel corrosion is discussed, as well as some aspects that are known to increase corrosion rates. Furthermore, typical methods that have been applied to mitigate corrosion are presented, such as the use of corrosion inhibitors, barrier coatings, and the incorporation of corrosion inhibitors into coatings for the development of better protective systems. The use of environmentally friendly alternatives for the substituition of volatile organic compounds (VOC) found in traditional coatings is discussed

in detail, along with the problems associated with toxic corrosion inhibitors. The general objective of this Chapter is to introduce the reader into fundamental concepts applied in this doctoral project, that aims the development of efficient and sustainable systems for mitigation of metallic corrosion.

1.2 Steel Corrosion

According to thermodynamics, all matter that is not in its natural lowest energy state is inclined to return to that first condition[9,10]. Therefore, materials such as metals, plastics, ceramics, and composites will eventually degrade if not protected[9]. The word “corrosion” is frequently related to the undesired degradation of metallic materials[9]. It happens by means of physicochemical interactions between the metal (i.e. steel) and its environment, resulting in changes in the physicomechanical properties of the metal (steel)[5].

The driving force for metallic corrosion is the difference of potential between the anodic and cathodic sites of the metal itself[5], where an anodic site loses electrons to a cathodic site (Figure 1.1). The product of oxidation, Fe^{2+}, reacts with oxygen dissolved in an electrolyte (a water droplet or even a thin film of moisture), forming hydrated iron oxides (rust) that are similar in chemical composition to the original iron ore[11]. To balance this charge transfer, ions in the media move between these sites of oxidation and reduction[12]. The rate of corrosion is generally determined by the electrolyte and the difference in mobility between the metals or the relative ratio of electrolyte to steel surface area[13]. Metallic corrosion is intensified under harsh conditions such as high salinity (marine environment), high humidity, low pH, and/or high temperatures[3]. It is also known that the presence of microorganisms such as bacteria, fungi, archaea, and microalgae on the steel surface also promotes corrosion, which is referred to as microbiologically

influenced corrosion (MIC)[14–16].

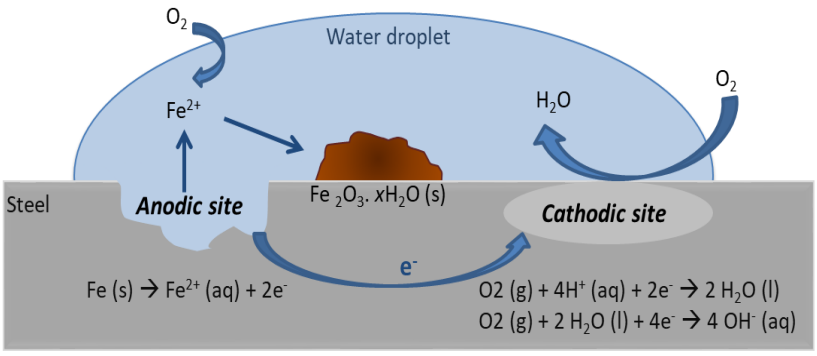

Figure 1.1: Representation of rust formation from the processes of steel corrosion[17,18].

Although the process of corrosion is natural and inevitable, there are methods used to slow its progress toward the equilibrium state[11]. Some common approaches to mitigate corrosion include the use of protective coatings to cover the metallic surface, and the use of corrosion inhibitors[17] and biocides[14] which are either injected in solution or incorporated into coatings[14,18,19].

1.3 Corrosion Inhibitors

Corrosion inhibitors are chemicals that can diminish or control corrosion when added to the metal environment, even in small concentrations (ppm range)[19,20]. They are commonly used into water tanks, pipelines, streams or incorporated into paint coatings[21]. There are different classes of compounds that are effective corrosion inhibitors; chromates, nitrites, phosphates, molybdates and vanadates are examples of inorganic inhibitors, while carboxylates, quarternary amines, and triazoles are well established organic inhibitors[12,17,22]. Chromate-based inhibitors are known to be the most efficient; nevertheless, they have been banned in nearly all cases due

to the toxic and carcinogenic nature of hexavalent chromium[13,17]. Hence, there is an increasing interest in the study of alternative environmentally friendly inhibitors[17]. The efficiency of new corrosion inhibitors are routinely tested in solution via cyclic potentiodynamic polarization (CPP), a technique that provides information such as corrosion rate, corrosion potential and changes in the anodic and cathodic reactions.

Organic inhibitors have been extensively studied due to their relative ease of synthesis, and high corrosion protection ability[23]. The mechanism of action of such compounds are still poorly understood[20]. Heteroatoms of phosphorus (P), oxygen (O), nitrogen (N), and sulfur (S), are commonly found in the structure of organic inhibitors, either non-bonding or in the form of polar functional groups, as well as π-electrons in the form of extensive conjugation[23]. The organic molecules adsorb on the metal surface, forming a protective hydrophobic film through an association of physisorption and chemisorption interactions (Figure 1.2 a)[17,18]. The physical adsorption is based on electrostatic interactions between the charged metal surface and charged inhibitor molecule. On the other hand, chemical adsorption occurs via sharing of the non-bonding electrons and π-electrons of aromatic rings and multiple bonds between the inhibitor and metallic d-orbital[23].

Naturally occurring organic compounds based on carboxylates, such as salicylate and cinnamates, were found to be promising corrosion inhibitors in solution, when used at relatively high concentrations, predominantly reducing anodic reaction rates[21,24–28]. Amongst the carboxylates, p-coumaric acid (trans-4-hydroxycinnamate) has sparked interest since it is widely found in fruits (e.g. apples, pears, grapes, oranges, tomatoes and berries), vegetables (e.g. beans, potatoes and onions), cereals (e.g. maize, oats and wheat), plants and mushrooms[29]. Furthermore, its bioactivity, including both antioxidant and anti-inflammatory properties, have been studied in recent years[29,30]. Cinnamate-based compounds have been discussed as

candidates for the substitution of toxic inhibitors[25]. The influence of the position of substitution of the aromatic ring of 2-, 3-, and 4- hydroxycinnamate (Figure 1.2 b - f), and the combination of the compound with rare earth metal cations have been studied in terms of their of corrosion efficiency[31], with the most promising results reported for $La(4OHCinn)_3$. On the other hand, it was reported that 4-hydroxycinnamate (p-coumaric acid) improved the performance of sol-gel formulations after the successful incorporation of lanthanum[32,33]. Recently, ionic coumarate corrosion inhibitors were incorporated into acrylic UV coatings, showing promising results in terms of corrosion inhibition[34–36].

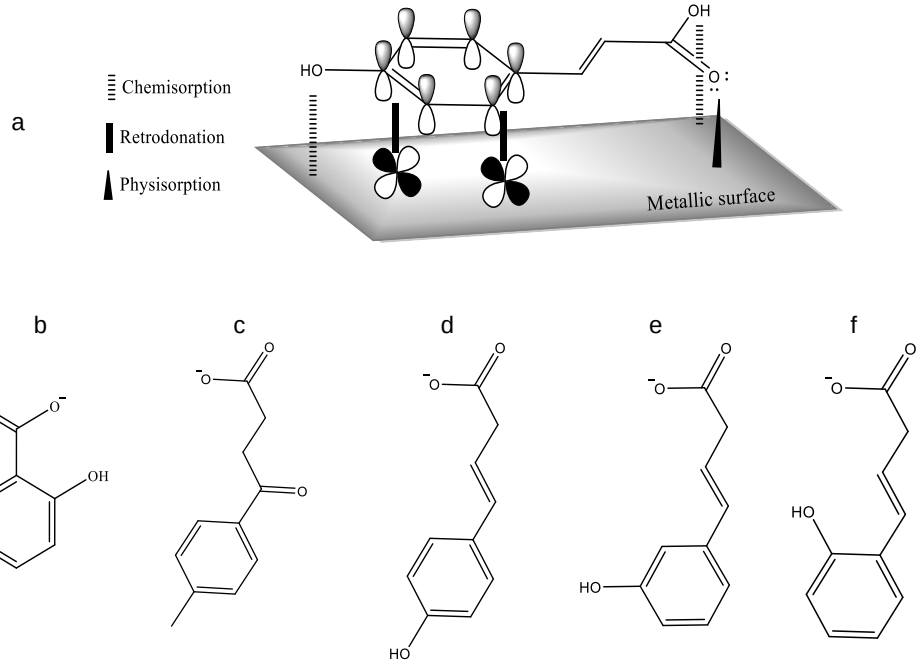

Figure 1.2: Chemical structures of carboxylate inhibitors; a) molecular structure of p-coumaric acid interacting with a metallic surface, b) salicylate, c) 3-(4-methylbenzoyl) propionic acid, d) 4-hydroxycinnamate, e) 3-hydroxycinnamate, f) 2-hydroxycinnamate.

An interesting approach to study corrosion inhibition would be to study the efficiency of molecules based on variations of 4-hydroxycinnamate differing the functionality of the -OH substituent, as nonpolar radicals could be useful for forming a protective hydrophobic film when the molecule is attached to a metallic surface. On the other hand, a more suitable methodology for the industrial application of those carboxylate inhibitors in coatings would be to incorporate them into the binder of waterborne coatings. However, this approach has not been reported or extensively studied for anticorrosive applications.

Another promising approach to the development of corrosion inhibitors, which has been reported and studied by Forsyth and Somers *et al*., is the combination of onium cations with aromatic carboxylate anions inhibitors, that may produce a synergic effect to maximize the mitigation of corrosion[8]. One interesting molecule for this approach is hexadecyltrimethylammonium bromide (CTAB), a commercial molecule that is known to have biocidal[37] and anticorrosive properties[38] (Figure 1.3). CTAB was previously combined with a surface-active counter ion, 4-hydroxycinnamate anion, to produce the new inhibitor, CTA-4OHCinn, which shows high corrosion protection in corrosive media in neutral conditions[8,39–43]. In solution, CTA-4OHCinn forms micelles that are susceptible to concentration and pH dependent changes in morphology, which consequently affect the anticorrosive properties [39–42]. The length of the alkyl chain of the anion has also been suggested to modify the resulting micellar properties [42].

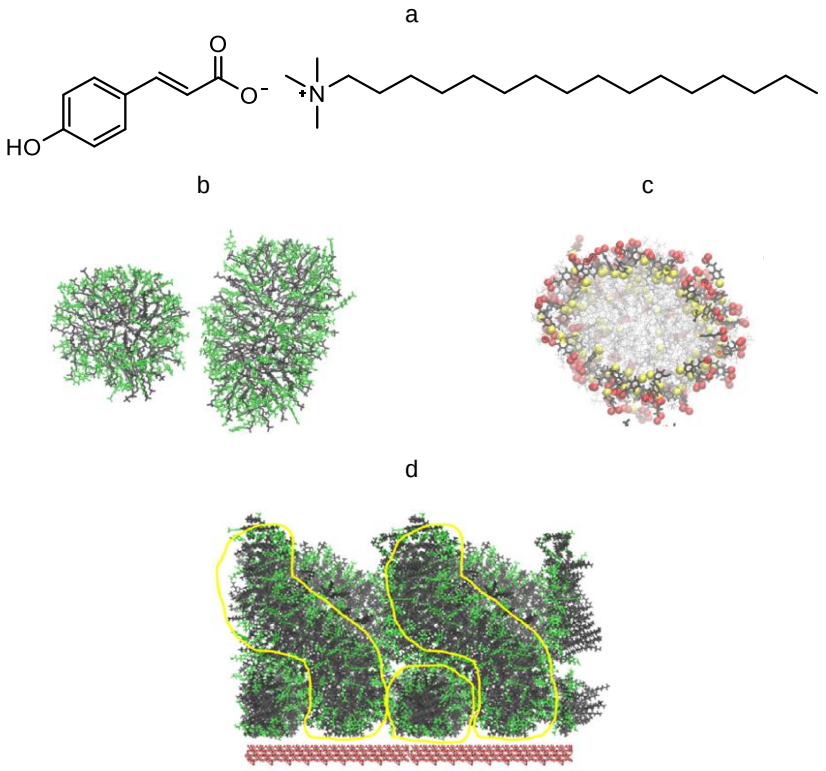

Figure 1.3: Chemical structure of CTA-4OHCinn; a) 4-hydroxycinnamate ion (green) with hexadecyltrimethylammonium bromide (CTAB) counter cation (gray), b) conformation of two cetrimonium 4-OH cinnamate micelles, formed after 160 ns dissolved in neutral water [41], c) cross-section of a micelle that shows the location of carboxylate (red) and hydroxyl groups (yellow spheres), cetrimonium is colored with gray[41], d) CTA-4OHCinn micelles adsorbed on oxide surface (purple). Yellow outlines indicate wormlike micelles either lying on the surface or growing in the horizontal direction[41].

1.4 Organic Coatings

1.4.1 Nanocomposite Coatings and Microencapsulation of Active Agents

The development of hybrid nanocomposite materials attempts to combine properties of each of the individual components to reach a better performance than the sum of the parts[44]. In

the case of nanocomposite coatings, typically, an inorganic hard particle is dispersed within a polymeric matrix[44]. Nanocomposite films with metallic nanoparticles have been the standard in corrosion resistance; where the inclusion of materials such as chromium, nickel, aluminium, and zinc has provided sacrificial cathodic/anodic protection[44]. The incorporation of ceramic nanoparticles used as diffusion barriers/reservoirs for anionic and molecular active corrosion inhibitors dates back to the early 1950s, and more recently, the use of carbon nanoparticles (graphene and carbon nanotubes) serving as diffusion barriers has been explored[44].

A promising route for the development of high performance, functional coatings is the incorporation of microcapsules loaded with biocides, anti-fouling species, superhydrophobic additives, or anticorrosive agents, into the coating matrix [7,45,46]. The encapsulation may be carried out by different methods, including via chemical (interfacial, suspension, emulsion polymerization), physicochemical (ionic gelation, coacervation, sol-gel), and physicomechanical (spray drying, solvent evaporation) approaches[47,48]. The final shape of the microcapsules (mononuclear, polynuclear, matrix and multi wall) is dependent on the core material and the deposition methods of the shell[47,48]. The microencapsulation of materials is widely used in the food industry, pharmaceuticals for drug delivery, cosmetics, agriculture, and textile industries[45,47], usually to protect sensitive substances from an external environment or to obtain controlled release kinetics.

In a simple coating system with incorporated microcapsules, the content of the capsules is continuously released over time, while more complex coatings are designed to enable controlled/selective release that can be triggered by changes in the surrounding environment such as pH, temperature and humidity[45,46,49]. Microcapsules have also been used for the development of self-healing coatings[49,50]. For example, an autonomic mechanism of healing was reported[50] for a system composed of an epoxy matrix embedded with microcapsules loaded with

a healing agent and a catalytic chemical trigger. When the epoxy is damaged, the crack breaks the microcapsules of the surrounds, releasing the healing agent into the crack though capillary action. The healing agent contacts the catalyst, triggering a polymerization reaction that closes the crack.

The high cost of microencapsulation and the numerous steps required for the process negatively impacts the final price of the product. However, the direct encapsulation of organic inhibitors into the binder of a waterborne latex through the polymerization reaction is an easy, one step process that, to the best of our knowledge, has not been reported in the literature.

1.4.2 Waterborne Coatings

Organic coatings are complex systems; they are composed of solvents, pigments, extenders, and additives contained within a continuous polymeric phase known as the binder[5,51]. The binder is specifically responsible for the cohesion of all the materials in the coating and the adhesion to the substrate[51]. Efficient coatings should be relatively easy and quick to manufacture, have good chemical and mechanical resistance, provide good substrate wetting and adhesion, appropriate film formation, and promote environmental stability and compliance[52]. The major function of a corrosion protection coating is to form a physical protective barrier, limiting the diffusion of ions and other species from the corrosive media to the metal[52,53]. Therefore, the barrier protection is commonly dependent on the coating thickness and typically multilayers with different purposes are included in a system[5].

The industry of coatings has been through significant changes in the past decades due to the development of new technologies, increasing regulations and cost pressures[5,53,54]. Conventional coatings are casted from organic solvent solutions. However, due to environmental

regulation requirements for reducing the concentration of VOCs, waterborne coatings have become more industrially appealing as alternatives to the traditional solvent-based paints[53]. Other advantages over solvent-based coatings are their low viscosity, reduced flammability, reduced odor, and easy application using conventional equipment[54]. Nowadays, waterborne coatings are employed as inks, exterior and interior decorative coatings, and also as protective coatings. However, the use of waterborne coatings in metallic surfaces is especially challenging since the relatively high starting concentration of water contributes to the formation of flash rusting; a general and rapid corrosion that instantly occurs when metals are exposed to corrosive environments[55,56].

Common polymers used for the production of waterborne coatings include vinyl acetate copolymers, styrene-butadiene or styrene-acrylic copolymers and fully acrylic copolymers. In typical acrylic formulations, methyl methacrylate (MMA) and butyl acrylate (50 wt% each) are polymerized, since the copolymer forms transparent polymeric films with good flexibility at room temperature.

Besides the physical protection given by the polymeric coating, the inclusion of active anticorrosive properties is also desired to protect the system from the heterogeneities and defects inherent to the film formation process [57], and from the inevitable failings produced during the life of the coating[44].

1.4.2.1 Synthesis

Different polymerization techniques can be used to produce waterborne latexes, such as dispersion polymerization, emulsion polymerization, and miniemulsion polymerization. They have different mechanisms of reaction and may lead to distinct products. Therefore, it is

important to understand their differences to choose the most suitable technique for reaching the desired product. In dispersion polymerization, the system is initially composed of a single homogeneous phase containing monomer(s), initiator, surfactant (stabilizer), and a solvent. As the reaction proceeds, amphiphilic species produced by grafting of stabilizer molecules self-aggregate, forming polymer particles that grow by absorption of monomer and further polymerization[58,59] (Figure 1.4 a).

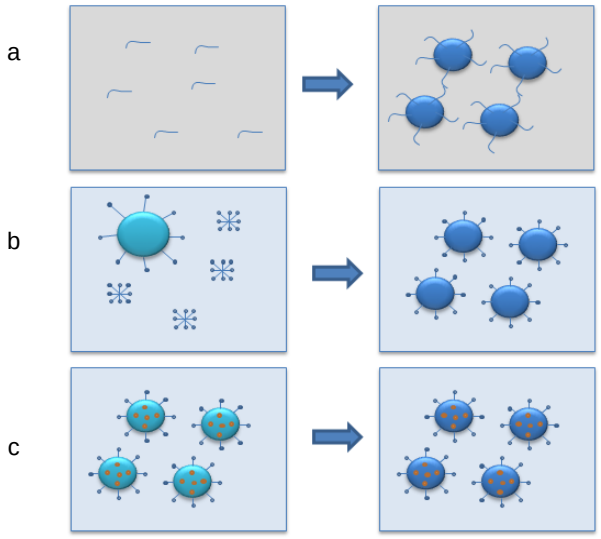

Figure 1.4: General scheme of methodologies for latex production; a) dispersion polymerization, b) emulsion polymerization, and c) miniemulsion polymerization.

The use of an organic solvent is not needed in emulsion polymerization (Figure 1.4 b), which makes this technique more environmentally friendly. Emulsion polymerization is the most common and simple technique for the production of waterborne polymeric dispersions [59–62]. The mechanism of an ab-initio batch emulsion polymerization initiated by aqueous phase soluble

initiators can be summarized in three intervals:[63] a) Nucleation of polymer particles by entry of oligoradicals into micelles or by precipitation of oligoradicals absorbing surfactant (first interval), b) Particle growth by diffusion of monomer from the droplets to the growing particles (2nd interval), and c) Once the monomer droplets are depleted, the remaining monomer in the polymer particles is consumed (3rd interval) to produce the final polymer particle dispersion or latex[60]. The final polymer particles obtained by emulsion polymerization are typically smaller than the initial drops of monomer (Figure 1.4 b).

The conventional emulsion polymerization is not suitable in the presence of very hydrophobic reactants or for the encapsulation of compounds such as corrosion inhibitors. In those cases, miniemulsion polymerization is employed (Figure 1.4 c)[64], where energy is applied to a coarse emulsion to reduce the size of the monomer droplets, producing a dispersion of monomer nanodroplets. This nanodroplet dispersion is polymerized by the addition of an initiator, and degradation of the monomer nanodroplets (so called Ostwald ripening) is prevented by the use of a co-stabilizer. The co-stabilizer, a water-insoluble compound, retards miniemulsion degradation by molecular diffusion because its slow rate of diffusion would permit the monomer to remain essentially equilibrated among the nanodroplets of different size[64]. In this case, the final particles of polymer are the same size as the initial monomer droplets (Figure 1.4 c).

Surfactants are amphiphilic molecules that play a crucial role in the preparation and stabilization of latexes. However, they may also be the cause of problems such as being trapped at particle/particle boundaries, creating hydrophilic pathways in the film, or migration toward the film-air or film-substrate interface[65,66]. To avoid those drawbacks, an alternative is the use of polymerizable surfactants in the reactions, which maintain the essential amphiphilic structure of

conventional surfactants but have a double bond in their structure, which can copolymerize with the monomers during the course of the polymerization[65].

1.4.2.2 Film formation

Once the latex is deposited on a surface, the water starts to evaporate, increasing the concentration of the dispersed polymeric particles up to the point at which they are tightly packed[57,67] (Figure 1.5 a). If the temperature is higher than the minimum film formation temperature (MFFT), particles will be deformed due to interfacial tensions and capillary forces[57,67,68]. In the next step, there is inter-diffusion of the polymeric chains across particle boundaries and the coalescence of particles, resulting in a continuous film[68,69].

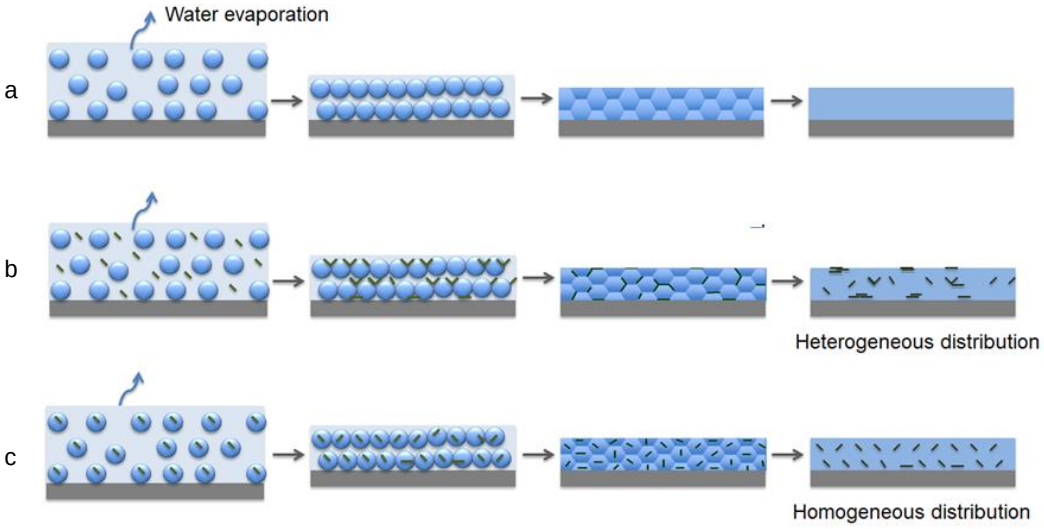

Figure 1.5: Schemes of latex film formation; a) latex with no inhibitor in its composition, b) latex with blended inhibitor (black lines) leading to a heterogeneous distribution in the final film, and c) latex with inhibitor incorporated into the particles (blue circles) of the latex, leading to homogeneous distribution into the final film.

As previously mentioned, active anticorrosive protection can be achieved by the incorporation of corrosion inhibitors into the coating formulation[18,50,55]. However, depending on the location of the inhibitor molecules in the latexes, their final location in the coating film will be dependent on this film formation process. The most common and simple technique to incorporate inhibitors in latexes is the mechanical blending of inhibitors soluble in the continuous phase into the final formulation. In this case, the inhibitors, initially dispersed in the aqueous continuous phase may aggregate or migrate to the surfaces during the film formation process, which may results in a heterogeneous distribution of the inhibitor in the coating and this may contribute to their premature leaching (Figure 1.5 b)[26]. An alternative option is the incorporation of inhibitors into the particles during the polymerization reaction. In this case, the inhibitors will be located within the polymer particles, which would restrain their movement during film formation, allowing a more homogeneous distribution of inhibitors and the increase of their leaching time (Figure 1.5 c)[5,26,55]. Therefore, the distribution of corrosion inhibitors into the coating formulation are likely to affect the final corrosion protection properties of the film.

Furthermore, it has to be taken into account that the corrosive media will permeate the coating during its service life. Depending on the hydrophilicity of the inhibitors, they will be more or less free to diffuse toward the metallic substrate to form an inhibiting layer that protects the surface[9]. Therefore, care must be taken in the selection of the inhibitor to be incorporated into the coating, since highly hydrophilic molecules would be quickly leached out of the coating and therefore be unable to give long term protection to the system, while highly hydrophobic ones would not be able to diffuse and give protection to the surface[70,71].

The process of development of a new paint is long and arduous[51]. Even when the properties of the individual components are well-known, when combined within formulated products, the overall outcome is not predictable[51]. Therefore, quantitative and qualitative

analyses of the final properties of the proposed films/coating are of great importance. The properties of metallic surfaces/coatings and their changes during exposure to corrosive environments are commonly analyzed by electrochemical impedance spectroscopy (EIS)[72,73]. EIS is a nondestructive method in which an AC voltage of varying frequency is applied to the sample[74]; the high frequency range is associated with fast reactions taking place and the low frequency range to the slow reactions. This technique is able to simultaneously measure the deterioration of the coating and the increase of corrosion rate of the metallic substrate[72–74]. Good anticorrosive coatings are expected to show higher values of impedance and a phase angle that approaches –90°, characteristic of a pure capacitor[74,75].

The mathematical results obtained from EIS analysis should be critically analyzed and compared to the visual aspect of the samples. As a sole method for corrosion quantification, it may be problematic in terms of quantitative prediction of corrosion performance[76]. However, when considering series of comparative and duplicated tests, EIS is useful, as a proof of concept, in determining performance and mechanisms.

1.5 Objectives of the work

This thesis is focused on the study of the anticorrosive properties of new cinnamate based corrosion inhibitors for their posterior incorporation into waterborne polymeric latexes by different techniques such as emulsion, miniemulsion and dispersion polymerization. Acrylic polymers will be prioritized as they are commonly used for exterior protection and industrial coating applications.

In the first part of this thesis, molecules derived from 4-hydroxycinnamate (p-coumaric acid) were investigated for their potential application as free corrosion inhibitors in solution. The promising molecules will be incorporated into waterborne coatings. The polymerization reactions will be proposed and optimized according to the viability of the system.

At a later point, the anticorrosive efficiency of a cetrimonium cinnamate cationic surfactant combined with counter-ions derived from 4-hydroxycinnamate with different alkyl chain length, will be studied in acidic conditions, as free inhibitors. The promising systems will be incorporated into waterborne coatings by blending it or incorporating the molecules as surfactants.

The effectiveness of all proposed corrosion inhibitors and coatings are going to be investigated by electrochemical analysis.

1.6 Outline of the thesis

This thesis is composed of six Chapters. The present chapter (Chapter 1), comprises an introduction of fundamental concepts applied in the development of this doctoral project.

Chapter 2 outlines the optimization process for incorporating the organic corrosion inhibitors into waterborne coatings. p-coumaric acid (4-hydroxycinnamic acid) was modified by a butyl radical and its effectiveness as an anticorrosive free inhibitor in solution was confirmed by potentiodynamic polarization. The molecule was then successfully incorporated into waterborne polymeric binders by employing different polymerization techniques in dispersed media. Whenever possible, the inhibitor was also blended into the bare latexes to compare the effect of

the incorporating method. The anticorrosion performance of the obtained coatings was tested and compared by electrochemical analysis.

In Chapter 3, the corrosion protection efficiency of four p-coumaric acid based inhibitors, methyl (H1), butyl (H4), trifluoromethoxy (HCF3), and p-4-ethyloxymethacrylate p-coumaric acid (HMA), is investigated. The inhibitors were incorporated into environmentally friendly waterborne polymeric binders by batch miniemulsion polymerization. The barrier corrosion protection of the coatings produced from these hybrid latexes was analyzed by electrochemical impedance spectroscopy (EIS) of intact and scratched coated steel substrates.

Chapter 4 reports the attempt to further improve the corrosion properties of the coating formed with 1% H1, which is presented in Chapter 3. By semibatch emulsion polymerization, a phosphate surfmer (Sipomer® PAM-200) was further incorporated into the system. The phosphate groups, attached to the particles are supposed to interact with the hydroxyl groups of the surface of the steel producing a passive iron phosphate layer, covalently bonded to the polymeric film when dried under specific conditions. The barrier corrosion protection of the coatings produced from these hybrid latexes was analyzed by electrochemical impedance spectroscopy (EIS) of intact and scratched coated steel substrates.

In Chapter 5, cetrimonium cinnamates cationic surfactants were studied as free inhibitors in solution in acidic corrosive environments (pH 1 and 2). The inhibitors were found to have excellent properties at low pH, especially at pH 1. As a proof of concept that those inhibitors would also work when incorporated into a coating, they were mechanically blended into a dispersion latex. The samples were dried and the coatings were analysed by EIS when in contact with a corrosive solution at pH 1, yielding promising results. Emulsion polymerization reactions were also produced with a cetrimonium cinnamates inhibitor as a surfactant.

Finally, in Chapter 6 the main conclusions of this PhD thesis are reported.

1.7 References

(1) Weng, Y.; Dong, H.; Yong, G. Advanced Steel and Our Society: Better Steel, Better World (Opening Address and the Introduction of the Specific Proceedings). In *Advanced Steels The Recent Scenario in Steel Science and Technology*; 2011; p 523. https://doi.org/10.1007/978-3-642-17665-4_47.

(2) Vinutha, M. R.; Venkatesha, T. V. Review on Mechanistic Action of Inhibitors on Steel Corrosion in Acidic Media. *Port. Electrochim. Acta* **2016**, *34* (3), 157–184. https://doi.org/10.4152/pea.201603157.

(3) Chuka, C. E.; Odio, B. O.; Chukwuneke, J. L.; Sinebe, J. E. Investigation Of The Effect Of Corrosion On Mild Steel In Five Different Environments. *Int. J. Sci. Technol. Res.* **2014**, *3* (7), 306–310.

(4) Koch, G.; Varney, J.; Thopson, N.; Moghissi, O.; Gould, M.; Payer, J. International Measures of Prevention , Application , and Economics of Corrosion Technologies Study. *NACE Int.* **2016**, 1–216.

(5) Sørensen, P. A.; Kiil, S.; Dam-Johansen, K.; Weinell, C. E. Anticorrosive Coatings: A Review. *J. Coatings Technol. Res.* **2009**, *6* (2), 135–176. https://doi.org/10.1007/s11998-008-9144-2.

(6) Petrovic, Z. Catastrophes Caused by Corrosion. *Vojnoteh. Glas.* **2016**, *64* (4), 1048–1064. https://doi.org/10.5937/vojtehg64-10388.

(7) Montemor, M. F. Functional and Smart Coatings for Corrosion Protection: A Review of Recent Advances. *Surf. Coatings Technol.* **2014**, *258*, 17–37. https://doi.org/10.1016/j.surfcoat.2014.06.031.

(8) Forsyth, M.; Somers, A.; Ghorbani, M. Organic Corrosion Inhibitors. WO 2021/097532 A1, 2022.

(9) Brooman, E. W. Modifying Organic Coatings to Provide Corrosion Resistance-Part I: Backgrund and General Principles. *Met. Finish.* **2002**, *100* (6), 104–110. https://doi.org/10.1016/S0026-0576(02)80446-9.

(10) Davis, J. R. Corrosion: Understanding the Basics. *ASM Int.* **2000**, 1–21. https://doi.org/10.1361/cutb2000p001.

(11) Shaw & Kelly. What Is Corrosion? *Electrochem. Soc. Interface* **2006**, *15* (1), 24–26. https://doi.org/10.1179/000705978798276131.

(12) Kendig, M.; Mills, D. J. An Historical Perspective on the Corrosion Protection by Paints. *Prog. Org. Coatings* **2017**, *102*, 53–59. https://doi.org/10.1016/j.porgcoat.2016.04.044.

(13) Prochaska, S.; Tordonato, D. Review of Corrosion Inhibiting Mechanisms in Coatings. In *Research and Development Office Science and Technology Program (Final Report) ST-2017-1703*; 2017; p 24.

(14) Little, B. J.; Blackwood, D. J.; Hinks, J.; Lauro, F. M.; Marsili, E.; Okamoto, A.; Rice, S. A.; Wade, S. A.; Flemming, H. C. Microbially Influenced Corrosion—Any Progress? *Corros. Sci.* **2020**, *170* (November 2019), 108641. https://doi.org/10.1016/j.corsci.2020.108641.

(15) Mansfeld, F. The Interaction of Bacteria and Metal Surfaces. *Electrochim. Acta* **2007**, *52* (27 SPEC. ISS.), 7670–7680. https://doi.org/10.1016/j.electacta.2007.05.006.

(16) Little, B.; Wagner, P.; Mansfeld, F. An Overview of Microbiologically Influenced Corrosion. *Electrochim. Acta* **1992**, *37* (12), 2185–2194. https://doi.org/10.1016/0013-4686(92)85110-7.

(17) Forsyth, M.; Seter, M.; Hinton, B.; Deacon, G.; Junk, P. New “Green” Corrosion Inhibitors Based on Rare Earth Compounds. *Aust. J. Chem.* **2011**, *64* (6), 812–819. https://doi.org/10.1071/CH11092.

(18) Brycki, B. E.; Kowalczyk, I. H.; Szulc, A.; Kaczerewska, O.; Pakiet, M. Organic Corrosion Inhibitors. In *Corrosion Inhibitors, Principles and Recent Applications*; Intech, Ed.; 2017; p 36. https://doi.org/10.5772/intechopen.72943.

(19) Taghavikish, M.; Dutta, N. K.; Choudhury, N. R. Emerging Corrosion Inhibitors for Interfacial Coating. *Coatings* **2017**, *7* (12), 1–28. https://doi.org/10.3390/coatings7120217.

(20) Sharma, S.; Ko, X.; Kurapati, Y.; Singh, H.; Nešić, S. Adsorption Behavior of Organic Corrosion Inhibitors on Metal Surfaces—Some New Insights from Molecular Simulations. *Corrosion* **2019**, *75* (1), 90–105. https://doi.org/10.5006/2976.

(21) Chong, A. L.; Mardel, J. I.; MacFarlane, D. R.; Forsyth, M.; Somers, A. E. Synergistic Corrosion Inhibition of Mild Steel in Aqueous Chloride Solutions by an Imidazolinium Carboxylate Salt. *ACS Sustain. Chem. Eng.* **2016**, *4* (3), 1746–1755. https://doi.org/10.1021/acssuschemeng.5b01725.

(22) Deacon, G. B.; Forsyth, M.; Junk, P. C.; Leary, S. G.; Lee, W. W. Synthesis and Characterisation of Rare Earth Complexes Supported by Para-Substituted Cinnamate Ligands. *Zeitschrift fur Anorg. und Allg. Chemie* **2009**, *635* (6–7), 833–839. https://doi.org/10.1002/zaac.200801379.

(23) Goyal, M.; Kumar, S.; Bahadur, I.; Verma, C.; Ebenso, E. E. Organic Corrosion Inhibitors for Industrial Cleaning of Ferrous and Non-Ferrous Metals in Acidic Solutions: A Review. *J. Mol. Liq.* **2018**, *256* (February), 565–573. https://doi.org/10.1016/j.molliq.2018.02.045.

(24) Forsyth, M.; Forsyth, C. M.; Wilson, K.; Behrsing, T.; Deacon, G. B. ATR Characterisation of Synergistic Corrosion Inhibition of Mild Steel Surfaces by Cerium Salicylate. *Corros. Sci.* **2002**, *44* (11), 2651–2656. https://doi.org/10.1016/S0010-938X(02)00024-0.

(25) Somers, A. E.; Deacon, G. B.; Macfarlane, D. R.; Junk, P. C.; Forsyth, M. Recent Developments in Environment-Friendly Corrosion Inhibitors for Mild Steel. *J. Indian*

Inst. Sci. **2016**, *96* (4), 285–292.

(26) Somers, A. E.; Hinton, B. R. W.; de Bruin-Dickason, C.; Deacon, G. B.; Junk, P. C.; Forsyth, M. New, Environmentally Friendly, Rare Earth Carboxylate Corrosion Inhibitors for Mild Steel. *Corros. Sci.* **2018**, *139* (May), 430–437. https://doi.org/10.1016/j.corsci.2018.05.017.

(27) Deacon, G. B.; Junk, P. C.; Lee, W. W.; Forsyth, M.; Wang, J. Rare Earth 3-(4′-Hydroxyphenyl)Propionate Complexes. *New J. Chem.* **2015**, *39* (10), 7688–7695. https://doi.org/10.1039/c5nj00787a.

(28) Blin, F.; Leary, S. G.; Wilson, K.; Deacon, G. B.; Junk, P. C.; Forsyth, M. Corrosion Mitigation of Mild Steel by New Rare Earth Cinnamate Compounds. *J. Appl. Electrochem.* **2004**, *34* (6), 591–599. https://doi.org/10.1023/B:JACH.0000021932.87043.7b.

(29) Pei, K.; Ou, J.; Huang, J.; Ou, S. P-Coumaric Acid and Its Conjugates: Dietary Sources, Pharmacokinetic Properties and Biological Activities. *J. Sci. Food Agric.* **2016**, *96* (9), 2952–2962. https://doi.org/10.1002/jsfa.7578.

(30) Pragasam, S. J.; Venkatesan, V.; Rasool, M. Immunomodulatory and Anti-Inflammatory Effect of p-Coumaric Acid, a Common Dietary Polyphenol on Experimental Inflammation in Rats. *Inflammation* **2013**, *36* (1), 169–176. https://doi.org/10.1007/s10753-012-9532-8.

(31) Seter, M.; Girard, G. M. A.; Lee, W. W.; Deacon, G.; Junk, P.; Hinton, B.; Forsyth, M. The Influence of Organic Structure and Rare Earth Metal Cation on the Corrosion Efficiency Observed on AS1020 Steel Compared with La(4OHCin)3. *AIMS Mater. Sci.* **2015**, *2* (1), 1–15. https://doi.org/10.3934/matersci.2015.1.1.

(32) Suárez-Vega, A.; Agustín-Sáenz, C.; O'Dell, L. A.; Brusciotti, F.; Somers, A.; Forsyth, M. Properties of Hybrid Sol-Gel Coatings with the Incorporation of Lanthanum 4-Hydroxy Cinnamate as Corrosion Inhibitor on Carbon Steel with Different Surface Finishes. *Appl. Surf. Sci.* **2021**, *561*, 149881.

https://doi.org/10.1016/j.apsusc.2021.149881.

(33) Suarez Vega, A.; Agustín-Sáenz, C.; Brusciotti, F.; Somers, A.; Forsyth, M. Effect of Lanthanum 4-Hydroxy Cinnamate on the Polymerisation, Condensation and Thermal Stability of Hybrid Sol–Gel Formulations. *J. Sol-Gel Sci. Technol.* **2020**, *96* (1), 91–107. https://doi.org/10.1007/s10971-020-05315-x.

(34) Udabe, E.; Sommers, A.; Forsyth, M.; Mecerreyes, D. Cation Effect in the Corrosion Inhibition Properties of Coumarate Ionic Liquids and Acrylic UV-Coatings. *Polymers (Basel).* **2020**, *12* (11), 1–16. https://doi.org/10.3390/polym12112611.

(35) Udabe, E.; Forsyth, M.; Somers, A.; Mecerreyes, D. Metal-Free Coumarate Based Ionic Liquids and Poly(Ionic Liquid)s as Corrosion Inhibitors. *Mater. Adv.* **2020**, *1* (4), 584–589. https://doi.org/10.1039/d0ma00243g.

(36) Udabe, E.; Somers, A.; Forsyth, M.; Mecerreyes, D. Design of Polymeric Corrosion Inhibitors Based on Ionic Coumarate Groups. *ACS Appl. Polym. Mater.* **2021**, *3* (4), 1739–1746. https://doi.org/10.1021/acsapm.0c01266.

(37) Gopi, D.; Govindaraju, K. M.; Manimozhi, S.; Ramesh, S.; Rajeswari, S. Inhibitors with Biocidal Functionalities to Mitigate Corrosion on Mild Steel in Natural Aqueous Environment. *J. Appl. Electrochem.* **2007**, *37* (6), 681–689. https://doi.org/10.1007/s10800-007-9300-x.

(38) El-Maksoud, S. A. A. The Effect of Hexadecyl Pyridinium Bromide and Hexadecyl Trimethyl Ammonium Bromide on the Behaviour of Iron and Copper in Acidic Solutions. *J. Electroanal. Chem.* **2004**, *565* (2), 321–328. https://doi.org/10.1016/j.jelechem.2003.10.026.

(39) Ghorbani, M.; Soto Puelles, J.; Forsyth, M.; Catubig, R. A.; Ackland, L.; Machuca, L.; Terryn, H.; Somers, A. E. Corrosion Inhibition of Mild Steel by Cetrimonium Trans-4-Hydroxy Cinnamate: Entrapment and Delivery of the Anion Inhibitor through Speciation and Micellar Formation. *J. Phys. Chem. Lett.* **2020**, *11* (22), 9886–9892. https://doi.org/10.1021/acs.jpclett.0c02389.

(40) Puelles, J. S.; Ghorbani, M.; Yunis, R.; MacHuca, L. L.; Terryn, H.; Forsyth, M.; Somers, A. E. Electrochemical and Surface Characterization Study on the Corrosion Inhibition of Mild Steel 1030 by the Cationic Surfactant Cetrimonium Trans-4-Hydroxy-Cinnamate. *ACS Omega* **2021**, *6* (3), 1941–1952. https://doi.org/10.1021/acsomega.0c04733.

(41) Soto Puelles, J.; Ghorbani, M.; Crawford, S.; Ackland, M. L.; Chen, F.; Forsyth, M.; Somers, A. E. Modelling Cetrimonium Micelles as 4-OH Cinnamate Carriers Targeting a Hydrated Iron Oxide Surface. *J. Colloid Interface Sci.* **2022**, *610*, 785–795. https://doi.org/10.1016/j.jcis.2021.11.139.

(42) Ghorbani, M.; Soto Puelles, J.; Forsyth, M.; Zhu, H.; Crawford, S.; Chen, F.; Cáceres-Vélez, P. R.; Jusuf, P. R.; Somers, A. Engineering Advanced Environmentally Friendly Corrosion Inhibitors, Their Mechanisms, and Biological Effects in Live Zebrafish Embryos. *ACS Sustain. Chem. Eng.* **2022**, *10* (9), 2960–2970. https://doi.org/10.1021/acssuschemeng.1c07958.

(43) Tuck, B.; Watkin, E.; Forsyth, M.; Somers, A.; Ghorbani, M.; Machuca, L. L. Evaluation of a Novel, Multi-Functional Inhibitor Compound for Prevention of Biofilm Formation on Carbon Steel in Marine Environments. *Sci. Rep.* **2021**, *11* (1), 1–12. https://doi.org/10.1038/s41598-021-94827-9.

(44) Dennis, R. V.; Patil, V.; Andrews, J. L.; Aldinger, J. P.; Yadav, G. D.; Banerjee, S. Hybrid Nanostructured Coatings for Corrosion Protection of Base Metals: A Sustainability Perspective. *Mater. Res. Express* **2015**, *2* (3), 0–22. https://doi.org/10.1088/2053-1591/2/3/032001.

(45) Ghosh, S. K. *Functional Coatings and Microencapsulation: A General Perspective*; Wiley, 2006. https://doi.org/10.1002/3527608478.ch1.

(46) Shchukin, D. G.; Grigoriev, D. O.; Möhwald, H. Application of Smart Organic Nanocontainers in Feedback Active Coatings. *Soft Matter* **2010**, *6* (4), 720–725. https://doi.org/10.1039/b918437f.

(47) Jyothi, N. V. N.; Prasanna, P. M.; Sakarkar, S. N.; Prabha, K. S.; Ramaiah, P. S.; Srawan, G. Y. Microencapsulation Techniques, Factors Influencing Encapsulation Efficiency. *J. Microencapsul.* **2010**, *27* (3), 187–197. https://doi.org/10.3109/02652040903131301.

(48) Jamekhorshid, A.; Sadrameli, S. M.; Farid, M. A Review of Microencapsulation Methods of Phase Change Materials (PCMs) as a Thermal Energy Storage (TES) Medium. *Renew. Sustain. Energy Rev.* **2014**, *31*, 531–542. https://doi.org/10.1016/j.rser.2013.12.033.

(49) Nazeer, A. A.; Madkour, M. Potential Use of Smart Coatings for Corrosion Protection of Metals and Alloys: A Review. *J. Mol. Liq.* **2018**, *253*, 11–22. https://doi.org/10.1016/j.molliq.2018.01.027.

(50) S. R. White, N. R. Sottos, P. H. Geubelle, J. S. Moore, M. R. Kessler, S. R. Sriram, E. N. Brown, S. V. Autonomic Healing of Polymer Composites. *Nature* **2001**, *409*, 794–817. https://doi.org/10.1038/35057232.

(51) Lyon, S. B.; Bingham, R.; Mills, D. J. Advances in Corrosion Protection by Organic Coatings: What We Know and What We Would like to Know. *Prog. Org. Coatings* **2017**, *102*, 2–7. https://doi.org/10.1016/j.porgcoat.2016.04.030.

(52) Chimenti, S.; Vega, J. M.; Lecina, E. G.; Grande, H. J.; Paulis, M.; Leiza, J. R. Combined Effect of Crystalline Nanodomains and in Situ Phosphatization on the Anticorrosion Properties of Waterborne Composite Latex Films. *Ind. Eng. Chem. Res.* **2019**, *58* (46), 21022–21030. https://doi.org/10.1021/acs.iecr.9b02233.

(53) Wan, H.; Song, D.; Li, X.; Zhang, D.; Gao, J.; Du, C. A New Understanding of the Failure of Waterborne Acrylic Coatings. *RSC Adv.* **2017**, *7* (61), 38135–38148. https://doi.org/10.1039/c7ra04878e.

(54) Russell, J. Paint and Coatings : A Mature Transition Industry. *Science (80-.).* **1997**, *22* (96), 203–245.

(55) ISO 12944-4. Paints and Varnishes — Corrosion Protection of Steel Structures by

Protective Paint Systems. *ISO* **1998**.

(56) Momber, A. Colour-Based Assessment of Atmospheric Corrosion Products, Namely of Flash Rust, on Steel. *Mater. Corros.* **2012**, *63* (4), 333–342. https://doi.org/10.1002/maco.201005831.

(57) Keddie, J. L. Film Formation of Latex. *Mater. Sci. Eng. R Reports* **1997**, *21* (3), 101–170. https://doi.org/10.1016/S0927-796X(97)00011-9.

(58) Richez, A. P.; Yow, H. N.; Biggs, S.; Cayre, O. J. Dispersion Polymerization in Non-Polar Solvent: Evolution toward Emerging Applications. *Prog. Polym. Sci.* **2013**, *38* (6), 897–931. https://doi.org/10.1016/j.progpolymsci.2012.12.001.

(59) Gilbert, R. G. *Emulsion Polymerization: A Mechanistic Approach*; Academic Press, 1997; Vol. 38.

(60) Asua, J. M. Emulsion Polymerization: From Fundamental Mechanisms to Process Developments. *J. Polym. Sci. Part A Polym. Chem.* **2004**, *42* (5), 1025–1041. https://doi.org/10.1002/pola.11096.

(61) Thickett, S. C.; Gilbert, R. G. Emulsion Polymerization: State of the Art in Kinetics and Mechanisms. *Polymer (Guildf).* **2007**, *48* (24), 6965–6991. https://doi.org/10.1016/j.polymer.2007.09.031.

(62) Lovell, P. A.; El-Aasser, M. S. Emulsion Polymerization and Emulsion Polymers. In *Emulsion polymerization and emulsion polymers*; Wiley, 1998; Vol. 36, pp 104–105. https://doi.org/10.1016/s1381-5148(97)84204-6.

(63) Smith, W. V.; Ewart, R. H. Kinetics of Emulsion Polymerization. *J. Chem. Phys.* **1948**, *16* (6), 592–599. https://doi.org/10.1063/1.1746951.

(64) Asua, J. M. Miniemulsion Polymerization. *Prog. Polym. Sci.* **2002**, *27* (7), 1283–1346. https://doi.org/10.1016/S0079-6700(02)00010-2.

(65) Aguirreurreta, Z. *Water-Borne Coatings and Water Pressure Sensitive Adhesives -*

Sensitive Adhesives Produced with Polymerizable Produced with Polymerizable Surfactants; PhD thesis, University of the Basque Country UPV/EHU, 2016.

(66) Keddie, J. L.; Routh, A. F. *Fundamentals of Latex Film Formation: Processe and Properties*; Springer: Dortecht, The Netherland, 2010. https://doi.org/10.1007/978-90-481-2845-7.

(67) Steward, P. A.; Hearn, J.; Wilkinson, M. C. Overview of Polymer Latex Film Formation and Properties. *Adv. Colloid Interface Sci.* **2000**, *86* (3), 195–267. https://doi.org/10.1016/S0001-8686(99)00037-8.

(68) Du Chesne, A.; Gerharz, B.; Lieser, G. The Segregation of Surfactant upon Film Formation of Latex Dispersions: An Investigation by Energy Filtering Transmission Electron Microscopy. *Polym. Int.* **1997**, *43* (2), 187–196. https://doi.org/10.1002/(sici)1097-0126.

(69) Butler, L. N.; Fellows, C. M.; Gilbert, R. G. Effect of Surfactant Systems on the Water Sensitivity of Latex Films. *J. Appl. Polym. Sci.* **2004**, *92* (3), 1813–1823. https://doi.org/10.1002/app.20150.

(70) Brooman, E. W. Modifying Organic Coatings to Provide Corrosion Resistance: Part II-Inorganic Additives and Inhibitors. *Met. Finish.* **2002**, *100* (5), 42–53. https://doi.org/10.1016/S0026-0576(02)80382-8.

(71) Zheludkevich, M. L.; Shchukin, D. G.; Yasakau, K. A.; Möhwald, H.; Ferreira, M. G. S. Anticorrosion Coatings with Self-Healing Effect Based on Nanocontainers Impregnated with Corrosion Inhibitor. *Chem. Mater.* **2007**, *19* (3), 402–411. https://doi.org/10.1021/cm062066k.

(72) Mansfeld, F. Basic Analysis and Interpretation of EIS Data for Metals and Alloys. In *An Introduction to Electrochemical Impedance Measurement*; 1999; pp 1–77.

(73) Loveday, D.; Peterson, P.; Rodgers, B. Evaluation of Organic Coatings with Electrochemical Impedance Spectroscopy: Part 1: Fundamentals of Electrochemical Impedance Spectroscopy. *CoatingsTech* **2004**, *1* (8), 46–52.

(74) Loveday, D.; Peterson, P.; Rodgers, B. Evalution of Organic Coatings with Electrochemical Impedance Spectroscopy Part 2: Application of EIS to Coatings. *CoatingsTech* **2004**, *1* (10), 88–93.

(75) Murray, J. N. Electrochemical Test Methods for Evaluating Organic Coatings on Metals: An Update. Part III: Multiple Test Parameter Measurements. *Prog. Org. Coatings* **1997**, *31* (4), 375–391. https://doi.org/10.1016/S0300-9440(97)00099-4.

(76) Mills, D. J.; Jamali, S. S. The Best Tests for Anti-Corrosive Paints. And Why: A Personal Viewpoint. *Prog. Org. Coatings* **2017**, *102*, 8–17. https://doi.org/10.1016/j.porgcoat.2016.04.045.

Chapter 2

Incorporation of a coumarate based corrosion inhibitor in waterborne polymeric binders for corrosion protection applications

2.1 Introduction

As previously mentioned in Chapter 1, one of the most common and effective method for mitigation of corrosion in metallic materials is the use of organic coatings[1,2]. Waterborne coatings have become an industrially viable alternative to fulfill such environmental regulations to dimish the use of volatile organic compounds (VOCs) present in traditional solvent based coatings [3–6]. One of the major challenges to overcome for the industrial application of waterborne coatings on metallic surfaces is that the presence of water can contribute to the formation of flash rust [7,8].

The main function of a coating is to form a physical protective barrier, limiting the diffusion of ions and other species from the corrosive media to the metal surface[3,9]. In organic coatings, the barrier property is mainly provided by the polymer matrix. Corrosion inhibitors may be added to the coating by different methodologies to provide extra protection[10–12]. The most common technique for the inclusion of corrosion inhibitors into a coating is via mechanical blending of inhibitors into the final formulation, which results in a heterogeneous distribution of the inhibitor in the coating but may contribute to premature leaching of the inhibitors[13], as previously shown in Chapter 1 (Figure 1.5). An alternative technique is the incorporation of inhibitors into the binder during the polymerization reaction, which allows for a more homogeneous distribution of inhibitors and increases the leaching time[5,11,13] (Figure 1.5).

Amongst the promising carboxylate compounds, p-coumaric acid (4-hydroxycinnamic acid) combined with new rare earth elements, has been reported to be an efficient free corrosion inhibitor in solution[1,13–15]. A better performance was observed in 4-hydroxy cinnamate based sol-gel formulations after the successful incorporation of lanthanum[16,17]. Recently, ionic coumarate corrosion inhibitors have been incorporated into acrylic UV coatings showing promising results

in terms of corrosion inhibition[18–20]. An interesting methodology for the industrial application of those carboxylate inhibitors would be to incorporate them into waterborne latexes. Conversely, common latexes have an anionic surfactant component in their composition, making them unstable in the presence of ions, which could cause a rapid coagulation of the particles. Therefore, the acid forms of the carboxylate inhibitors are more suitable for waterborne systems.

For this present chapter, the molecule of p-coumaric acid (Figure 2.1) was modified by the addition of a butyl (H4) radical to its structure, according to the technique proposed by Naciri et *al.*[21] (the synthesis was carried out by Daniele Mantione in the University of the Basque Country). The nonpolar radical is supposed to contribute to the formation of a protective hydrophobic film where the molecule is adsorbed onto a metal substrate, in addition to decreasing its solubility in water, preventing a rapid leaching profile. The aim of the present work was to investigate the anticorrosive properties of H4 in order to incorporate it into a waterborne polymeric binder by industrially viable methodologies; dispersion, emulsion, and miniemulsion polymerization reactions. Whenever possible, the inhibitor was also blended into the final latexes to compare the effect of incorporating it into the polymer particles. The effectiveness of the obtained coatings was compared by electrochemical analysis.

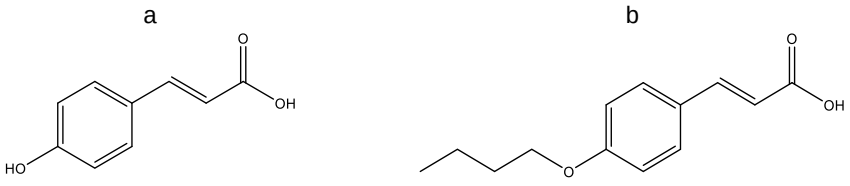

Figure 2.1**.** Chemical structures of a) p-coumaric acid (4-hydroxycinnamic acid) and b) Butylcoumaric acid (H4).

2.2 Experimental Section

2.2.1 Electrochemical analysis of H4 as a free inhibitor

The anticorrosive properties of H4 in solution were evaluated by electrochemical impedance spectroscopy (EIS) and potentiodynamic polarization (PP) experiments using a low current channel of the potentiostat BIO-LOGIC VMP3 and EC Lab V11.26 software. The experiments were performed at room temperature and open to air, with a cell composed of reference electrode of Ag/AgCl (saturated with KCl), medium carbon steel substrates as the working electrode, and a graphite rod counter electrode. The tests were carried out using an exposure area of 1.1 cm^2.

The open circuit voltage (OCV) was monitored for 47 minutes over the frequency range from 100 kHz to 10 mHz, followed by EIS at a scan rate of 0.167 mV/s with 6 points per decade and a sinoidal amplitude of 10 mV. Impedance responses were monitored for 24 hours, followed by a PP experiment. 0.3 mM of the inhibitor was dissolved in a 0.01M NaCl corrosive solution of ethanol and water. Ethanol was added to enhance the solubility of the inhibitor, and the solution was heated for 2 hours at low temperature to evaporate the ethanol. For comparison purposes, a control experiment with no inhibitor was also performed.

The corrosion current density (I_{corr}) and corrosion potential (E_{corr}) values were extracted from the PP curves by Tafel extrapolation. The linearity of the curves was found to be over a range of 10-25 mV at both sides of E_{corr}. The value of I_{corr} corresponds to the point on the graph in which the linear extrapolations of the anodic and the cathodic sections of the curves intersect. The inhibitor efficiency (IE) was calculated by Equation 2.1.

$$\mathrm{IE} = \frac{I_{corr\ control} - I_{corr\ inhibited}}{I_{corr\ control}} \times 100 \quad (2.1)$$

2.2.2 Bulk polymerization in the presence of H4

Bulk polymerization reactions were monitored by carbon NMR in order to analyze the effect of the presence of H4 in the conversion of the monomers, MMA and BA (50 / 50), to be used in the polymerization reactions. The bulk polymerizations were carried out at 70 °C, with inhibitor concentrations including 0, 1, and 3 % (g H4/100 g monomer). AMBN was used as the initiator at a concentration of 1 % (g AMBN /100 g monomer). The reaction conversion was followed by monitoring the decrease area of the peak related to one of the double bonds of MMA at 5.6 ppm.

2.2.3 Synthesis of low solids content waterborne poly(MMA/BA) latex by dispersion polymerization

Dispersion polymerization reactions were carried out in a 100 mL round bottom flask immersed in a bath of ethylene glycol (Figure 2.2). The system was initially composed of a single homogeneous phase prepared according to the recipe presented in Table 2.1. The solution was mixed for 10 minutes, then continuously agitated (250 rpm) and fed with N_2 for at least 15 minutes before addition of the initiator at 70 °C. Latexes were produced with a H4 inhibitor concentration of 3 % (g H4/100 g monomer), and a control latex with no inhibitor was also prepared for comparison purposes. The final latexes have a solids content of 30 %.

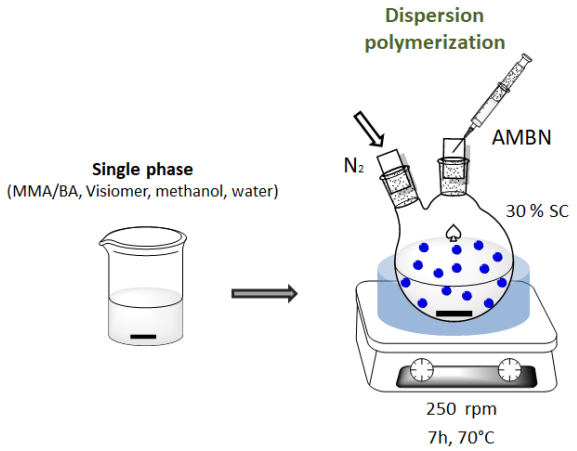

Figure 2.2. Schematic representation of dispersion polymerization of poly(MMA/BA).

Table 2.1. Recipe used for the dispersion polymerization reactions.

	Components	Mass (g)
Single phase	MMA	6.15
	BA	6.15
	VISIOMER® MPEG 2005 50% (22 % wbm*)	5.4
	H4 (0/3 % wbm*)	0 /0.37
	methanol/water (30/70 %)	22.3
Solution of initiator	AMBN (1.7 % wbm*)	0.2
	methanol/water (30/70 %)	10

*weight based on monomer

Additionally, as H4 is soluble in methanol, the inhibitors were mechanically blended into the control latex to form a final concentration of 3 % (g H4 / 100 g monomer), equivalent to the latexes with the inhibitors incorporated. The purpose was to compare both methodologies to analyze which one is more promising in terms of corrosion inhibition efficiency. The partition of H4 between the polymer particles and the continuous phase is expected to be the main difference between both methods of inhibitor addition to the dispersion latex. In order to quantify the amount

of inhibitor in the aqueous phase of the final latexes, calibration curves of H4 in methanol/water (70 / 30, m / m) were constructed using ultraviolet spectroscopy (UV 2550, Shimadzu). Then, samples of latex with H4 incorporated and with H4 blended were centrifuged for 6 hours at - 4 °C and 13000 rpm. The serum was analyzed in UV in triplicate. Using the data obtained by the calibration curve, the concentration of H4 located outside the particles was calculated.

2.2.4 Synthesis of low solids content waterborne poly(MMA/BA) by emulsion polymerization

An attempt of incorporating H4 inhibitor in latexes by emulsion polymerization was also performed (Figure 2.3). The reactions were prepared according to the recipe described in Table 2.2, to obtain latexes with 20 % solids content. Initially the aqueous and organic phases were mixed, agitated for 10 minutes, and finally placed in the round bottom flask. The solution was continuously agitated (250 rpm) and fed with N_2 for at least 15 minutes before addition of initiator. When the system reached 70 °C, the initiator solution was added, commencing the reaction.

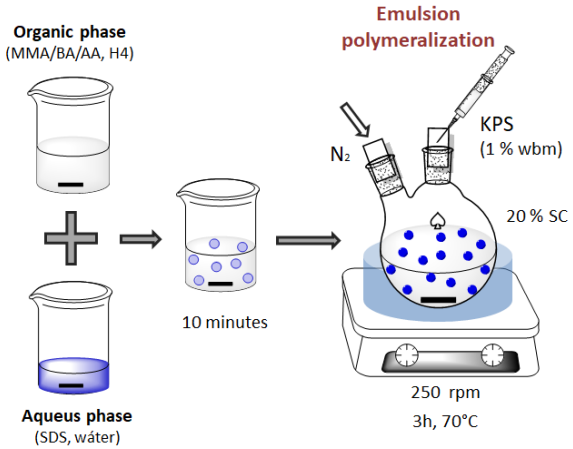

Figure 2.3. Schematic representation of emulsion polymerization of poly(MMA/BA/AA).

Table 2.2. Recipe used for the emulsion polymerization reaction with 20 % solids content

	Components	Mass (g)
Organic phase	MMA	4.95
	BA	4.95
	AA	0.1
	H4	0 / 0.1
Aqueous phase	SDS	0.2
	H_2O	35
Initiator solution	KPS	0.1
	H_2O	5.0

2.2.5 Synthesis of low solids content waterborne poly(MMA/BA) by miniemulsion polymerization

H4 inhibitor was incorporated in latexes by miniemulsion polymerization (Figure 2.4). The recipe is presented in Table 2.3, to obtain latexes with 20 % solids content. Aqueous and organic phases were mixed together and agitated for 10 minutes. Then, the mixture was utrasonicated with a Branson Ultrasonics Sonifier 450 for 5 minutes (operating at 1 - output control and 80% duty cycle in an ice bath and under magnetic stirring of 300 rpm), and finally placed in the round bottom flask. The solution was continuously agitated (250 rpm) during reaction, and fed with N_2 for at least 15 minutes before addition of initiator. When the system reached 70 °C, the initiator solution was added, commencing the reaction.

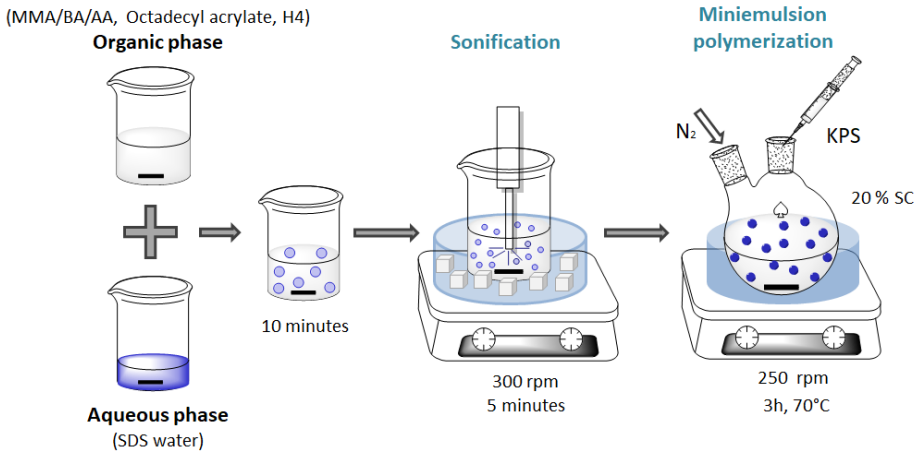

Figure 2.4. Schematic representation of emulsion polymerization of poly(MMA/BA/AA).

Table 2.3. Recipe used for the minimulsion polymerization reaction with 20 % solids content

	Components	Mass (g)
Organic phase	MMA	4.95
	BA	4.95
	AA	0.1
	Octadecyl acrylate	0.4
	H4	0 / 0.1
Aqueous phase	SDS	0.2
	H_2O	35
Initiator solution	KPS	0.1
	H_2O	5.0

2.2.6 Synthesis of high solids content latexes (50 % SC) by semibatch emulsion polymerization

In order to increase the solids content of the latexes containing the H4 inhibitor, a two stage seeded semibatch emulsion polymerization process was implemented (Figure 2.5). The seed latexes were prepared by miniemulsion polymerization containing H4 inhibitor. These polymerization reactions were carried out under N_2 atmosphere in a 250 mL glass-jacketed

reactor. The temperature was maintained at 75 °C, and the impeller rotation speed at 200 rpm. Initially, a seed of 30 % solids content with 1 % H4 inhibitor (g H4/ 100 g monomer) was prepared by miniemulsion polymerization. The mixture was utrasonicated using a Branson Ultrasonics Sonifier 450 for 5 minutes (operating at 1 - output control and 80% duty cycle in an ice bath and under magnetic stirring of 300 rpm). In the second stage, a pre-emulsion of MMA, BA, water, and surfactant was continuously fed for 3 hours in order to increase the solids content of the latex to 50 %. Therefore, the concentration of H4 in the final latex was 1.5 mg H4/g polymer (0.15 % H4). A post polymerization step was performed at 90 °C for one hour to eliminate traces of monomer. A control latex with no H4 was also produced for comparison purposes. The recipe used for the polymerizations is presented in Table 2.4.

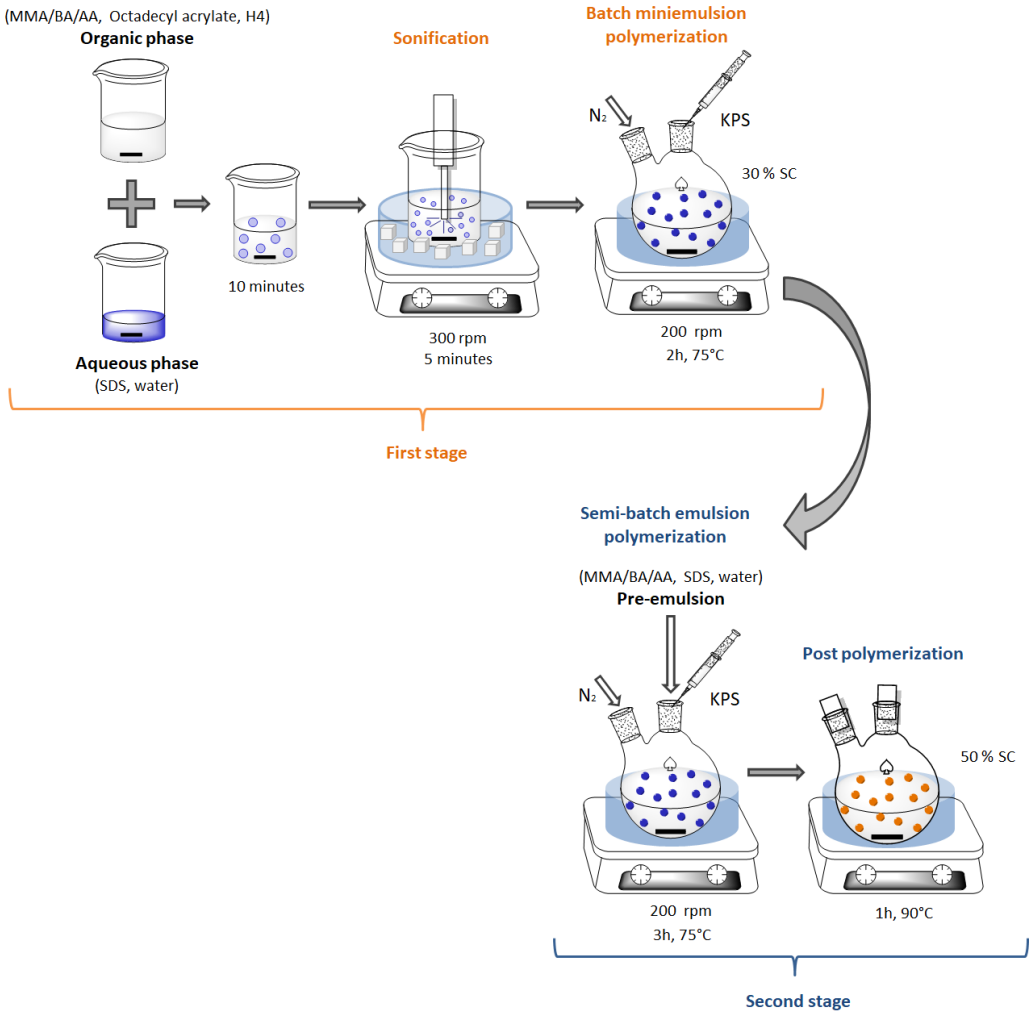

Figure 2.5. Schematic representation of semibatch emulsion polymerization of poly(MMA/BA/AA).

Table 2.4. Recipe used for the two stage seeded semibatch emulsion polymerization reactions.

Seed		
	Components	Mass (g)
Organic phase	MMA	14.85
	BA	14.85
	AA	0.3
	Octadecyl acrylate	1.2
	H4 (0/ 1 % wbm)	0/0.3
Aqueous phase	SDS (2 %wbm)	0.6
	H_2O	55
Initiator solution	KPS (1 % wbm)	0.3
	H_2O	15
Preemulsion		
	Components	Mass (g)
Organic phase	MMA	34.65
	BA	34.65
	AA	0.7
Aqueous phase	SDS (1 % wbm)	0.7
	H_2O	15
Initiator solution	KPS (0.5 % wbm)	0.35
	H_2O	15

2.2.7 Characterization of latexes

2.2.7.1 Monomer conversion and particle size

Monomer conversion was followed by gravimetry. Samples were taken from the reaction over time and placed in a pre-weighed aluminum pan with droplets of hydroquinone (1 wbm %) to stop the reaction. The pans were dried until a constant weight was obtained. The instantaneous conversion of each sample was obtained by Equation 2.2.

$$X(t) = \frac{(solids\ content) - (fraction\ of\ non\ polymerizable\ material)}{fraction\ of\ monomers} \quad 2.2$$

2.2.7.2 Dynamic light scattering

The polymer particle sizes were measured by dynamic light scattering (DLS) using a Zetasizer Nano Series (Malvern instrument) after diluting the samples with deionized water. The equipment was operated at 20 °C and the values reported were the average of three repeated measurements.

2.2.7.3 Water absorption of free films

To analyze the absorption of water in the films, latex samples were placed in silicone molds and dried at room temperature for 7 days. The films were peeled from the molds and immersed in distilled water. The water uptake was followed for 11 days, in triplicate and it was measured by the difference between the weight of the film after immersion in water and the initial weight.

2.2.8 Preparation of steel substrates and EIS of coatings

The steel substrate surfaces were used as received. The substrates were cleaned with abundant acetone and dried with compressed air before deposition of the latex. The samples were dried at room temperature for at least one day. The final thickness of the coatings was measured with a coating thickness gauge to ensure that the final film had an average thickness of 45 µm.

Electrochemical impedance spectroscopy (EIS) was performed over 24 hours according to the same procedure reported in section 2.2, except that the concentration of the corrosive

solution used was 0.005 M NaCl. In addition to these EIS measurements on the intact films, EIS measurements were also carried out for films in which an artificial scratch (1.1 cm in size and 0.1 mm thick) was made. EIS analyses were performed on the scratched coatings to determine if H4 imparts any active anticorrosive properties to the system where the barrier properties of the coating was removed.

2.3 Results and Discussion

2.3.1 Electrochemical analysis of H4 as a free inhibitor

The anticorrosive property of H4 was investigated by EIS (Figure 2.6.a (control) and Figure 2.6.b (0.3 mM H4)). This concentration was chosen as it is approximately the maximum solubility observed for the component in the system. The molecules of H4 dispersed in the corrosive solution are expected to diffuse from the bulk of the solution and adsorb onto steel surfaces, forming a protective layer. In first hour of immersion, the solution with H4 shows higher impedance values (10^4 Ω) in the low frequency range and also a higher phase angle (27 degrees) when compared to the control ($10^{3.2}$ Ω, 14 degrees), demonstrating that H4 molecules do provide a degree of corrosion protection to the metal surface even at such low concentrations. However, a decrease in the impedance and phase is observed after 6 hours of experiment, indicating that the concentration of inhibitors was not sufficient to maintain the corrosion protection of the system for 24 hours.

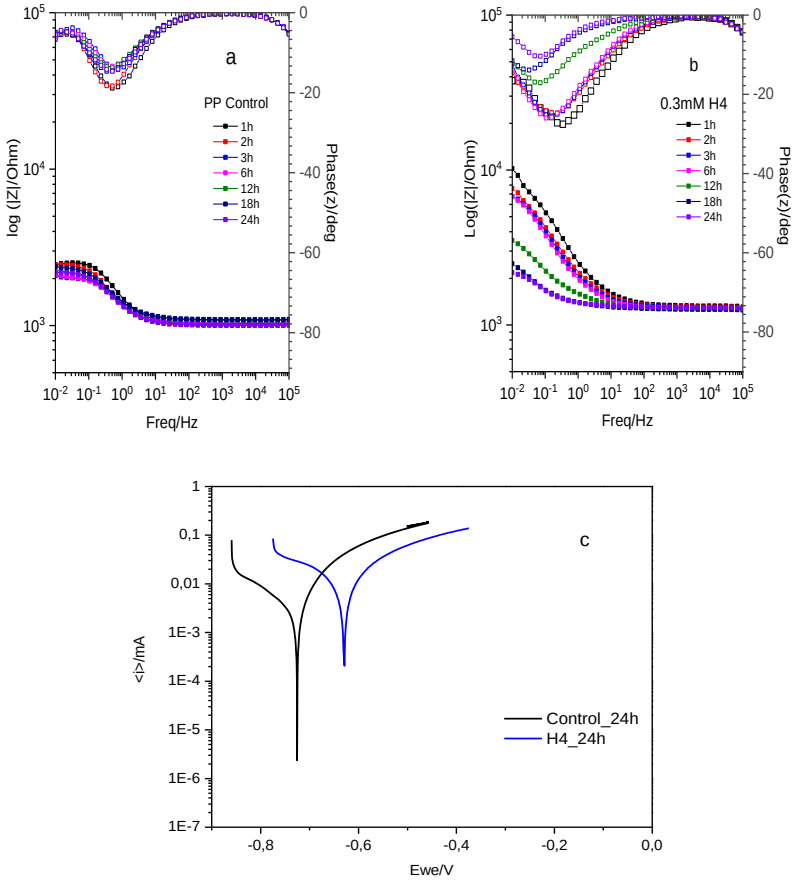

Figure 2.6. Bode spectra of steel immersed in a) the control solution (0.01 M NaCl) and b) the solution containing the H4 inhibitor (0.3 mM H4 in 0.01 M NaCl) over 24 hours; c) Potentiodynamic polarization curves of the control and H4 solutions (as described for a and b) after 24 hours at OCV.

The PP spectra are shown in Figure 2.6.c. A shift in the corrosion potential (E_{corr}) towards a more positive value is observed in the solution of inhibitor. The E_{corr} of the control was -635 mV, whereas the solution with H4 yielded an E_{corr} of -704 mV, indicating that H4 primarily suppresses the anodic reaction of corrosion. The corrosion current of the control was found to

be 2.720 A/cm^2 while the solution with H4 had a current of 0.704 A/cm^2, giving an inhibition efficiency of 74.1 %.

The inhibitor molecule is required to be incorporated in higher concentration into the coating in order to provide longer term protection. It is important to highlight though, that even when the property of an inhibitor is well known, the outcome of its incorporation into a coating is not predictable[12].

2.3.2 Bulk polymerization

In order to analyze the effect that H4 inhibitor molecules may have on the rate of monomer polymerization, radical polymerization of the MMA/BA mixture was carried out in bulk, in the absence and presence of H4 molecules. This study was monitored by NMR. It was observed that the conversion of MMA/BA is retarded in the presence of H4 at 70 °C (Figure 2.7). It is known that compounds with aromatic rings in their composition may retard free radical polymerization reactions [22]. The kinetic profile observed in the system with 1 % H4 (g H4/ 100 g monomer) is very similar to the one with 3 % H4 (g H4/ 100 g monomer), and since precipitation of some of the H4 was observed in the bottom of the NMR tube containing the system prepared with 3 % H4 (indicating that the concentration was over its solubility), a H4 concentration of 1 % was adopted as the limit for the solubility/dispersibility of H4 into the MMA / BA (50 / 50) monomer mixture.

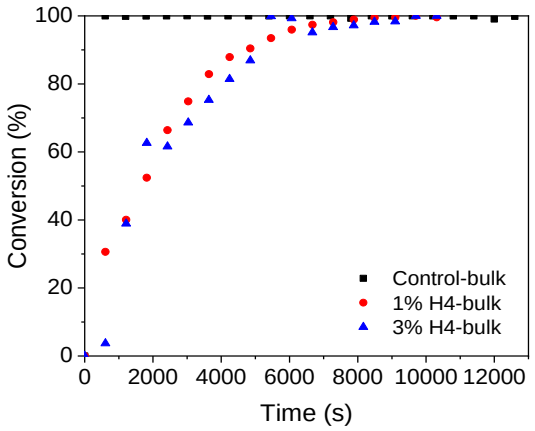

Figure 2.7. Conversion of MMA/BA in bulk radical polymerization in the presence of H4, as measured by NMR.

2.3.3 Coatings made by dispersion polymerization reactions with H4 incorporated / blended

Once the inhibitory effect of H4 on the radical polymerization of MMA/BA was identified, the first attempts to incorporate it in waterborne binders were carried out by dispersion polymerization. H4 is soluble in the initial methanol/water/monomer phase used in the dispersion polymerization recipe, so its incorporation is more straightforward by this technique. The kinetics of the dispersion polymerization reactions performed in both the absence (control-dispersion) and presence (3 % H4) of H4 molecules are presented in Figure 2.8. In principle, the radical reaction inhibitory effect of H4 is not so evident from these reactions, even though the final monomer conversion achieved in the presence of H4 was slightly lower than the control. Thus, the H4 molecules were successfully incorporated into the polymer particles dispersed in the continuous methanol/water phase. The average particle size of the control-dispersion latex,

135 nm, was determined to be larger than that of the latex with H4, which was 115 nm. Additionally, the control-dispersion latex was blended with H4 after the polymerization step, in order to analyze the effect of having the H4 molecules mainly in the continuous methanol/water phase.

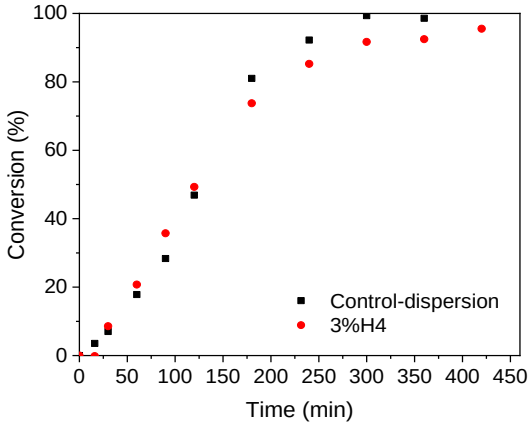

Figure 2.8. Kinetics of batch dispersion polymerization reactions of MMA/BA carried out in the absence (control-dispersion) and presence of H4 (3 %).

To analyze the partition of the inhibitor between the continuous media and the polymer particles, a calibration curve of H4 in methanol/water (70 / 30) was constructed, and then the continuous phase of both latexes (after centrifugation) was analyzed. For the latex with H4 incorporated, 48 % of the total amount of inhibitor was in the media, with the remaining 52 % of the inhibitor in the polymer particles. On the other hand, as expected in the latex with H4 blended, 100 % of the inhibitor was found in the media. Therefore, it is expected that this difference in availability of the H4 inhibitor will vary the corrosion inhibiting effect of the films produced from these latexes.

The free films formed from both the control-dispersion latex and the latex with H4 incorporated are transparent (Figure 2.9.a). However, the free film obtained from the latex with H4 blended is opaque. It is likely that the opacity is due to an accumulation of inhibitor molecules in the interstices of the particles during film formation. This is in contrast to the events occurring during film formation from latex with H4, as the incorporation of H4 in the particles results in its higher dispersion in the final film (Figure 1.5 b, and c of Chapter 1). The water uptake of these three films is shown in Figure 2.9 b. The absorption of water is nearly the same for the control film and the film with H4 blended, however, the film with H4 incorporated absorbs less water. These results indicate that the incorporation of H4 into the polymer particles and hence, its higher distribution during film formation, contributes to the film being more hydrophobic.

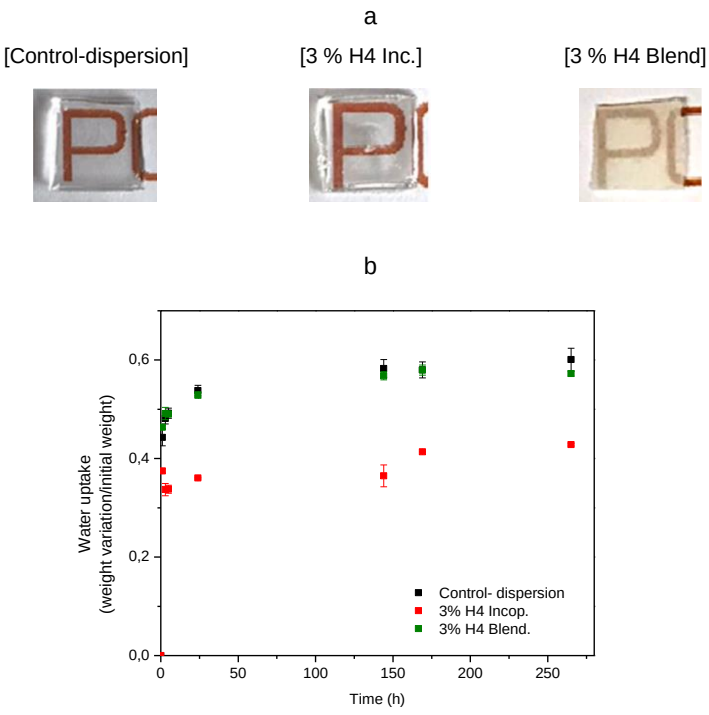

Figure 2.9. a) Images of the free latex films formed from control dispersion, dispersion with 3 % H4 incorporated and 3 % H4 blended; b) Water absorption of the free films over time.

Finally, the corrosion inhibitory effect of these three films coated on steel was analyzed by EIS (Figure 2.10 a - d), optical images of the sample before and after the experiment was also taken. The Bode spectra of the control-dispersion coating (Figure 2.10 b) is characteristic of soft coatings that allow diffusion of water, and it has no phase angle peaks at high frequencies that are normally associated with a barrier coating[23]. The control-dispersion coating offers no significant anticorrosive protection to the bare steel substrate (Figure 2.10 a and b). Therefore, any increase in impedance that is observed in the other coatings will exclusively result from the anticorrosive properties of the inhibitors in the films. Higher impedances are observed in the first 3 hours of analysis for the coating with H4 blended and in the first hour for the film with H4 incorporated, highlighting the anticorrosive properties of H4. The difference between the two may be due to the availability of H4 in the system; in the coating in which H4 is incorporated, almost half of it is attached to the polymeric particles, as previously determined by calculation of the partition of H4 into the phases. On the other hand, in the coating with the blended H4, all of it is free in the medium. Therefore, when the coating is applied on the steel, a higher amount of H4 molecules are free to diffuse onto the metal surface to produce the corrosion inhibitory effect in the blended system than in the case of the incorporated system. In any case, the anticorrosive effect of H4 does not last for 24 hours in this system; this may be due to the poor barrier properties of the control-dispersion film or the low concentration of H4 in the system.

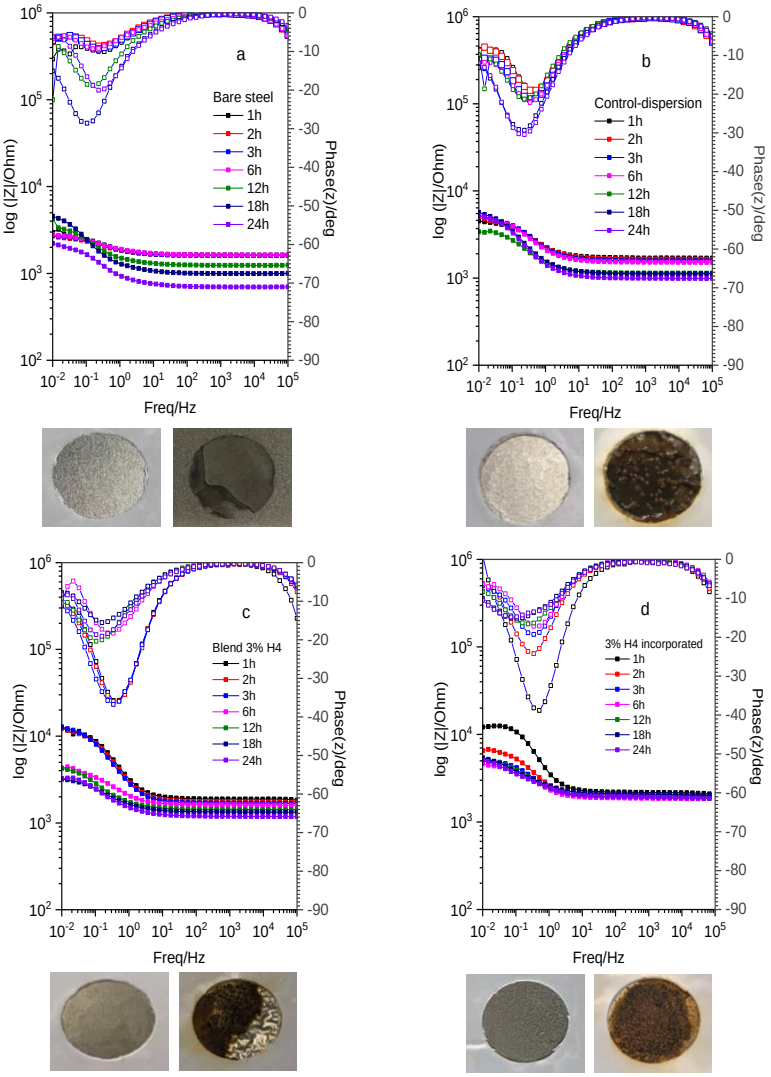

Figure 2.10**.** Electrochemical impedance spectra of bare steel and of coatings made by dispersion polymerization followed by optical images of the samples before (on the left) and after the experiment (on the right). a) Bare steel; b) Control coating; c) Coating with 3% H4 blended; and d) Coating with 3% H4 incorporated.

2.3.4 Coatings made by emulsion polymerization with H4 incorporated

As seen above, the inhibitory effect of H4 was indicated in the dispersion latex coatings, but the low barrier properties of the control-dispersion film itself led to low corrosion protection films. This could be explained by the large amount of stabilizer (PEGMA) present in the recipe, which can increase the hydrophilicity and water permeability of the final films[24]. Therefore, in an effort to decrease the amount of stabilizer/emulsifier required to produce waterborne latexes containing H4, an emulsion polymerization strategy was tried. However, two main drawbacks were found when this polymerization technique was used. On one hand, as evident from Figure 2.11 a, the conversion of the monomers was retarded by the presence of H4 molecules in the system. On the other hand, even if a stable latex was obtained from both formulas, a supernatant was observed at the end of the reaction from the H4 containing latex, which was confirmed to be mainly composed of H4 by NMR (Figure 2.11 b). Therefore, due to the hydrophobic character of H4, its diffusion from the droplets of monomer to the polymer particles during the emulsion polymerization is difficult, preventing its incorporation in the polymer particles. Therefore, H4 segregates and phase separates, ending up on the surface of the latex. Thus, the incorporation of H4 was not successful by emulsion polymerization.

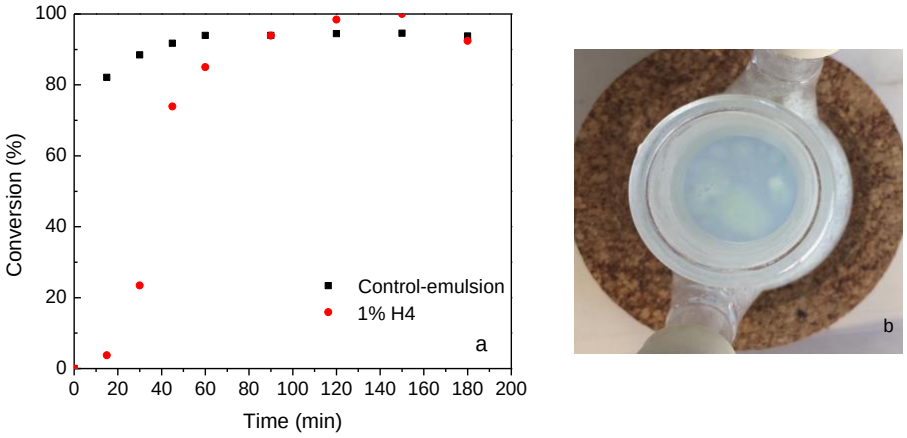

Figure 2.11**.** a) Kinetics of emulsion polymerization reactions (20 % SC); and b) supernatant observed at the end of the reaction with H4.

2.3.5 Coatings made by miniemulsion polymerization

Once the emulsion polymerization technique was discarded for the incorporation of H4 inhibitor to waterborne coatings, the miniemulsion polymerization technique was pursued. In this polymerization technique, the monomer polymerizes directly in the monomer droplets, without needing to be transported through the water phase. Therefore, it was hypothesized that if the H4 molecules can be initially placed in the monomer droplets, they would remain in the final polymer particles. Two types of processes were tried by miniemulsion polymerization; one as a single stage batch to obtain final low solids content latexes (20 % SC), and another using a two stage seeded semibatch emulsion polymerization, to achieve higher final solids content (50 % SC). In the latter, the first stage was a batch miniemulsion polymerization where the H4 was incorporated.

2.3.5.1 Single stage batch, low solids content (20 %) latexes

Initially the batch miniemulsion polymerizations were carried out in the absence and presence of H4. It was observed that at 70 °C, the reaction was also retarded by the presence of 1 % of H4 (Figure 2.12 a). On the other hand, the presence of H4 in the system seems to contribute to the formation of smaller particles, as the average particle size of the control-miniemulsion latex was 90 nm, while that of the latex with 1 % H4 was 80 nm. These latexes were applied onto steel substrates, and a brownish color, characteristic of flash rust was observed on the surface of the metal (Figure 2.12 b). This flash rust was attributed to the high concentration of water in contact with the steel substrate for these low solids content (high water content) latexes. Therefore, as an attempt to prevent the flash rust, the formulation of the latexes was optimized in order to increase their solids content.

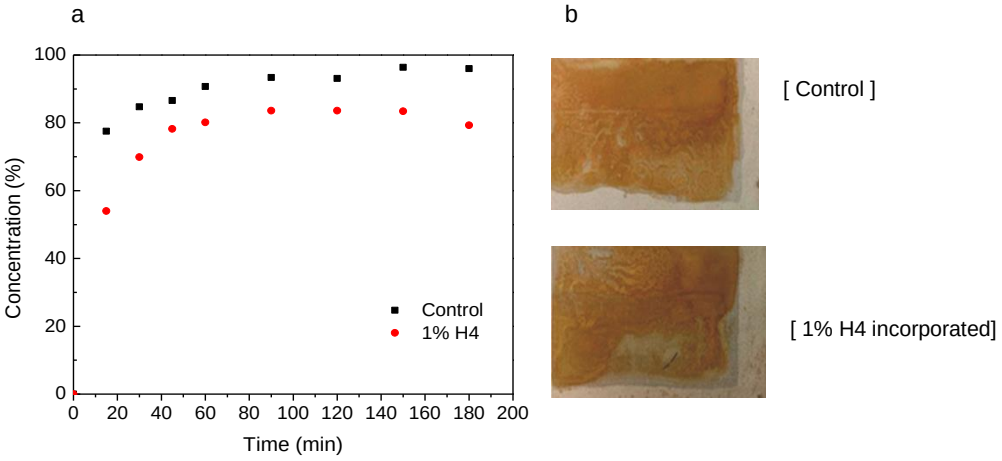

Figure 2.12. a) Kinetics of miniemulsion polymerization reactions (20 % SC); and b) Images of the steel substrates coated with the latexes obtained with 20 % SC, showing clear evidence of flash rust.

2.3.5.2 Two stage seeded semibatch emulsion polymerization (50 wt% solids content)

Due to the exothermic character of polymerization reactions, batch polymerization reactions at high solids contents are not recommended, due to the thermal runaway that could occur in these conditions. Therefore, first a low solids content latex was synthesized by miniemulsion polymerization incorporating all the amount of the inhibitor H4 (1 % based on the monomers in this step) in the formulation. This latex was then used as seed in the semibatch emulsion polymerization where the remaining MMA/BA monomers needed to produce a dispersion with 50 % solids content were added as a preemulsion and polymerized. This way, the final H4 concentration in the latex was 0.15 % based on total monomers. The reactions kinetics of this second process are presented in Figure 2.13 a. It was observed that at 75 °C, the reaction was not retarded by the addition of H4. H4 may be partially hidden from the initiator radicals by the polymer in the seed, and its polymerization retardation effect may be therefore notably reduced. The instantaneous conversions are high and similar for both the control latex and the latex with H4. The evolution of the particle size over time is shown in Figure 2.13 b. A similar particle size evolution can be seen in both cases, reaching 160 nm for the control-semibatch latex and 154 nm for the latex containing H4.

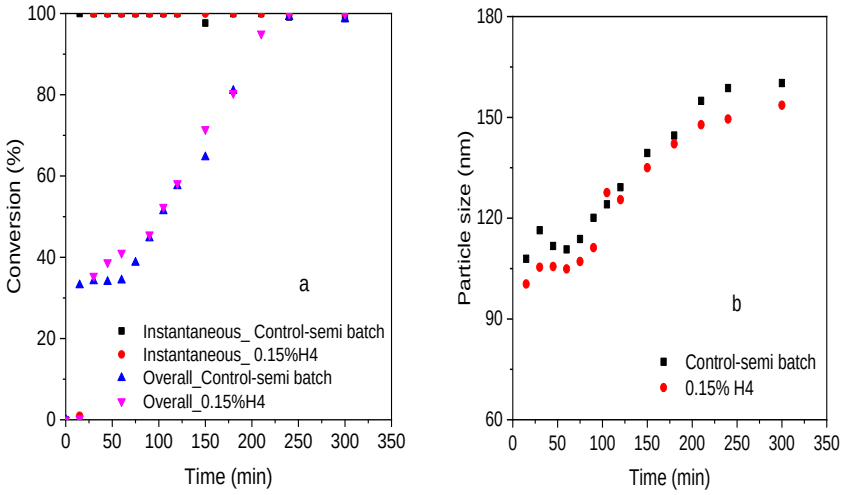

Figure 2.13**.** a) Kinetics of the semibatch emulsion polymerization reaction; and b) The average particle size obtained over the duration of the reaction.

The water uptake of the free films is shown in Figure 2.14. The profile of the absorption of water is considerably different from the one observed in the films made via dispersion (Figure 2.9 c). In the dispersion films, the absorption of water was rapid; the control-dispersion reaches the maximum, 0.5 (weight variation/real weight), after 24 hours and remains constant until the end of the experiment. However, in the case of the films made by semibatch emulsion polymerization, the absorption of water is gradual, and the control-semibatch reaches 0.35 (weight variation/initial weight) at the end of the experiment, after 24h. This is related to the higher concentration of stabilizer (PEO based macromonomer) used in the dispersion polymerization recipe, which is known to contribute to the absorption of water in waterborne films[24]. There is no significant difference between the absorption of water of the free films formed from the emulsion-0.15 % H4 and the control-semibatch over 24 hours of immersion. This is an indication that the concentration of H4 incorporated into the film does not change the hydrophobicity of the film.

However, after 144 hours of immersion, the water uptake of the emulsion-0.15 % H4 films is slightly higher than the control. This may be due to the creation of pores in film emulsion-0.15 % H4 film, as the inhibitor is leached out.

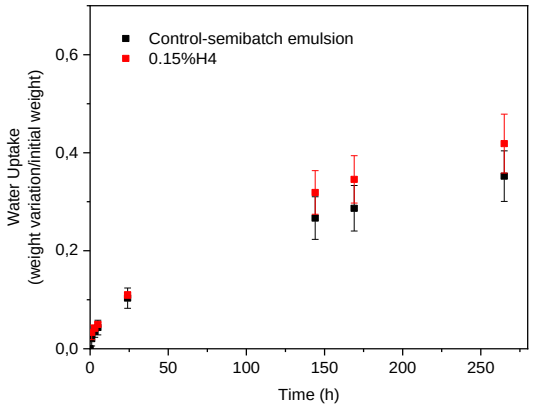

Figure 2.14**.** Water absorption of free semibatch emulsion films over time.

When these high solids content latexes were applied onto steel substrates, no flash rusting was formed. Therefore, their corrosion protection properties were measured by EIS, optical images of the sample surfaces before and after the experiment were also taken (Figure 2.15). A phase angle peak at high frequencies, normally associated with a barrier coating[23], is seen for the control-semibach emulsion and also for the semibatch emulsion-0.15 % H4. The EIS spectra indicates that the control-semibatch emulsion coating (Figure 2.15 b) offers an effective barrier protection to the bare steel substrate (Figure 2.15 a), showing impedances in the range of $10^{5.2}$ to 10^{6} Ω and phases angles of 54 to 72° from the moment immersed to 24 hours after immersion in the corrosive medium. The coating with H4 incorporated shows more effective corrosion protection of 10^{6} to $10^{6.7}$ Ω and phases angles of 65 to 80 degrees (Figure 2.15 c) over the 24 hours of immersion.

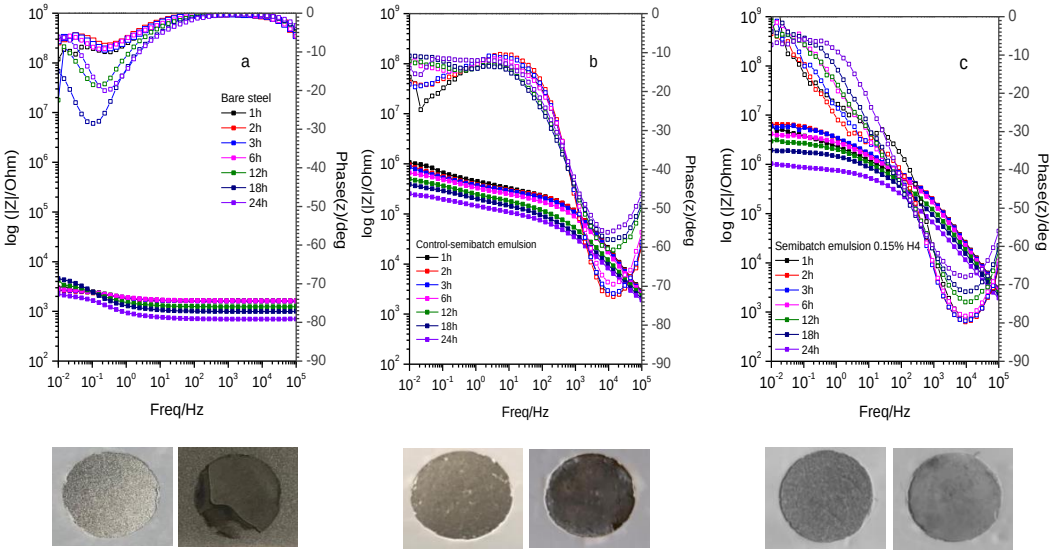

Figure 2.15**.** Electrochemical impedance spectra of coatings made by seeded semibatch emulsion polymerization and optical images of the sample before (on the left) and after the experiment (on the right) for a) the bare steel; b) the control coating; and c) the coating with H4.

The phase angle approaches that for highly effective barrier coatings that show a capacitor behavior – phase angle of 90 degrees[23]. Optical images in Figure 2.15 of the bare steel and of the two coated systems before and after the 24 hours of immersion also show the effective protection that the H4 containing semibatch emulsion gives the steel from corrosion. Therefore, it was confirmed that H4 is able to provide extra anticorrosive protection to the system, even in such low concentrations (1.5 mg H4/g polymer).

In a further analysis to assess the corrosion performance of the coatings when a defect is present, a scratch was made to both coatings applied on steel, and EIS measurements were conducted on these scratched samples. The spectra of the coatings with a scratch and the optical images of the sample surfaces before and after the experiment are presented in Figure 2.16 along with optical images before and after immersion. The impedance of the control-semibatch

emulsion (Figure 2.16 a) drops considerably faster than the one of the coating with H4 (Figure 2.16 b). This phenomenon is mainly visible in the first hours of the experiment (1-6 hours); the impedance of the coating with H4 incorporated dropped from $10^{4.2}$ to $10^{3.9}$ Ω, whereas the impedance of the control coating dropped from $10^{4.2}$ to $10^{3.6}$ Ω. This is an indication that even if H4 is incorporated into the polymer particles of the coating, it can be released and impart corrosion inhibiting properties. The effect does not last for long, probably because the concentration of inhibitor is low in this system.

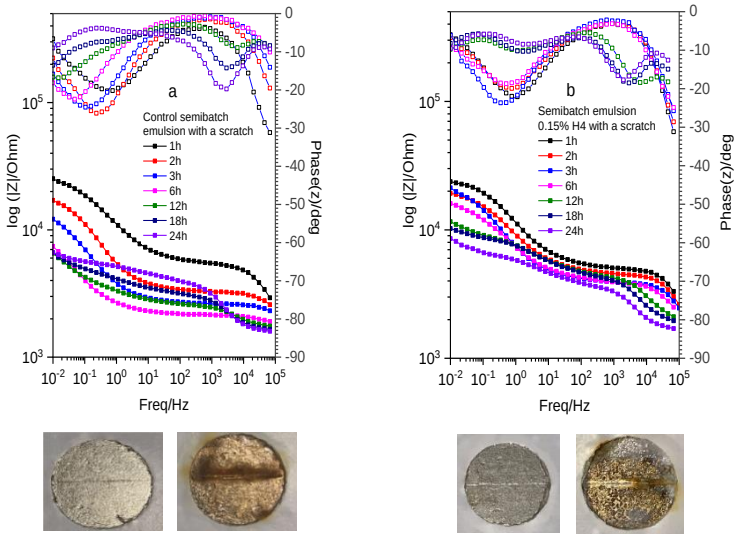

Figure 2.16. Electrochemical impedance spectra of coatings with a controlled scratch and optical images of the sample surfaces before (on the left) and after the experiment (on the right) for a) the control coating; and b) the coating with H4.

The optimum concentration of H4 is still under investigation. A higher amount of inhibitor in the system will most likely be required, but the solubility of the inhibitor in the monomer system is limiting. It is also important to highlight that the recipe of the coating itself without inhibitors

could be optimized to improve protection against corrosion, for instance by using more hydrophobic monomers and surfactants.

2.4 Conclusions

The anticorrosive property of H4 was confirmed by potentiodynamic polarization analysis making it a suitable candidate to investigate as part of a coating system. It was not possible to incorporate H4 by emulsion polymerization due to its resistance of diffusion through the water phase. However, H4 was successfully incorporated into the waterborne polymeric binder by dispersion, batch miniemulsion, and seeded semibatch emulsion polymerization with the H4 incorporated in the seed.

Blending H4 into the final latex, as opposed to incorporation into the separate polymer particles was possible only in the case of dispersion polymerization due to the presence of methanol that dissolves the inhibitor. The coatings made by dispersion did not provide effective barrier protection to the steel substrate but in the presence of H4, either incorporated or blended, higher impedances were reached in the first hours of experiment. These results prove the concept that the presence of H4 in a coating can provide extra protection to the system. The coating with H4 blended provided protection for 6 hours, while the one with H4 incorporated only provided it for the first hour. This difference may be related to the availability of H4 in the system, as when blended, the inhibitor has higher mobility.

The coatings obtained by batch miniemulsion polymerization with low solids content were not able to avoid flash rust when applied to steel substrates. However, this could be avoided by increasing the solids content of the latex by seeded semibatch emulsion polymerization.

These high solids content latexes provided an effective barrier protection to the steel surface and when the inhibitor was incorporated it gave extra protection to the system. Therefore, this methodology seems promising for the incorporation of inhibitors into the binder for development of waterborne coatings with anticorrosive properties. In the next chapter, coatings with higher concentration of inhibitors are obtained by batch polymerization of high solids content miniemulsions.

2.5 References

(1) Somers, A. E.; Hinton, B. R. W.; de Bruin-Dickason, C.; Deacon, G. B.; Junk, P. C.; Forsyth, M. New, Environmentally Friendly, Rare Earth Carboxylate Corrosion Inhibitors for Mild Steel. *Corros. Sci.* **2018**, *139* (May), 430–437. https://doi.org/10.1016/j.corsci.2018.05.017.

(2) Kendig, M.; Mills, D. J. An Historical Perspective on the Corrosion Protection by Paints. *Prog. Org. Coatings* **2017**, *102*, 53–59. https://doi.org/10.1016/j.porgcoat.2016.04.044.

(3) Wan, H.; Song, D.; Li, X.; Zhang, D.; Gao, J.; Du, C. A New Understanding of the Failure of Waterborne Acrylic Coatings. *RSC Adv.* **2017**, *7* (61), 38135–38148. https://doi.org/10.1039/c7ra04878e.

(4) Asua, J. M. Miniemulsion Polymerization. *Prog. Polym. Sci.* **2002**, *27* (7), 1283–1346. https://doi.org/10.1016/S0079-6700(02)00010-2.

(5) Sørensen, P. A.; Kiil, S.; Dam-Johansen, K.; Weinell, C. E. Anticorrosive Coatings: A Review. *J. Coatings Technol. Res.* **2009**, *6* (2), 135–176. https://doi.org/10.1007/s11998-008-9144-2.

(6) Asua, J. M. Emulsion Polymerization: From Fundamental Mechanisms to Process Developments. *J. Polym. Sci. Part A Polym. Chem.* **2004**, *42* (5), 1025–1041. https://doi.org/10.1002/pola.11096.

(7) ISO 12944-4. Paints and Varnishes — Corrosion Protection of Steel Structures by Protective Paint Systems. *ISO* **1998**.

(8) Momber, A. Colour-Based Assessment of Atmospheric Corrosion Products, Namely of Flash Rust, on Steel. *Mater. Corros.* **2012**, *63* (4), 333–342. https://doi.org/10.1002/maco.201005831.

(9) Chimenti, S.; Vega, J. M.; Lecina, E. G.; Grande, H. J.; Paulis, M.; Leiza, J. R. Combined Effect of Crystalline Nanodomains and in Situ Phosphatization on the Anticorrosion Properties of Waterborne Composite Latex Films. *Ind. Eng. Chem. Res.* **2019**, *58* (46), 21022–21030. https://doi.org/10.1021/acs.iecr.9b02233.

(10) Dennis, R. V.; Patil, V.; Andrews, J. L.; Aldinger, J. P.; Yadav, G. D.; Banerjee, S. Hybrid Nanostructured Coatings for Corrosion Protection of Base Metals: A Sustainability Perspective. *Mater. Res. Express* **2015**, *2* (3), 0–22. https://doi.org/10.1088/2053-1591/2/3/032001.

(11) Nazeer, A. A.; Madkour, M. Potential Use of Smart Coatings for Corrosion Protection of Metals and Alloys: A Review. *J. Mol. Liq.* **2018**, *253*, 11–22. https://doi.org/10.1016/j.molliq.2018.01.027.

(12) Lyon, S. B.; Bingham, R.; Mills, D. J. Advances in Corrosion Protection by Organic Coatings: What We Know and What We Would like to Know. *Prog. Org. Coatings* **2017**, *102*, 2–7. https://doi.org/10.1016/j.porgcoat.2016.04.030.

(13) Somers, A. E.; Deacon, G. B.; Macfarlane, D. R.; Junk, P. C.; Forsyth, M. Recent Developments in Environment-Friendly Corrosion Inhibitors for Mild Steel. *J. Indian Inst. Sci.* **2016**, *96* (4), 285–292.

(14) Deacon, G. B.; Junk, P. C.; Lee, W. W.; Forsyth, M.; Wang, J. Rare Earth 3-(4′-Hydroxyphenyl)Propionate Complexes. *New J. Chem.* **2015**, *39* (10), 7688–7695. https://doi.org/10.1039/c5nj00787a.

(15) Blin, F.; Leary, S. G.; Wilson, K.; Deacon, G. B.; Junk, P. C.; Forsyth, M. Corrosion Mitigation of Mild Steel by New Rare Earth Cinnamate Compounds. *J. Appl.*

Electrochem. **2004**, *34* (6), 591–599. https://doi.org/10.1023/B:JACH.0000021932.87043.7b.

(16) Suárez-Vega, A.; Agustín-Sáenz, C.; O'Dell, L. A.; Brusciotti, F.; Somers, A.; Forsyth, M. Properties of Hybrid Sol-Gel Coatings with the Incorporation of Lanthanum 4-Hydroxy Cinnamate as Corrosion Inhibitor on Carbon Steel with Different Surface Finishes. *Appl. Surf. Sci.* **2021**, *561*, 149881. https://doi.org/10.1016/j.apsusc.2021.149881.

(17) Suarez Vega, A.; Agustín-Sáenz, C.; Brusciotti, F.; Somers, A.; Forsyth, M. Effect of Lanthanum 4-Hydroxy Cinnamate on the Polymerisation, Condensation and Thermal Stability of Hybrid Sol–Gel Formulations. *J. Sol-Gel Sci. Technol.* **2020**, *96* (1), 91–107. https://doi.org/10.1007/s10971-020-05315-x.

(18) Udabe, E.; Somers, A.; Forsyth, M.; Mecerreyes, D. Design of Polymeric Corrosion Inhibitors Based on Ionic Coumarate Groups. *ACS Appl. Polym. Mater.* **2021**, *3* (4), 1739–1746. https://doi.org/10.1021/acsapm.0c01266.

(19) Udabe, E.; Forsyth, M.; Somers, A.; Mecerreyes, D. Metal-Free Coumarate Based Ionic Liquids and Poly(Ionic Liquid)s as Corrosion Inhibitors. *Mater. Adv.* **2020**, *1* (4), 584–589. https://doi.org/10.1039/d0ma00243g.

(20) Udabe, E.; Sommers, A.; Forsyth, M.; Mecerreyes, D. Cation Effect in the Corrosion Inhibition Properties of Coumarate Ionic Liquids and Acrylic UV-Coatings. *Polymers (Basel).* **2020**, *12* (11), 1–16. https://doi.org/10.3390/polym12112611.

(21) Naciri, J.; Shenoy, D. K.; Grüeneberg, K.; Shashidhar, R. Molecular Structure and Pretilt Control of Photodimerized-Monolayers (PDML). *J. Mater. Chem.* **2004**, *14* (23), 3468–3473. https://doi.org/10.1039/b403656e.

(22) Tudos, F., & Foldesberezsnich, T. Free-Radical Polymerization: Inhibition and Retardation. *Prog. Polym. Sci.* **1989**, *14* (6), 717–761.

(23) Murray, J. N. Electrochemical Test Methods for Evaluating Organic Coatings on Metals: An Update. Part III: Multiple Test Parameter Measurements. *Prog. Org.*

Coatings **1997**, *31* (4), 375–391. https://doi.org/10.1016/S0300-9440(97)00099-4.

(24) Butler, L. N.; Fellows, C. M.; Gilbert, R. G. Effect of Surfactant Systems on the Water Sensitivity of Latex Films. *J. Appl. Polym. Sci.* **2004**, *92* (3), 1813–1823. https://doi.org/10.1002/app.20150.

Chapter 3

Comparison of corrosion inhibition ability of different coumarate based compounds incorporated into waterborne binders

3.1 Introduction

In Chapter 2, the inhibitory property of the butoxy p-coumaric acid (H4) derived from p-coumaric acid was investigated as a free inhibitor in solution and when incorporated into waterborne latexes by different polymerization techniques[1]. A waterborne coating made by semibatch seeded emulsion polymerization showed promising results for corrosion mitigation, even when the inhibitor was as low as 0.15 % based on polymer. Chapter 2 also included the incorporation of H4 by dispersion polymerization in a continuous methanol/water phase, as well as its blending at the final control latex (without inhibitor), aiming a higher concentration of inhibitor into the system (3% based on polymer) but it resulted in poor coatings.

In the present chapter, a different method of inhibitor incorporation into the latex will be investigated to increase their concentration in the final coatings, while maintaining its homogenous distribution within the film. Instead of the previously used seeded semibatch emulsion polymerization technique, the latexes will be produced by batch miniemulsion polymerization, since it enables the incorporation of a higher concentration of hydrophobic inhibitors[2].

Hydrophobicity is an important factor for improving the ability of a coating to act as a barrier[3]. It was reported that polymeric films containing Dowfax 2A1 showed lower absorption of water compared to the standards anionic surfactants such as Sodium dodecyl sulfate (SDS)[4]. Therefore, Dowfax 2A1 will be used as surfactant in the polymerization reaction in order to obtain a more hydrophobic film that would be more resistant to the absorption of corrosive solutions.

H4 and three other derivatives of the p-coumaric acid (p-CA), namely methoxy p-coumaric acid (H1), trifluoromethoxy p-coumaric acid (HCF3) and p-4-ethyloxymethacrylate p-

coumaric acid (HMA) (Figure 3.1) will be investigated as free inhibitors in solution and then will be incorporated into the waterborne polymeric binder (Figure 3.1).

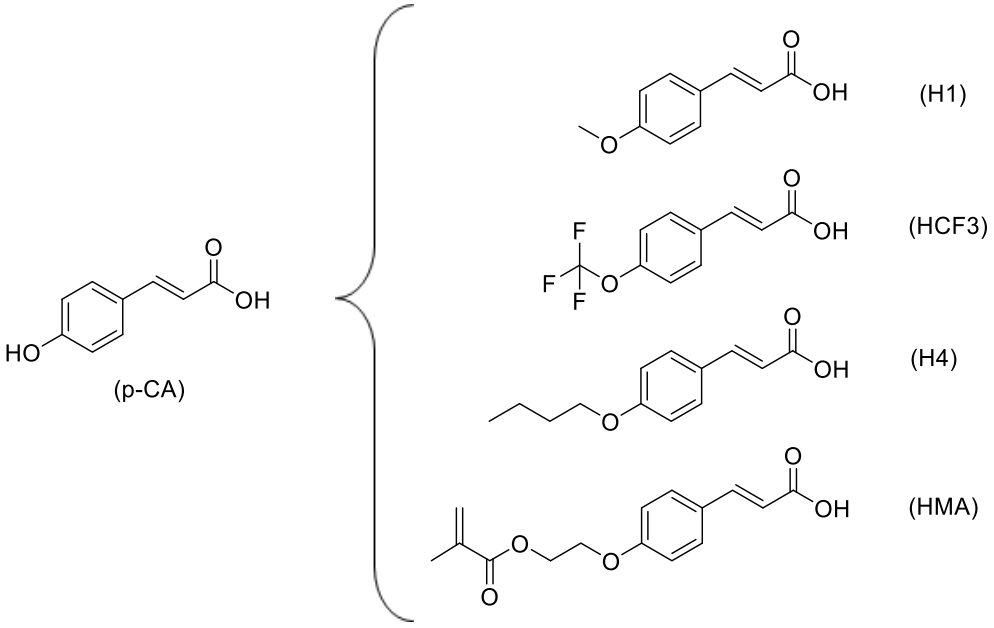

Figure 3.1. Chemical structure of anticorrosive inhibitors; p-coumaric acid (p-CA), metoxy p-coumaric acid (H1), trifluoromethoxy p-coumaric acid (HCF3), butoxy p-coumaric acid (H4), and p-4-ethyloxymethacrylate coumarate (HMA).

H1, HCF3, and H4 have been synthesized according to the technique proposed by Naciri et al.[5] (the reactions were carried out by Daniele Mantione), and the synthesis of HMA is described in the Appendix. H1, H4 and HCF3 do not react with the monomers used to produce the polymer, so they are supposed to act as additive incorporated into the binder. The methoxy (H1) and buthoxy (H4) radicals were chosen to analyze the contribution of the length of the radical, and therefore the water solubility of the inhibitor, on the corrosion protection. The use of the fluorinated radical (HCF3) was justified by the characteristics observed in fluorinated coatings such as low surface tension, non-wettability by water and oil, non-adhesive nature and antifouling

properties[6]. HMA has a methacrylate moiety that can copolymerize with the monomers of the binder, and consequently, it is supposed to be incorporated in the polymer chains. HMA was chosen to compare the differences between using an inhibitor as an additive, unattached to the polymer chain, and one incorporated in the copolymer chain. The anticorrosive properties of the intact coatings were evaluated by Electrochemical Impedance Spectroscopy (EIS). Later, the analysis was repeated on coatings with a controlled scratch in order to analyze the active protection given by the inhibitors.

The in-situ incorporation of the proposed new organic inhibitors into the binder of waterborne latexes is a novelty for the coatings research field, in contrast to reported works that uses epoxy with inorganic inhibitors[7,8]. The polymerization methodology contributes to lowering the environmental footprint through the reduction of VOCs, and the use of environmentally friend inhibitors prevent the need of P, heavy metals, or even Zn in the system.

3.2 Experimental Section

3.2.1 Incorporation of H1, H4, HCF3, and HMA into waterborne poly(MMA/BA) latex by batch miniemulsion polymerization

Miniemulsion polymerization reactions were carried out in a round bottom flask of 100 mL, immersed in a bath of ethylene glycol (Figure 3.2). The temperature was maintained at 70 °C, under agitation of 250 rpm, and N_2 atmosphere. The reactions were prepared according to the recipe described in Table 3.1. The inhibitors were initially dissolved/dispersed into the monomers (organic phase). Then, the phases were mixed and agitated for 10 minutes. The mixture was utrasonicated using a Branson Ultrasonics Sonifier 450 for 5 minutes (operating at 1-output control and 80% duty cycle in an ice bath and under magnetic stirring of 300 rpm), and

placed in the round bottom flask. The solution was continuously agitated and fed with N_2 for 15 minutes before the addition of the initiator solution. Latexes were produced with the concentration of 4 mg inhibitor/g latex (1 g inhibitor/100 g monomer), and a control latex, with no inhibitor, was prepared for comparison purposes. A latex containing simultaneously 1 % H1 (non-reactive inhibitor) and 1% HMA (reactive inhibitor) was also synthesized in other to analyze if the incorporation of those inhibitors together in a latex would result in a coating with synergistic protection. The final latexes have a solids content of 40 %.

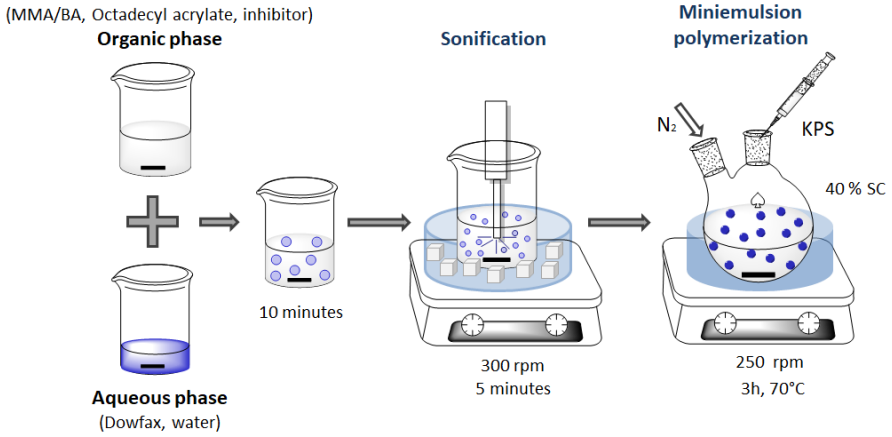

Figure 3.2. Schematic representation of miniemulsion polymerization of poly(MMA/BA).

Table 3.1. Recipe of miniemulsion polymerization latexes with 40% solids content

	Components	Mass (g)
Organic phase	MMA	10
	BA	10
	Octadecyl Acrylate	0.8
	Inhibitor (1 wbm%)	0.2
Aquous phase	Dowfax 2A1 (solution 45%)	0.88
	H_2O	25
Solution of initiator	KPS	0.2
	H_2O	5.0

3.2.2 Leaching tests

Leaching tests were performed in order to analyze the release of the additive inhibitors from the coatings to the aqueous media. Initially, calibration curves of the inhibitors dissolved in water were constructed using ultraviolet spectroscopy (UV 2550, Shimadzu). Then, free films of known weight were immersed in closed vials with 5 mL of MiliQ water. After 1, 5, and 24 hours, the vials ware opened and the aqueous media was analyzed by UV. Using the data obtained from the calibration curve, the concentration of inhibitor leached was calculated.

3.2.3 Preparation of steel substrates and EIS of coatings

The procedure of preparation of the metallic substrates and the details used for measurement of the EIS of the coatings are explained in section 2.2.6 of Chapter 2.

3.3 Results and Discussion

3.3.1 Analysis of inhibitors in solution and polymerization kinetics

Firstly, electrochemical analysis of p-CA, H1, H4, HCF3, and HMA as metal free inhibitors (in solution) were performed using the same system and parameters reported in section 2.3.3 of Chapter 2 (Figure 3.3). 0.3 mM of the inhibitor was dissolved in the corrosive solution of 0.01M NaCl. Ethanol was added to enhance the solubility of the inhibitor, and the solution was heated for 2 hours at low temperature to evaporate the ethanol. This concentration was chosen as it is approximately the maximum solubility/dispensability of H4 in the monomers MMA/BA (50 % / 50 %) used for the polymerizations. For comparison purposes, a control experiment with no inhibitor was also carried out. Tests were performed at least in duplicate.

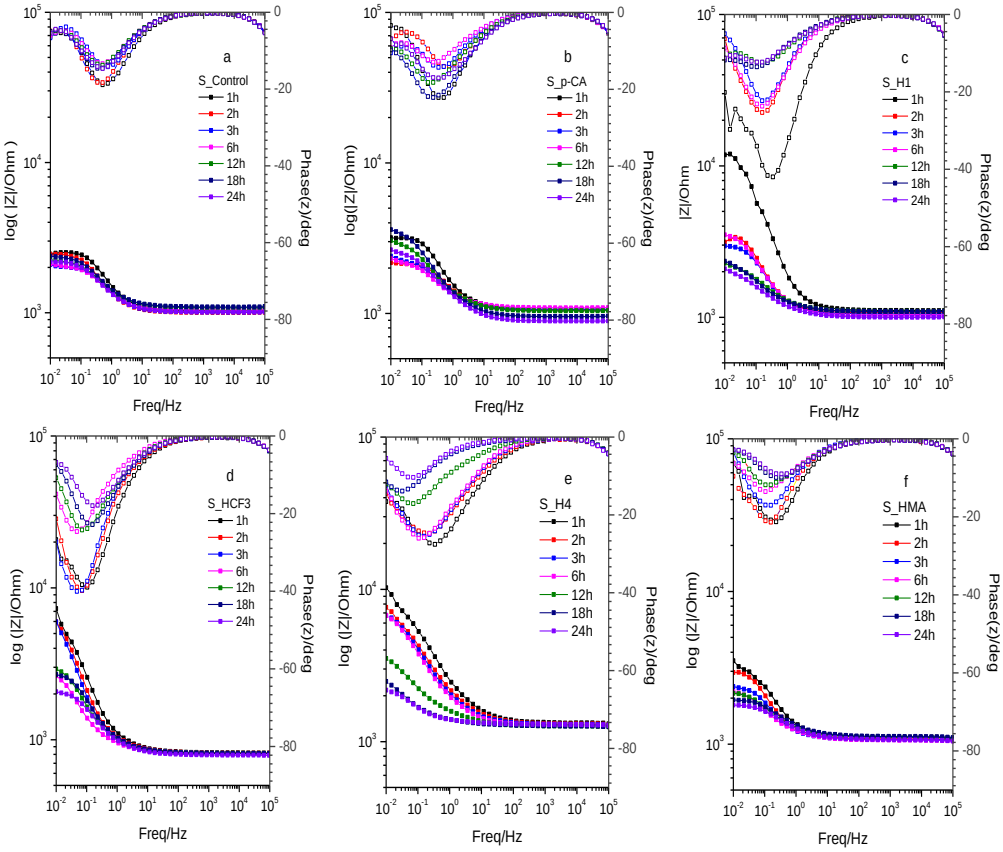

Figure 3.3. Electrochemical impedance spectra of solutions; a) control, b) p-CA, c) H1, d) HCF3, e) H4, and f) HMA, for 24 hours.

All of the studied molecules were able to provide protection to the system for the first hours of experiment, indicating anticorrosive properties. The molecules of the inhibitors dispersed in the corrosive solution were expected to migrate from the bulk of the solution to adsorb onto the steel surface, forming a protective layer. As seen in Figures 3.3 a-f, H1, H4 and HCF3 inhibitors seem to be promising. They show higher impedances in the first hours of experiment when compared to the control experiment without inhibitor or to the p-CA solution. However, they are unable to maintain the protection for the whole 24 hours of experiment, likely

due to the low concentration used compared to the corrosive species. The relatively poor performance of HMA in comparison to the other inhibitors may be due to its long chain that makes its diffusion through the solution more difficult and so the replacement of molecules initially absorbed on the surface is slower.

Whilst these results in solution may suggest that these inhibitors are not suitable for addition in an open solution environment for long term protection, their behaviour in the initial stages still warrants their investigation in an environment such as in a coating where their incorporation can have a positive effect on the metal coating interface and the exposed metal area requiring protection is significantly decreased. Therefore, all inhibitors were incorporated in the waterborne binders and their anticorrosion properties were tested.

Batch miniemulsion polymerization reactions were successfully performed and full conversion was reached after 2 hours of reaction (Figure 3.4 a) with a final particle size of 110-130 nm (Figure 3.4 b) for the latexes containing the different coumarate inhibitors and without inhibitor (Control latex). Conversion and particle size were measured as reported in Chapter 2 (2.2.6.1 and 2.2.6.2, respectively). Coagulum was not observed in the reactions, confirming that the inhibitors were incorporated into the latex particles. The reaction with H4 is initially retarded when compared to the others, probably due to the properties of the molecule, as previously observed in the bulk radical polymerization of MMA/BA in the presence of H4[1]. Therefore, by miniemulsion polymerization, 1 wbm % of the different inhibitors based on total polymer were incorporated in the latexes.

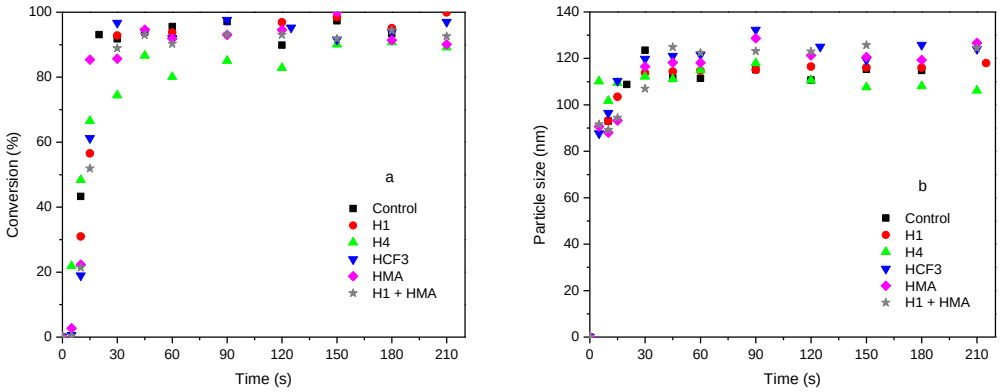

Figure 3.4. a) Kinetics of batch miniemulsion polymerization reactions; b) Particles size over time of reaction.

3.3.2 Leaching tests

Tests were performed to better understand the leaching of the additive inhibitors from the coatings when exposed to an aqueous media. Initially the tests were performed on the free films of the studied latexes made by miniemulsion polymerization. However, the inhibitors were not able to be detected by UV because the signals of the aromatic ring of the surfactant present in the films, Dowfax 2A1, mask the inhibitors signal. Therefore, the leaching tests were performed using the free films formed from latexes with inhibitors blended in a latex synthesized by dispersion polymerization with a surfactant that does not have aromatic rings, Visiomer MPEG 2005[1]. The concentration of inhibitor in the blend was 3% g inhibitor/monomer weight. The percentage of leaching of the additive inhibitors after 1, 5, and 24 hours in contact with water (pH 7) is shown in Figure 3.5. As expected, the leaching of the additive inhibitors in water is dependent of the solubility on the molecules in the media (H1>HCF3>H4).

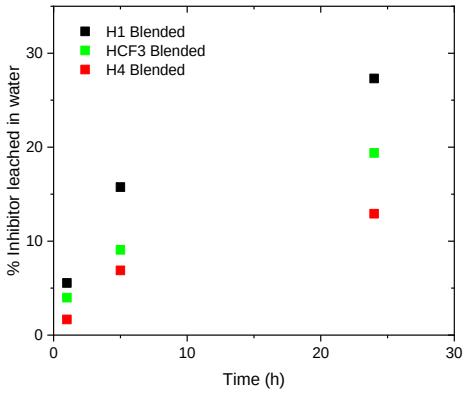

Figure 3.5. Percentage of leaching of additive inhibitors blended, from free films of dispersion polymerizations.

3.3.3 Electrochemical impedance spectroscopy of intact coatings and coatings with a controlled defect

The latexes prepared by miniemulsion polymerization were cast onto mild steel surfaces and the corrosion protection properties of the coatings were measured by EIS during immersion in 0.005 M NaCl over 24 hours. The spectra for bare steel in Figure 3.6 shows the maximum impedance of $10^{3.5}$ Ω and phase angles of 28 degrees. However, when the steel is covered with the poly(MMA/BA) latex coating, the system shows much higher impedances and phase angles that are relatively stable over 24 hours. The Control coating displayed maximum impedance of $10^{5.2}$ Ω and phase angle of 66° at high frequencies (Figure 3.6 b), indicating that the Control coating has an effective barrier protection[9]. The coatings with the inhibitors incorporated showed considerably better performances when compared to the Control latex.

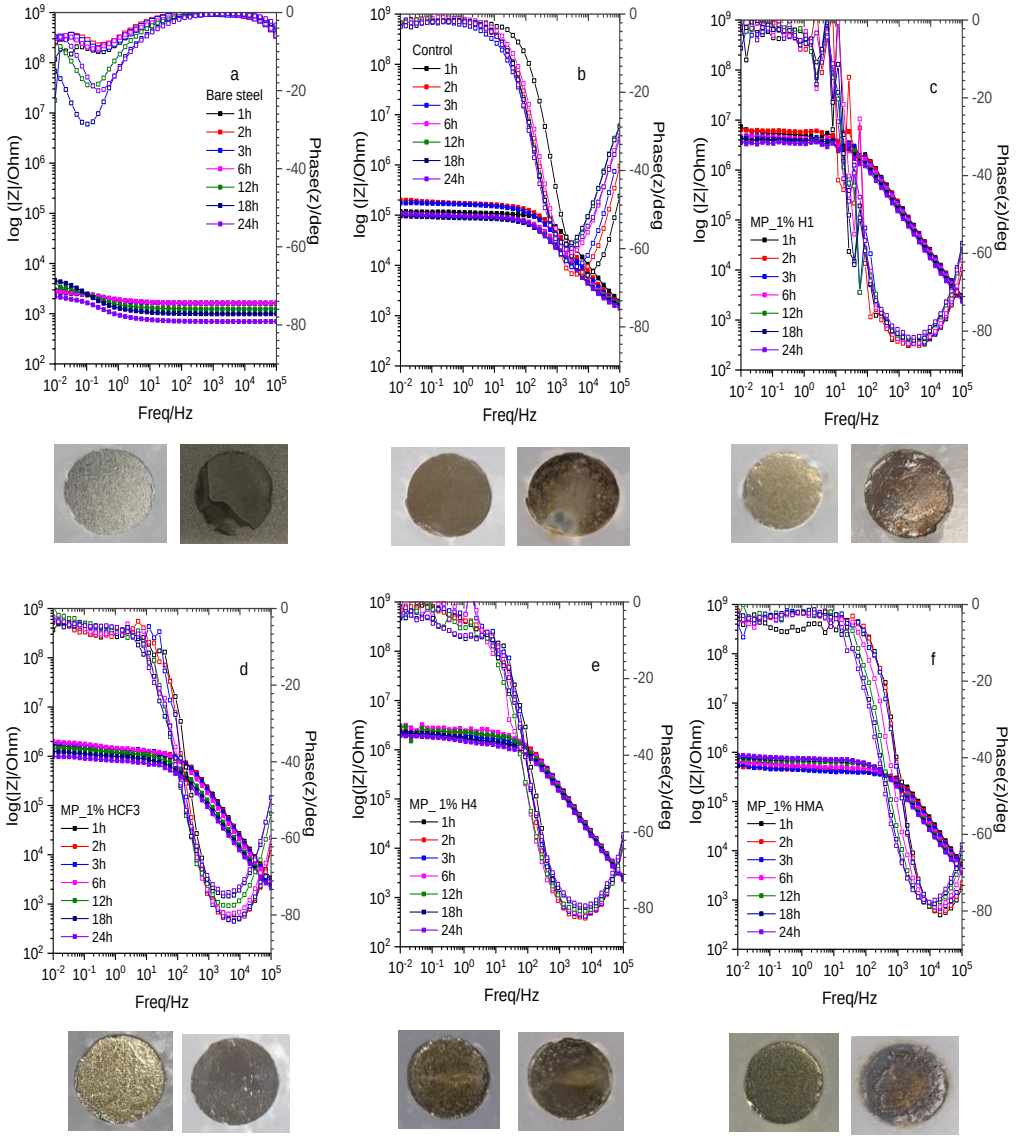

Figure 3.6. Electrochemical impedance spectra of bare steel and of coatings made by miniemulsion polymerization followed by optical images of the samples before (on the left) and after immersion in 0.005M NaCl (on the right). a) Bare steel; b) Control coating; c) Coating with 1% of H1, d) Coating with 1% of HCF3, e) Coating with 1% of H4, f) Coating with 1% of HMA.

The highest impedance is seen in the coating with H1 incorporated (Figure 3.6.c), with maximum impedance, $10^{6.7}$ Ω and phase angles of 84 degrees. The phase angle approaches 90 degrees, indicating a highly capacitive coating. The coating with HCF3 obtained the maximum impedance of $10^{6.2}$ Ω and phase angle of 82 degrees (Figure 3.6 d) and the one with H4 incorporated of $10^{6.3}$ Ω and phase angle of 82 degress (Figure 3.6.e). In comparison to a similar latex previously reported[1] in chapter 2, in which only 1.5 mg of H4/g latex (0.3 g of H4 / 100 g of monomer) could be incorporated by semi batch emulsion, the coating reported here has improved stability. While not showing as high an initial impedance, the coating reported here maintained an impedance around $10^{6.1}$ Ω and a phase angle around 80 degrees. For the previously reported coating the impedance reduced from $10^{6.7}$ to $10^{6.0}$ Ω and the phase angle from 80 to 65 degrees over 24 hours. This confirms that a higher concentration of inhibitor and the use of the more hydrophobic Dowfax 2A1 surfactant contributes to obtain better properties in the final coating. Finally, the coating obtained with a co-monomer inhibitor, HMA, showed impedances in the range of $10^{5.5}$ to $10^{5.9}$ Ω and phase angles of 78 - 82 degrees (Figure 3.6 f). Therefore, it was confirmed that the inhibitors were able to give extra anticorrosive protection to the systems when incorporated into this latex coating.

It seems that in the intact coatings, the performance of the additive inhibitors is directly related to their solubility in the media. As H1 is the most hydrophilic, it can easily diffuse from the coating to the metallic surface as the electrolyte solution moves through, giving better protection to the system when compared to HCF3 and H4. In the case of HMA, besides it low solubility in water, the molecule is attached to the polymeric chains of the binder, which prevents the molecules from diffusing and reaching the metallic surface easily.

To test the active protection of these inhibited coating systems, a scratch was made to the coatings applied on the steel, and EIS measurements were carried out over 24 hours in 0.005 M NaCl. The Bode spectra of the coatings with a scratch are presented in Figure 3.7. The impedance of the Control coating (Figure 3.7 a) drops from ≈ $10^{4.6}$ to $10^{4.1}$ Ω after the 24 hours of experiment meanwhile the impedances of the coatings with H1, HCF3, and H4 (Figure 3.7 b, c and d) only drop from ≈ $10^{4.6}$ to $10^{4.2}$ Ω. This is an indication that the additive inhibitors can be modestly released from the coating and provide protection to the exposed metallic surface. The scratched coating with HMA showed the best result, as the impedance after 24 hours was ≈$10^{4.3}$ Ω. In this case, as HMA is attached to the polymer it is not washed out of the area, therefore a better performance is observed when compared to the coatings with the more leachable inhibitors.

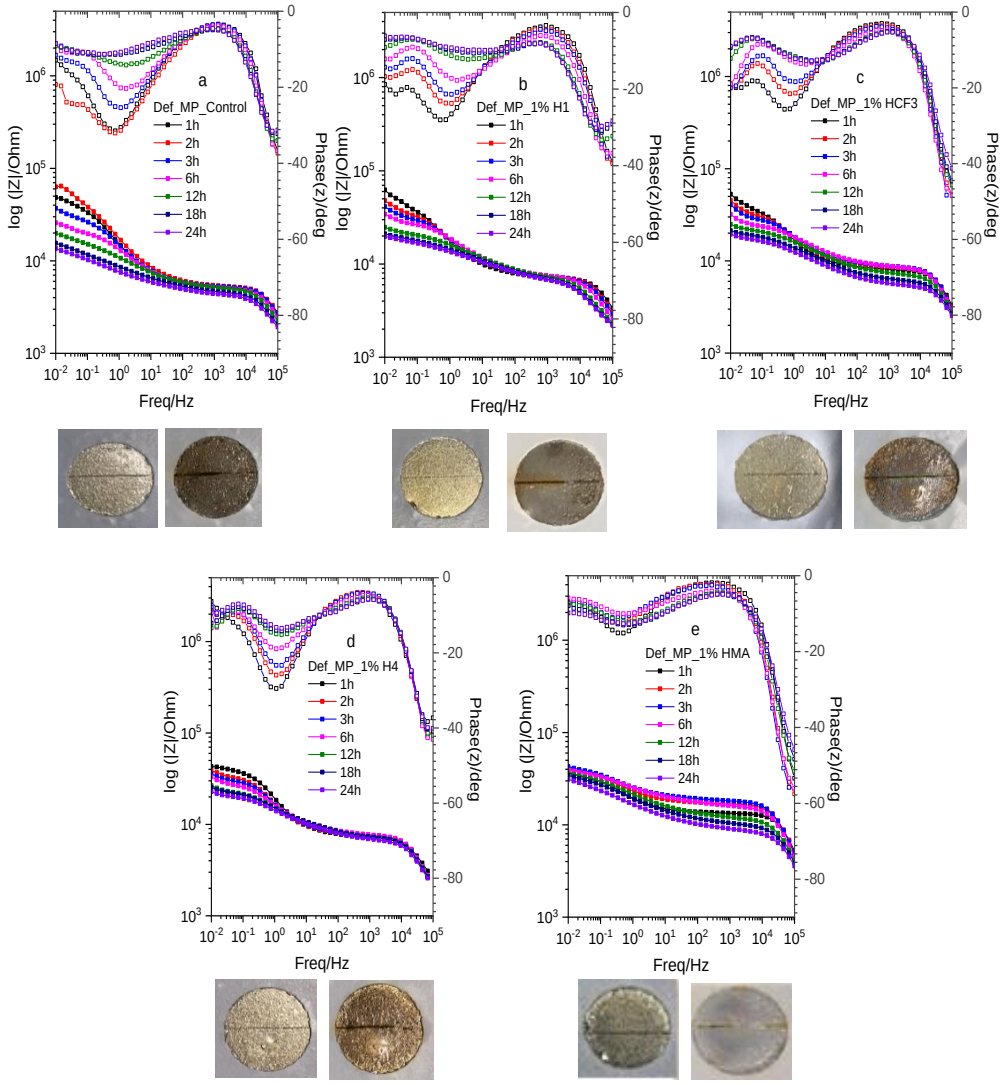

Figure 3.7. Electrochemical impedance spectra coatings with a controlled scratch followed by optical images of the samples before (on the left) and after the experiment (on the right). a) Control coating; b) Coating with 1% of H1, c) Coating with 1% of HCF3, d) Coating with 1% of H4, e) Coating with 1% of HMA.

Finally, in an attempt to combine the properties of the coating with H1 (non-reactive) that showed the highest impedances between the additive inhibitors and the properties of the

coating with HMA (reactive), that was able to maintain the impedance of the system with a controlled defect, a latex with 1% of H1 and 1% of HMA was also produced. The EIS obtained for the intact coating and for the coating with a controlled defect is shown in Figure 3.8.

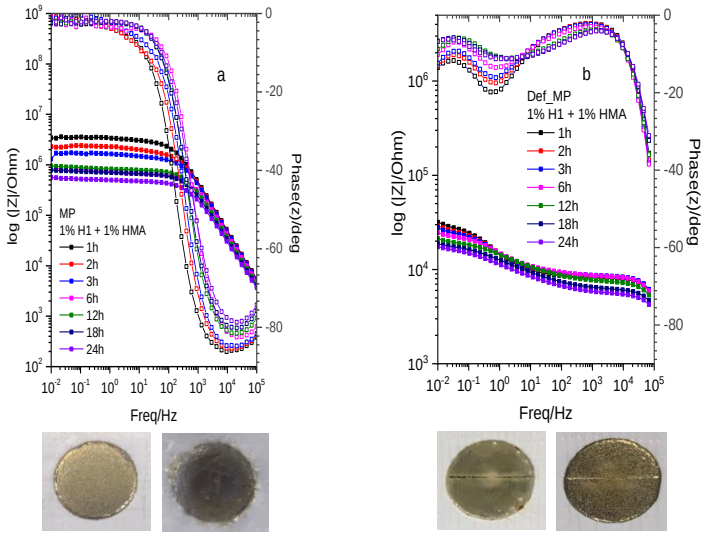

Figure 3.8. Electrochemical impedance spectra the coatings with 1% H1 and 1% HMA incorporated, a) intact coating, and b) coating with a controlled defect.

Initially, the properties of the intact coating with 1 % H1 and 1 % HMA (Figure 3.8 a) are similar to the one with H1 only (≈$10^{6.3}$ Ω, and 86 degrees), but with time, the impedance drops to values that are similar to those found in the coating with HMA (≈$10^{5.6}$ Ω, 78 degrees). Correspondingly, the defect coating with 1 % H1 and 1 % HMA seems to have intermediary properties between the coatings with H1 and the one with HMA. As both inhibitors act by adsorbing on the metallic surface, some competition may be occurring between them, causing the final properties of the coating to be less stable than the ones obtained when each of them was incorporated separately.

Whilst the low frequency impedance data is usually considered an important parameter to assess coating performance, careful observation of the full frequency spectra shows some significant differences in the intermediate frequency regions and thus a more quantitive analysis is warranted for these spectra. A typical equivalent circuit (EC) for representing coated metals (Figure 3.9) was used to fit the EIS spectra of the proposed coatings[9–11]. R_s represents the solution resistance, C_{coat} is the coating capacitance, R_{pore} is the resistance in the pores of the coating, C_{dl} represents the double layer capacitance at the interface, R_{ct} is the charge transfer resistance at the interface, and n_{coat} and n_{dl} characterize the capacitance behavior of C_{coat}/C_{dl} as it approaches 1. The fitting results for the samples after 1, 12, and 24 hours of experiment are shown in the Table 3.2.

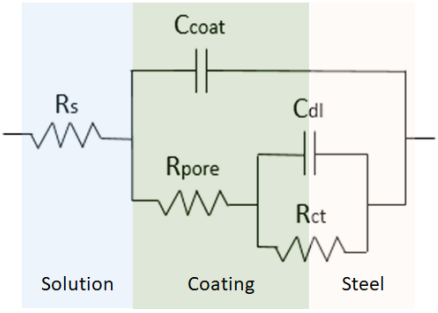

Figure 3.9. Equivalent circuit models used to fit EIS of the coatings.

The values of C_{coat}, obtained from the fit of the equivalent circuit (Figure 3.9), for the bare steel, are generally lower when compared to the values obtained for the intact control coatings. Of significance is that, in all of the intact coated systems, the values of R_{pore} were typically higher in the samples containing inhibitors than in the respective control, suggesting that the inhibitors are able to give additional protection to the systems by physisorption and chemisorption interactions with the metallic surface. Amongst all intact coating samples, lower C_{dl} values were obtained when the inhibitors are incorporated, which would indicate the

protection of the metal surface by the inhibitors, since a lower C_{dl} is typically associated with a less corroded surface (lower surface area)[12]. Therefore, the presence of inhibitors seems to contribute to a restricted motion of water/ions through the coating towards the metallic surface. Lower values of C_{dl} are also observed amongst the samples with inhibitors, where a scratch is present, when compared to the control sample.

As expected, from the low frequency impedance data, the values obtained for the charge transfer resistance at the interface of the system (R_{ct}) was considerably lower in the scratched samples when compared to the intact coatings, since part of the metallic surface is exposed. However, even though there is some scatter, the data continue to show a typically higher R_{ct}, higher pore resistance, and a lower C_{dl}, when the inhibitors are incorporated in the coating even after 24h exposure. This is in contrast to the un-inhibited sample, which shows a decreases in R_{ct} and pore resistance, in addition to increasing C_{dl} in the presence of a scratch defect. The scratched sample with HMA incorporated was the one with the highest values of R_{pore}, confirming better corrosion protection. It is also observed that only in the sample with HMA, R_{ct} increases with time, suggesting active protection in the system. The values obtained for the equivalent circuit elements of the scratched samples are consistent with the increased corrosion observed over time, in the experiments.

Table 3.2. Fitting results for intact and scratched coatings

	Sample	Time (h)	R_s (kΩ)	C_{coat} (nF.s^{n-1})	n_{coat}	R_{pore} (kΩ)	C_{dl} (μF.s^{n-1})	n_{dl}	R_{ct} (kΩ)	χ^2//Z/
	Bare steel	1	0.34	0.55	0.91	1.29	684500	0.67	1.34	0.00
		12	0.40	0.57	0.92	0.84	718500	0.65	3.04	0.00
		24	0.54	0.30	0.62	0.17	807500	0.65	1.83	0.01
Intact Coating	Control	1	1.09	6.73	0.87	6.17	438	0.35	98.15	0.01
		12	1.25	22.51	0.83	12.48	5511	0.89	76.98	0.01
		24	1.24	35.97	0.81	96.34	30120	1.00	1.72	0.11
	H1	1	1.09	1.24	0.94	487.78	0.10	0.12	9621	1.01
		12	1.32	1.55	0.94	114.86	0.00	0.48	3383	0.01
		24	1.04	2.14	0.93	1957	0.02	0.53	1559	0.34
	HCF3	1	1.33	1.13	0.94	975.20	1.33	0.46	885.20	0.03
		12	1.12	3.09	0.90	809.81	0.66	0.31	792.84	0.02
		24	1.42	3.48	0.91	143.40	0.04	0.46	727.90	0.04
	H4	1	0.93	1.14	0.96	1101	0.00	0.45	581.60	0.03
		12	1.09	1.67	0.93	144.84	0.04	0.27	2563	0.01
		24	1.14	2.06	0.93	367.83	0.01	0.46	996.55	0.02
	HMA	1	1.13	0.50	0.96	385.23	2.33	0.43	296.87	0.03
		12	1.30	1.22	0.92	19.57	0.02	0.33	632.33	0.01
		24	1.13	1.49	0.92	38.46	0.20	0.29	487.71	0.00
	H1/HMA	1	1.24	0.42	0.97	2472	0.02	0.67	803.18	0.03
		12	0.62	0.44	0.99	45.19	0.00	0.70	730.00	0.00
		24	0.58	0.99	0.94	13.30	0.01	0.47	478.02	0.00
Scratched Coatings	Control	1	0.89	3.74	0.86	4.33	24.65	0.61	50.04	0.02
		12	0.90	4.24	0.87	3.80	55.80	0.39	19.42	0.01
		24	1.07	4.17	0.91	2.95	116	0.32	16.66	0.00
	H1	1	1.03	1.32	0.93	6.86	34.28	0.52	60.76	0.06
		12	0.96	1.47	0.94	5.97	21.92	0.45	16.22	0.00
		24	0.96	1.57	0.94	4.31	32.44	0.44	14.72	0.00
	HCF3	1	1.15	1.96	0.90	5.86	29.86	0.51	77.27	0.04
		12	1.27	12.65	0.82	5.48	21.94	0.44	15.37	0.00
		24	1.35	23.61	0.79	5.17	22.02	0.46	9.71	0.01
	H4	1	0.83	10.75	0.79	6.57	18.58	0.66	47.22	0.00
		12	0.91	3.31	0.88	6.29	26.59	0.48	20.96	0.00
		24	1.07	2.68	0.90	5.51	28.93	0.44	18.46	0.01
	HMA	1	0.69	0.84	0.92	12.77	36.11	0.61	24.30	0.00
		12	0.77	1.42	0.90	10.62	32.79	0.39	32.56	0.00
		24	0.84	1.77	0.90	7.40	46.47	0.34	36.59	0.00
	H1/HMA	1	0.89	0.31	0.99	7.15	39.83	0.55	31.59	0.00
		12	1.03	0.49	0.98	6.14	36.98	0.41	15.93	0.00
		24	0.81	0.40	1.00	4.43	49.69	0.37	14.73	0.00

3.4 Conclusions

The p-coumaric derivative inhibitor compounds H1, HCF3, H4 and HMA were successfully incorporated into waterborne polymeric binders using batch miniemulsion polymerization at loadings of 4 mg inhibitor/g latex (1 g inhibitor/100 g monomer) and significant improvement was observed relative to an un-inhibited coating. EIS analyses were used to determine the corrosion protective properties of the films produced. Even though the control latex itself provided good barrier protection to the steel surface ($10^{5.2}$ Ω and 66 degrees), when the inhibitors were incorporated into the formulation, better performances were achieved in all cases. The coating with H4 incorporated showed impedances in the range of $10^{6.2}$ to $10^{6.3}$ Ω and phase angles of 80-82 degrees, considerably more stable than the ones obtained in the previous chapter in which 1.5 mg H4/g latex was incorporated by semi batch emulsion incorporation (≈10^{6} to $10^{6.7}$ Ω and phases angles of 65 to 80 degrees). This is an indication that a higher concentration of inhibitor provides better protection. However, the optimal concentration of inhibitor inside a coating is still under investigation.

Between the intact coatings studied, the one with H1 incorporated showed the highest impedances and phase angles ($10^{6.7}$Ω and 84°, respectively), which approaches capacitive behavior. The better performance of H1 when incorporated into the coating is probably due to its higher solubility in the media, which means that the molecule is able to efficiently migrate from the bulk of the coating to the metallic surface. In order to test the active protection of the systems, electrochemical analysis was also performed on the coatings, with a controlled scratch. All inhibitors provided an improvement in pore resistance and also lower corrosion as indicated by the C_{dl} values over 24 hours. The charge transfer resistance also remained higher over the 24 hours period compared to the control coating. The best results were obtained for the coating with

HMA incorporated. Its impedance was maintained at ≈$10^{4.3}$ Ω, for the 24 hours of experiment while for the control scratched sample the impedance droped from ≈ $10^{4.6}$ to $10^{4.1}$ Ω. This suggests that there is a benefit in bonding an inhibiting molecule into the polymer structure during the polymerization process. Unfortunately, our preliminary attempt to combine this polymerizing approach (HMA) together with the incorporation of a non reactive, leachable molecule (H1) to achieve synergistic protection was not successful. In the next chapter, an attempt of producing coatings with enhanced barrier properties and active inhibition by the incorporation of a polymerizable surfactant and a corrosion inhibitor will be investigated.

3.5 References

(1) Quites, D.; Leiza, J. R.; Mantione, D.; Somers, A.; Forsyth, M.; Paulis, M. Macromolecular Materials and Engineering Incorporation of a Coumarate Based Corrosion Inhibitor in Waterborne Polymeric Binders for Corrosion Protection Applications. *Macromol. Mater. Eng.* **2022**, *307*, 2100772. https://doi.org/https://doi.org/10.1002/mame.202100772.

(2) Asua, J. M. Miniemulsion Polymerization. *Prog. Polym. Sci.* **2002**, *27* (7), 1283–1346. https://doi.org/10.1016/S0079-6700(02)00010-2.

(3) Wan, H.; Song, D.; Li, X.; Zhang, D.; Gao, J.; Du, C. A New Understanding of the Failure of Waterborne Acrylic Coatings. *RSC Adv.* **2017**, *7* (61), 38135–38148. https://doi.org/10.1039/c7ra04878e.

(4) Aguirreurreta, Z.; de la Cal, J. C.; Leiza, J. R. Preparation of High Solids Content Waterborne Acrylic Coatings Using Polymerizable Surfactants to Improve Water Sensitivity. *Prog. Org. Coatings* **2017**, *112*, 200–209. https://doi.org/10.1016/j.porgcoat.2017.06.028.

(5) Naciri, J.; Shenoy, D. K.; Grüeneberg, K.; Shashidhar, R. Molecular Structure and Pretilt Control of Photodimerized-Monolayers (PDML). *J. Mater. Chem.* **2004**, *14* (23),

3468–3473. https://doi.org/10.1039/b403656e.

(6) Malshe, V. C.; Sangaj, N. S. Fluorinated Acrylic Copolymers: Part I: Study of Clear Coatings. *Prog. Org. Coatings* **2005**, *53* (3), 207–211. https://doi.org/10.1016/j.porgcoat.2005.03.003.

(7) Razizadeh, M.; Mahdavian, M.; Ramezanzadeh, B.; Alibakhshi, E.; Jamali, S. Synthesis of Hybrid Organic–Inorganic Inhibitive Pigment Based on Basil Extract and Zinc Cation for Application in Protective Construction Coatings. *Constr. Build. Mater.* **2021**, *287*, 123034. https://doi.org/10.1016/j.conbuildmat.2021.123034.

(8) Haddadi, S. A.; Alibakhshi, E.; Labani Motlagh, A.; Ramazani S.A., A.; Ghaderi, M.; Ramezanzadeh, B.; Mahdavian, M.; Arjmand, M. Synthesis of Methyltriethoxysilane-Modified Calcium Zinc Phosphate Nanopigments toward Epoxy Nanocomposite Coatings: Exploring Rheological, Mechanical, and Anti-Corrosion Properties. *Prog. Org. Coatings* **2022**, *171* (August), 107055. https://doi.org/10.1016/j.porgcoat.2022.107055.

(9) Murray, J. N. Electrochemical Test Methods for Evaluating Organic Coatings on Metals: An Update. Part III: Multiple Test Parameter Measurements. *Prog. Org. Coatings* **1997**, *31* (4), 375–391. https://doi.org/10.1016/S0300-9440(97)00099-4.

(10) Thomas, N. L. The Barrier Properties of Paint Coatings. *Prog. Org. Coatings* **1991**, *19* (2), 101–121. https://doi.org/10.1016/0033-0655(91)80001-Y.

(11) Peng, Y.; Hughes, A. E.; Deacon, G. B.; Junk, P. C.; Hinton, B. R. W.; Forsyth, M.; Mardel, J. I.; Somers, A. E. A Study of Rare-Earth 3-(4-Methylbenzoyl)-Propanoate Compounds as Corrosion Inhibitors for AS1020 Mild Steel in NaCl Solutions. *Corros. Sci.* **2018**, *145*, 199–211. https://doi.org/10.1016/j.corsci.2018.09.022.

(12) Loveday, D.; Peterson, P.; Rodgers, B. Evaluation of Organic Coatings with Electrochemical Impedance Spectroscopy: Part 1: Fundamentals of Electrochemical Impedance Spectroscopy. *CoatingsTech* **2004**, *1* (8), 46–52.

Chapter 4

Development of waterborne anticorrosive coatings by the incorporation of coumarate based corrosion inhibitors and phosphate functionalization

4.1 Introduction

As mentioned in the previous chapters, one of the best ways to protect mild steel from corrosion is the use of protective coatings, being waterborne coatings a more appealing choice due to their low toxicity when compared to conventional solvent based coatings. Surfactants are crucial for the production of waterborne coatings since they are responsible for the stability of the particles of the latex[1–3]. However, the presence of surfactants in the final polymeric film can be the source of problems such as the formation of hydrophilic pathways[4], creation of small pockets, aggregation through the formed film, or migration toward the film-air or film-substrate interface [5–7]. Migration of surfactant may adversely affect different properties of the final polymeric film such as adhesion, shear, and peel strength[8,9], as well as water resistance[1,8,9], and gloss impairment[9].

An alternative to the use of conventional surfactants that can avoid their negative effects is the use of reactive surfactants in the formulation[3,10,11]. The use of polymerizable surfactants, frequently referred as surfmers[3,12], has attracted special attention in the last few years[11,13]. A promising surfactant for the field of corrosion protection is Sipomer® PAM-200. The methacrylic function present in its structure allows the co-polymerization of this surfactant into the polymeric backbone while the hydrophilic part, represented by the phosphate group, provides efficient stabilization of the aqueous dispersion (Figure 4.1 a).

Recently, good corrosion resistance was found in waterborne (meth)acrylic films with phosphate functionality, achieved by using a phosphate polymerizable surfactant, Sipomer® PAM-200[14–18]. Excellent properties were obtained when the latex was dried under a slow drying rate with controlled conditions of temperature and relative humidity (23 °C, RH = 60 %)[16]. Besides the formation of more homogeneous films, lower drying rates allow the interaction of the

phosphate groups of the surfactant with the hydroxyl groups of the surface of the steel, producing a thin iron phosphate passive layer at the coating/metal interface, covalently bonded to the polymeric film[16] (Figure 4.1 b). Therefore, the phosphate functionalization of waterborne binders seems to be a promising strategy for reducing the water sensitivity of the final film and also increasing its barrier property due to the formation of the phosphate layer on the substrate.

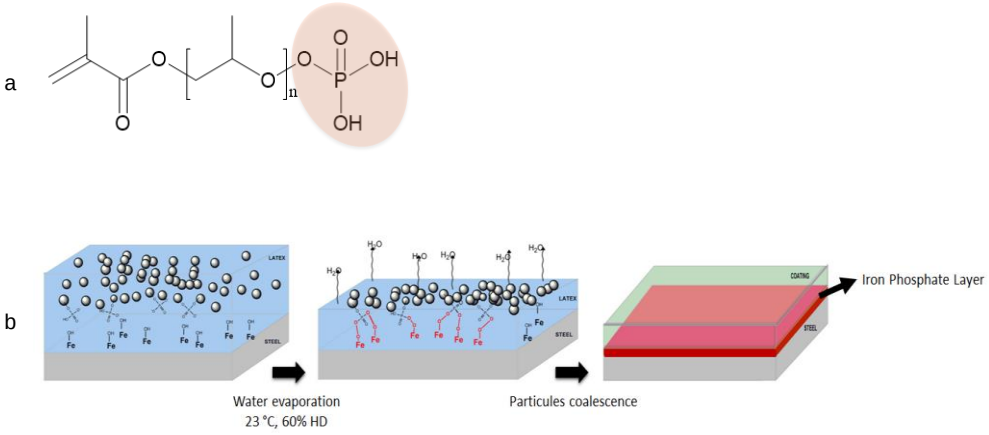

Figure 4.1. a) Chemical structure of Sipomer® PAM-200 (SIP), and b) representation of the in-situ phosphate layer formed with the polymeric film (adapted from ref[16]).

In Chapter 3, p-coumaric based inhibitors were incorporated into waterborne polymeric binders by batch miniemulsion polymerization in the concentration of 1 g inhibitor/100 g monomer. The barrier corrosion protection of the coatings produced from these hybrid latexes was analyzed by Electrochemical Impedance Spectroscopy (EIS) of intact and scratched coated steel substrates. Between the intact coatings, the one with methoxy p-coumaric acid (H1) incorporated, showed the highest impedances and phase angles ($10^{6.3}$ to $10^{6.7}$ Ω and 82-84

degrees, respectively), which approaches the capacitive behavior, and mild active corrosion protection was also observed in the scratched coatings.

Therefore, and in order to further improve the barrier properties of the coating with H1 inhibitor, the particles of the latex containing H1 were further functionalized by the incorporation of Sipomer® PAM-200 (SIP) by semibatch emulsion polymerization. The final latex with Sipomer® and H1 in its composition would ideally have higher barrier properties due to the combination of both components, and the active protection provided by H1 in case of the presence of a defect in the coating can be expected too. For practical reasons, in this chapter the latex with H1 incorporated, synthesized in Chapter 3 will be named Mp_H1. The control latex, with no inhibitor synthesized in Chapter 3 (Mp_Control) was also functionalized, for comparison purposes. The films formed from the new latex with phosphate functionality were cast on metal substrates and dried at two different conditions; 1) under non controlled room temperature conditions, and 2) under controlled conditions of T= 23 ºC and RH = 60 %. The coating corrosion protection ability was analyzed by EIS for both an intact coating and when a controlled scratch was made.

4.2 Experimental Section

4.2.1 Synthesis of phosphated poly (MMA/BA) waterborne latex by semibatch emulsion polymerization

Semibatch emulsion polymerization reactions were carried out to functionalize with phosphate moieties the latexes containing H1 inhibitor, previously synthesized by batch miniemulsion polymerization (Chapter 3). Reactions were carried out in a 100 mL round bottom flask immersed in a bath of ethylene glycol. The temperature was maintained at 70 °C, under

agitation of 250 rpm, and N_2 atmosphere. The reactions were prepared according to the scheme shown in Figure 4.2 and the recipe described in Table 4.1. Initially, the seed (Mp_Control or Mp_H1), synthesized in Chapter 3, was loaded in the round bottom flask. A buffer ($NaHCO_3$) was added to the seed to control the pH. The seed was continuously agitated and fed with N_2 for 15 minutes before the addition of the solution of initiator. A pre-emulsion composed of Sipomer® PAM-200 (SIP), monomer, and water was prepared and its pH was adjusted with drops of NH_4OH to be around 7. A pump was used for feeding this pre-emulsion into the round bottom flask at the rate of 0.157 mL/min during 3 hours. For maintaining the homogeneity of the pre-emulsion, it was continuously agitated on a stirring plate during the whole experiment. Two latexes with 40% solids content were produced at the end, one containing just phosphate functionality (Ep_SIP) and the second one containing H1 and phosphate functionality (Ep_H1_SIP). Ep_SIP latex had 5.3 mg of SIP/g latex (13.3 mg of SIP/g of polymer), and Ep_H1_SIP had 1.3 mg of H1/g latex (3.3 mg of H1/g polymer), and had 5.3 mg of SIP/g latex (13.3 mg of SIP/g of polymer).

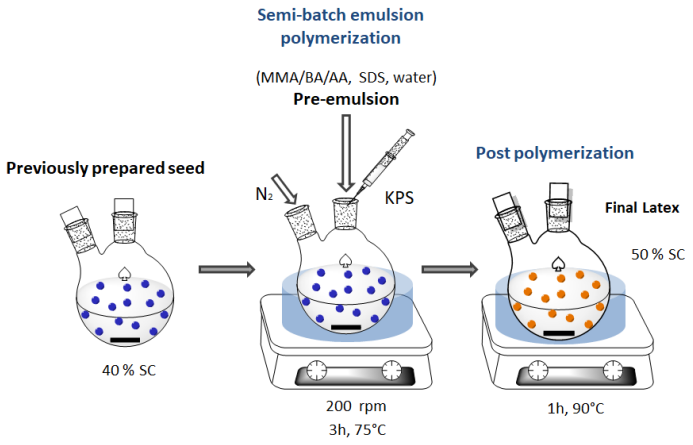

Figure 4.2. Synthesis of latexes containing H1 and phosphate functionalities by semibatch emulsion polymerization.

Table 4.1. Recipe of phosphated poly (MMA/BA) waterborne latex.

	Reactive	Initial load (g)	Stream (g)
Seed	Mp_Control / Mp_H1	15	-
	$NaHCO_3$	0.014	-
Pre-emulsion	MMA	-	6
	BA	-	6
	Sipomer® PAM-200 (SIP)	-	0.24
	H_2O	-	16
	NH_4OH	-	drops**
Solution of initiator		KPS	0.12
		H2O	2
Feed rate		0.157 mL/min	

**minimum quantity necessary for adjusting the solution to pH 7

A representation of the polymeric particles obtained by the polymerization reactions is represented in Figure 4.3. The particles of Ep_SIP latex are characterized for having phosphate functionalization (Figure 4.3 a), while particles of Ep_H1_SIP latex have in their composition Sipomer® and H1 incorporated (Figure 4.3 b). In order to analyze the influence of the particles composition into the final film, in terms of location/distribution of H1 and Sipomer® PAM-200, a blend of Mp_ H1 (seed) and Ep_SIP in a ratio1:1 of polymer particles was prepared. In the blend, half of the particles are functionalized with Sipomer® and the other half is loaded with H1 (Figure 4.3 c). Therefore, the blend has the final concentration of 2 mg of H1/g latex (5 mg of H1/g polymer) and 2.6 mg of SIP/g latex (6.6 mg of SIP/g polymer).

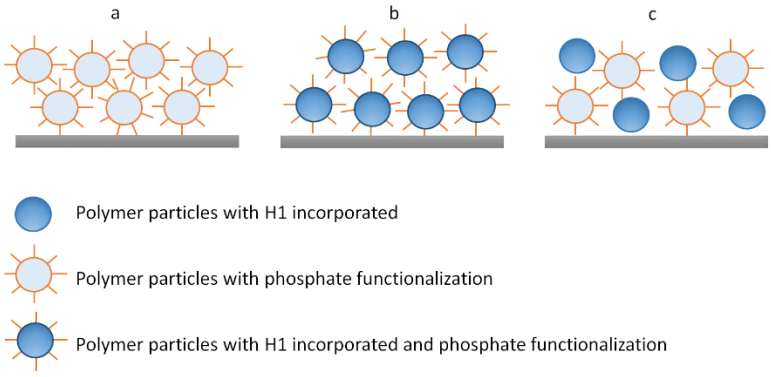

Figure 4.3. Representation of polymeric particles deposited on metallic substrate. a) Ep_SIP, b) Ep_H1_SIP, and c) Blend (Ep_SIP + Mp_ H1).

4.2.2 Coating of steel substrates and characterization of their corrosion protection properties

The metallic substrates were cleaned with abundant acetone and dried with compressed air before deposition of the latex. Samples were dried in two different conditions; 1) at room temperature without controlling the relative humidity, and 2) under controlled conditions of temperature and relative humidity (23 °C, RH = 60 %) in a humidity chamber, for at least 24 hours. The final thickness of the coatings was measured with a coating thickness gauge to ensure that the final film had an average thickness of 45 µm.

The details used for measurement of the EIS of the coatings are explained in section 2.2.6 of Chapter 2. Besides the EIS measurements on the intact films, tests were also carried out for coatings with an artificial scratch (1.1 cm long, 0.1 mm thick, and 45 µm deep) to determine if presence of H1 in the coating with Sipomer® PAM-200 (SIP), impart any active anticorrosive properties to the system with a damaged barrier properties.

4.3 Results and Discussion

4.3.1 Polymerization kinetics

Semibatch emulsion polymerization reactions were successfully performed using the latex with H1 incorporated (Mp_H1) or the one without it (Mp_Control), previously synthesized in Chapter 3, as seeds. Conversion and particle size were measured as reported in Chapter 2 (2.2.6.1 and 2.2.6.2, respectively). Full conversion was reached after 180 minutes of reaction for the reaction Ep_SIP, using Mp_Control as seed, and a conversion of 80% was obtained for the reaction Ep_H1_SIP, using Mp_H1 as seed (Figure 4.4 a).The lower conversion rate of this reaction may be due to some kind of retardation from the interaction of H1 with an increasing concentration of Sipomer® in the system. In both cases, the final particle size was 170-180 nm (Figure 4.4 b) and coagulum free latexes were obtained.

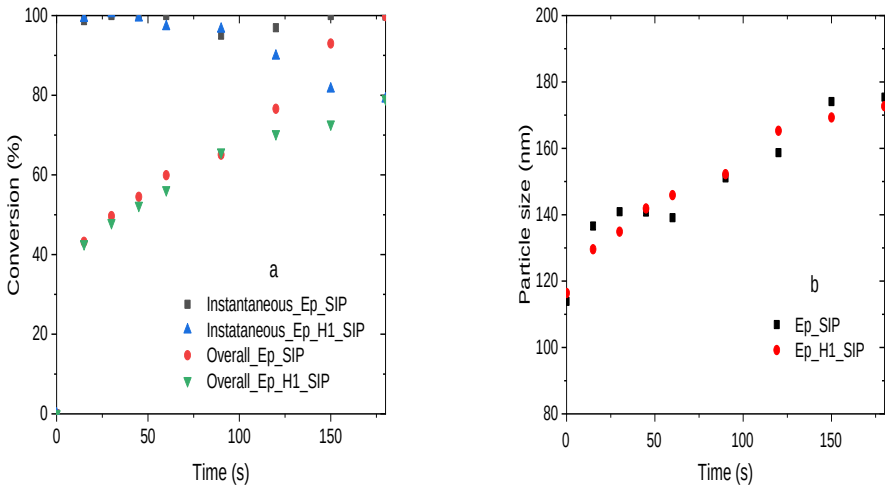

Figure 4.4: Batch emulsion polymerization reaction a) kinetics, and b) particles size over time of reaction.

The water absorption of free films made from Mp_H1, Mp_Control, Ep_H1_SIP, Ep_SIP, and the blend of Ep_H1_SIP and Ep_SIP was measured for 24 hours (Figure 4.5) according to the procedure reported in Chapter 2 (section 2.2.6.3). The coating Ep_SIP (13.3 mg of Sipomer®/g polymer) had the lowest absorption of water, as expected, since Sipomer® was reported to contribute to increase the hydrophobicity of the film[15,18]. On the other hand, the film with the highest water uptake was Mp_H1. This is due to the high concentration of H1 (10 mg H1/g polymer), that is sparingly soluble in water, as mentioned in Chapter 3. Therefore, the presence of H1 incorporated into the particles improves the hydrophilicity of the polymeric film. This is also supported by the considerably lower water uptake of Mp_Control (that has no H1 incorporated). Nevertheless, it is relevant to mention that, in this case, higher water uptake is not necessarily related to worse anticorrosive performance, as seen earlier in Chapter 3; Mp_H1 coating had shown higher impedances ($10^{6.7}$ Ω, and 84 degrees.) than Mp_Control ($10^{5.2}$ Ω and 66 degrees), due to the active anticorrosive protection given by H1.

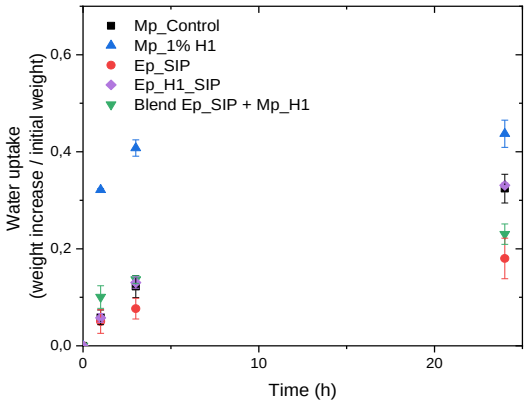

Figure 4.5. Water absorption of free films.

Ep_H1_SIP (3.3 mg of H1/g polymer, and 13.3 mg of SIP/g of polymer) film, showed considerably higher water uptake when compared to the Blend Ep_SIP + Mp_H1 (5 mg of H1/g polymer and 6.6 mg of SIP/g polymer), even though the blend has higher concentration of H1 in its composition. This is an indication that the distribution of H1 between the particles that form the film (Figure 4.3) have an influence in the absorption of water. When H1 is present in all of the particles, the absorption of water is higher (Figure 4.3).

4.3.2 Electrochemical characterization

In order to check their corrosion protection properties, the latexes were cast on metallic surfaces and dried at two different conditions; 1) room temperature with non-controlled RH, and 2) T = 23 °C and RH = 60%. The corrosion protection properties of the coatings were measured by EIS and presented in Figure 4.6.

When the coating Ep_SIP is dried at room temperature, it shows impedances of $10^{4.7}$-$10^{5.4}$ Ω, and phase angles of 78 - 82 degrees at high frequencies (Figure 4.6 a), which is very similar to those observed for the latex Mp_Control ($10^{5.2}$ Ω and 66 degrees) studied in Chapter 3, used as the seed. Therefore, the presence of Sipomer® did not show any significant improvement when compared to the seed, when dried under a condition that does not enable the formation of the phosphate layer[16]. When comparing Ep_SIP with Ep_H1_ SIP, dried at room temperature without controlling the relative humidity, it is observed that they have similar impedances and phase angles. Except that the impedance values obtained for Ep_H1_ SIP are more stable through the experiment, which is probably due to the presence of H1, that gives protection to the system.

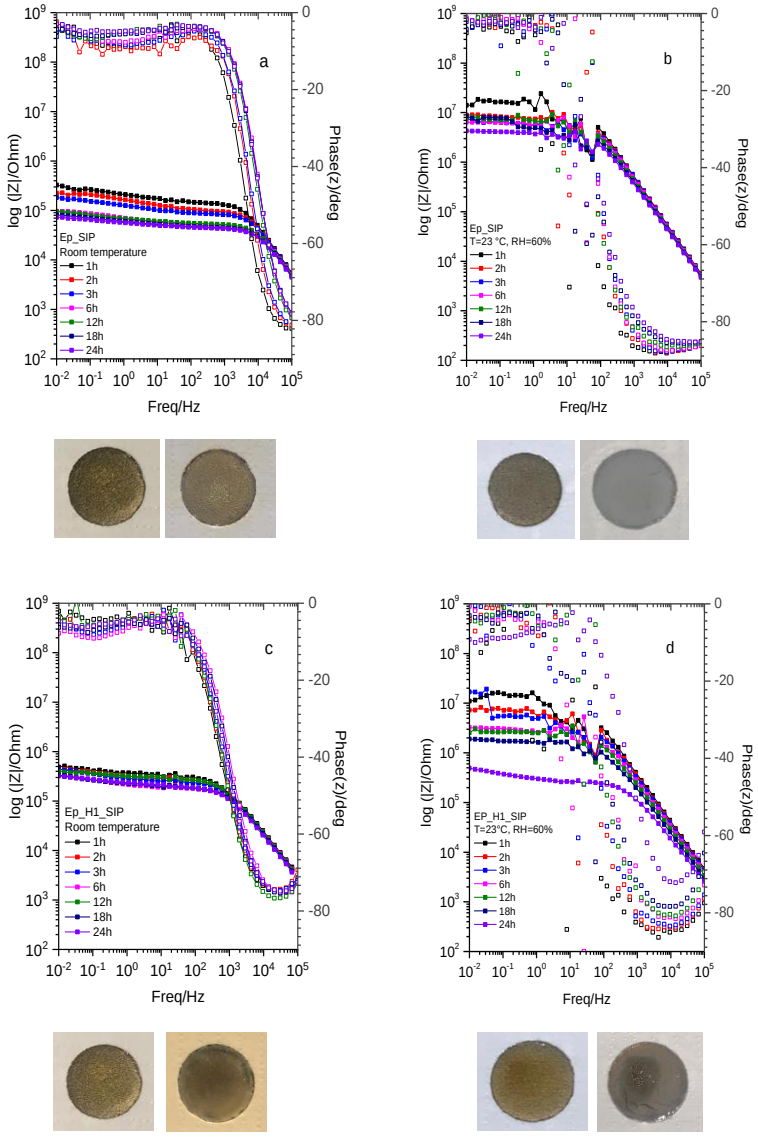

Figure 4.6: Electrochemical impedance spectra of coatings made by semi batch emulsion polymerization followed too by optical images of the samples before (on the left) and after the experiment (on the right). Ep_SIP dried at a) room temperature, and b) T = 23 °C and RH = 60%. Ep_H1_ SIP dried at c) room temperature, and d) T = 23 °C and RH = 60%.

However, when Ep_SIP is dried at T = 23 °C and RH = 60%, it shows considerably higher and constant impedances ($10^{7.1}$-$10^{6.4}$ Ω and phase angles of 84 - 88 degrees) throughout the 24 hour experiment time, similar to coatings previously reported with Sipomer®[16] (Figure 4.6 b). The improvement of impedance is due to the formation of the phosphate layer that provides extra barrier property to the system[16]. Nevertheless, the impedances obtained for Ep_H1_SIP dried in the same controlled conditions, are considerably less stable through the experiment. In the first three hours of experiment, Ep_H1_SIP shows impedances in the range of $10^{7.1}$-$10^{6.7}$ Ω and 96 - 72 of phase angle, similar to the values obtained for the Ep_SIP. However, the values drop with time reaching $10^{5.5}$ Ω and 72 degrees, after 24 hours of experiment, similar to the values obtained for Ep_H1_SIP, when dried at room temperature ($10^{5.3}$ - $10^{5.5}$ Ω and phase angles of 72 - 76 degrees), in which the phosphate layer is not formed. This may be an indication that the coexistence of H1 and Sipomer® incorporated into the binder is not compatible. Both Sipomer® and H1 are known for attaching to the metallic surface and forming a protective film. Therefore, it is likely that some kind of steric competition may be occurring, precluding the formation of an homogeneous phosphate layer.

In order to further investigate the influence of the disposition of H1 into the anticorrosive properties of the film, the latex Ep_SIP was blended with the latex Mp_H1 (Blend Ep_SIP + Mp_H1) in the proportion 1:1 (Figure 4.3 c). The EIS results for the sample dried at room temperature without controlling the relative humidity and for the one dried at T = 23 °C and RH = 60% are presented in Figure 4.7. The spectra of the sample dried at room temperature (Figure 4.7 a) has higher impedances and phase angles ($10^{5.3}$ - $10^{5.8}$ Ω and 80 - 75 degree), when compared to Ep_SIP dried in the same conditions (Figure 4.6 a), indicating that H1 was able to give some kind of extra protection to the system. On the other hand, the impedances obtained for the Blend Ep_SIP + Mp_H1, dried at T = 23 °C and RH = 60% (Figure 4.7.b) are very similar

to the ones obtained when the sample is dried at room temperature (Figure 4.7 a) and much lower than the impedances obtained for Ep_SIP dried under controlled conditions (Figure 4.6 b), indicating that the formation of a complete homogeneous phosphate layer was not possible due to the presence of the particles loaded with H1.

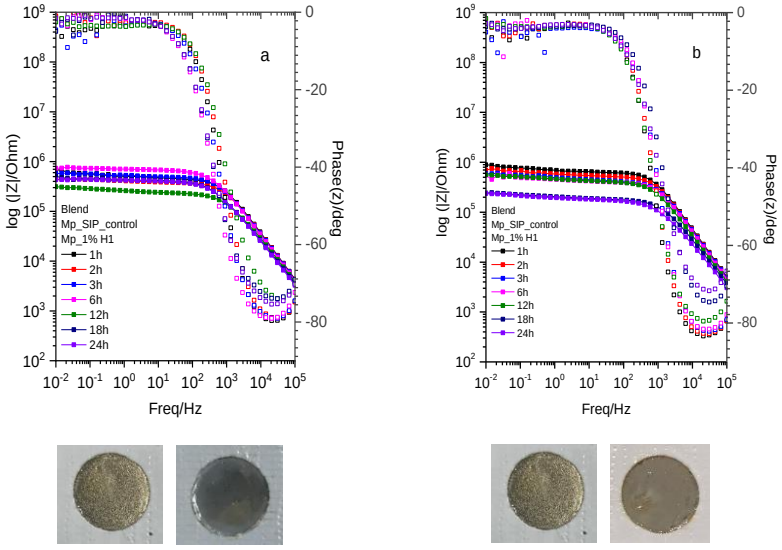

Figure 4.7. Electrochemical impedance spectra of the coating formed by the blend of the latex Ep_SIP + Mp_H1 (1:1), dried at; a) Room temperature ; b) T = 23 °C and RH = 60%.

To test the active protection of the proposed coating systems, samples were dried at T=23 °C and RH= 60%, and a scratch was made to the coatings applied on the steel, before the EIS measurements were carried out. The results are presented in Figure 4.8. A drop is observed in the impedance values of the coating Ep_SIP (Figure 4.8.a) in which the phosphate layer is homogeneous. However, while the impedance of Ep_SIP drops from $10^{4.4}$ to $10^{4.2}$ Ω after the 24 hours of experiment, while Mp_Control, studied in Chapter 3, dropped from ≈ $10^{4.6}$ to $10^{4.1}$ Ω

(Figure 3.5 a) in the same experiment. It is an indication that the phosphate present in Ep_SIP coating contributed to a more stable impedance profile when compared to Mp_Control.

The spectra obtained for the Ep_H1_SIP (Figure 4.8 b) is complex, with different processes taking place, as it is observed by the changes of profile in the phase angles and impedances along the experiment. Besides those changes, the impedances at low frequencies are maintained in $10^{4.2}$ Ω. The complexity of the system was already observed by the unstable impedances obtained for the intact coating (Figure 4.6 d), probably due to the configuration of the polymeric particle into the film (Figure 4.3 b). The lower drop is observed in the coating Ep_H1_SIP, that is an indication that H1 is providing some kind of active protection to the system when incorporated inside the particles with SIP (Figure 4.3 b). The same is not observed in the Blend Ep_SIP + Mp_H1, as H1 is distributed in a different configuration (Figure 4.3 c).

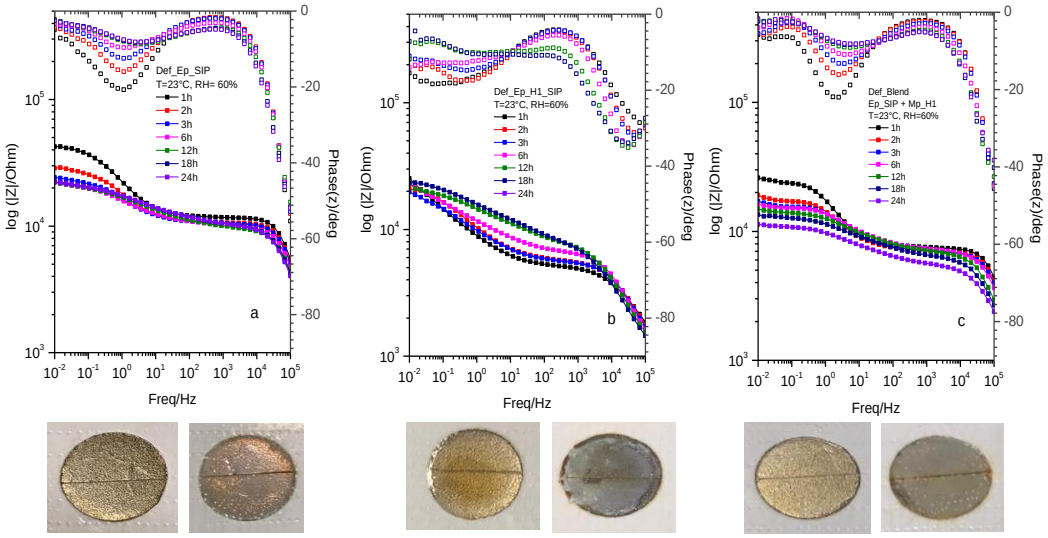

Figure 4.8. Electrochemical impedance spectra coatings dried at T = 23 °C and RH = 60%, with a controlled scratch followed by optical images of the samples before (on the left) and after the experiment (on the right). a) Ep_SIP, b) Ep_H1_SIP, c) Blend Ep_SIP + Mp_H1.

As an attempt to optimize the corrosion protection, a system composed of two layers of coatings was proposed, as shown in Figure 4.9. The first layer was prepared with the latex Ep_SIP dried at T = 23 °C and RH = 60%, that has previously shown the best impedance in the previous tests (10^7 Ω, Figure 4.6.b), and the second layer was prepared with the latex Mp_H1 that has shown high impedances (Figure 3.4) and some active protection due to the presence of H1 in its composition, reported in Chapter 3 (Figure 3.5). This sample was named 2L - Ep_SIP / Mp_H1. A control sample with the second layer prepared with the latex Mp_Control (Chapter 3) was also prepared for comparison propose (2L - Ep_SIP / Mp_Control). Each layer has the thickness of approximately 45 µm, therefore the final thickness of the system is of around 90 µm. The 2-layers-systems were measured by EIS, as intact systems and with an artificial scratch (1.1 cm long, 0.1 mm thick, and 90 µm deep), and the results are shown in Figure 4.10.

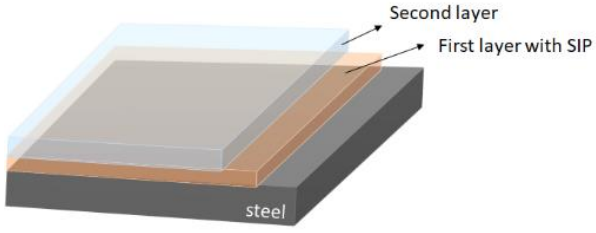

Figure 4.9: System composed of two layers, first layer prepared with the latex Ep_SIP dried at T = 23 °C and RH = 60%, and second layer Mp_Control / Mp_H1.

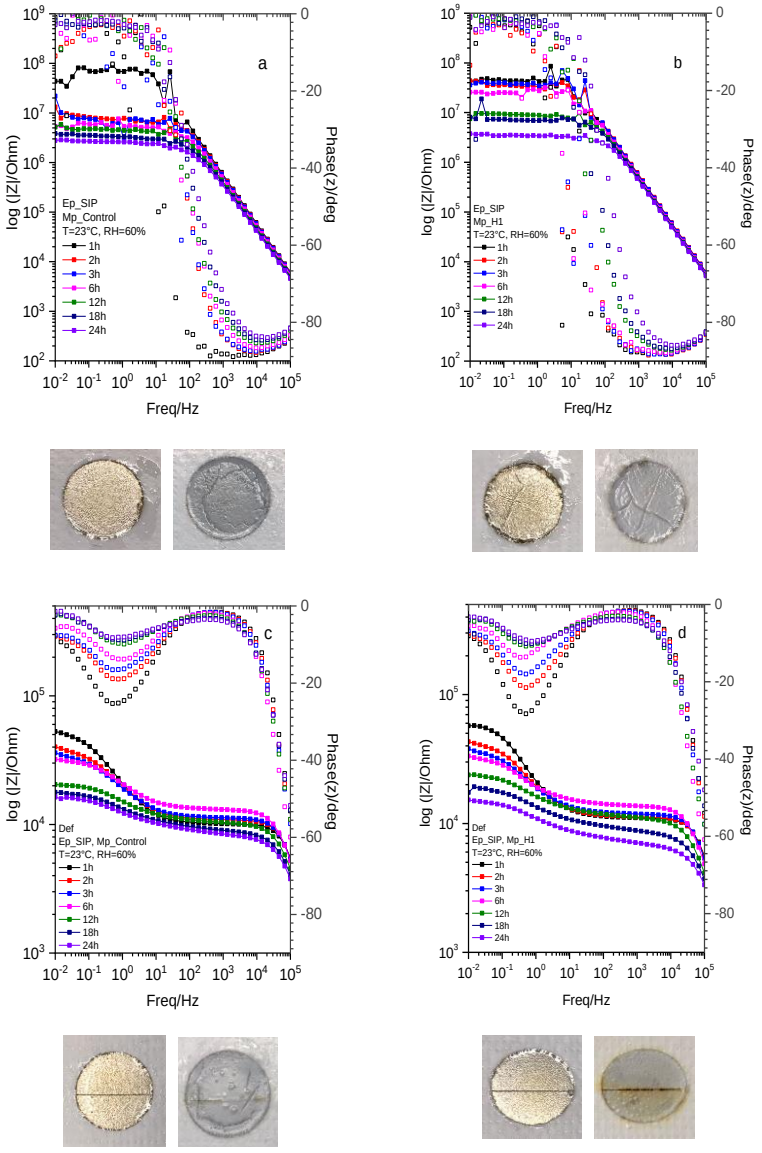

Figure 4.10. Electrochemical impedance spectra of 2-layer-coatings dried at T = 23 °C and RH = 60% of intact coatings a) 2L - Ep_SIP / Mp_Control, b) 2L - Ep_H1_SIP / Mp_H1, and coatings with a controlled scratch c) Def_2L - Ep_SIP / Mp_Control, d) Def_2L - Ep_H1_SIP / Mp_H1, followed by optical images of the samples before (on the left) and after the experiment (on the right).

The impedance spectra obtained for the 2-layer-coating Ep_SIP / Mp_Control is very similar to the one obtained for the 1 - layer coating Ep_SIP (Figure 4.6), even though the 2-layer-coating is thicker. The impedances obtained for the 2-layer-coating Ep_SIP / Mp_H1 (Figure 4.10.b) are higher in the first hours of experiment, when compared to the 2-layer-coating Ep_SIP / Mp_Control (Figure 4.10 a), indicating that the presence of H1 in the second layer of the coating contributes to improve the barrier properties of the proposed system. When a defect is present, the impedances of the system with H1 (Figure 4.10 d) drops slower in the first hours of the experiment, when compared to the system without the inhibitor (Figure 4.10 c), confirming that the presence of H1 is able to give mild corrosion protection to the system. Furthermore, the initial higher impedances of the scratched samples with the EP_SIP layer below indicate that the preparation of the phosphate and H1 bearing films favor the complete phosphatization of the surface, in the absence of H1.

4.4 Conclusions

The phosphate functionalization of a control latex and of the latex with H1 was performed by semi batch emulsion polymerization with the addition of Sipomer® PAM-200 (SIP). When dried at room temperature without controlling the relative humidity, in which the phosphate layer is not formed, the impedances obtained were comparable to the ones observed for the latexes without SIP. However, higher impedances were obtained when the latexes were dried under controlled conditions that allow the formation of the phosphate layer (23 °C, RH = 60 %). The control coating with SIP shows fairly stable impedances of $10^{7.1}$-$10^{6.4}$ Ω and phase angles of 84 - 88 degrees. However, the coating with H1 and SIP was less stable than the one of the control, with less stable impedances along time of $10^{7.1}$-$10^{6.7}$ Ω and phase angle of 96 – 94 degrees. This could be an indication that the coexistence of H1 and the phosphate function in

the particles is not compatible during the corrosion inhibition process. As both components are known for protecting the surface by being attached to it, some competition may be occurring between them.

The coating obtained from the blend of Ep_SIP with Mp_H1 (1:1), in which half of particles were loaded with SIP and the other half with H1 did not show higher impedances, when dried at 23 °C, RH = 60 %, as seen from the other coatings with SIP incorporated. This may be due to an impossibility of formation of the complete homogeneous phosphate layer caused by the presence of MP_H1 particles in contact with the metallic surface, that do not contain the phosphate on their particles´ surface.

The analysis obtained from the proposed 2-layer-coatings composed of a polymeric layer with SIP followed by a layer with H1 incorporated, has shown high impedances and that the presence of H1 in the second layer contributes for better corrosion protection of the system in the first hours of the experiment (~ 6 hours). Those results were observed for the intact coatings as well as for the coatings with a controlled scratch.

4.5 References

(1) Butler, L. N.; Fellows, C. M.; Gilbert, R. G. Effect of Surfactant Systems on the Water Sensitivity of Latex Films. *J. Appl. Polym. Sci.* **2004**, *92* (3), 1813–1823. https://doi.org/10.1002/app.20150.

(2) Asua, J. M. Emulsion Polymerization: From Fundamental Mechanisms to Process Developments. *J. Polym. Sci. Part A Polym. Chem.* **2004**, *42* (5), 1025–1041. https://doi.org/10.1002/pola.11096.

(3) Asua, J. M.; Schoonbrood, H. A. S. Reactive Surfactants in Heterophase

Polymerization. *Acta Polym.* **1998**, *49* (12), 671–686. https://doi.org/10.1002/(SICI)1521-4044(199812)49:12.

(4) Keddie, J. L.; Routh, A. F. *Fundamentals of Latex Film Formation: Processe and Properties*; Springer: Dortecht, The Netherland, 2010. https://doi.org/10.1007/978-90-481-2845-7.

(5) Aguirreurreta, Z. *Water-Borne Coatings and Water Pressure Sensitive Adhesives - Sensitive Adhesives Produced with Polymerizable Produced with Polymerizable Surfactants*; PhD thesis, University of the Basque Country UPV/EHU, 2016.

(6) Steward, P. A.; Hearn, J.; Wilkinson, M. C. Overview of Polymer Latex Film Formation and Properties. *Adv. Colloid Interface Sci.* **2000**, *86* (3), 195–267. https://doi.org/10.1016/S0001-8686(99)00037-8.

(7) Kientz, E.; Holl, Y. Distribution of Surfactants in Latex Films. *Colloids Surfaces A Physicochem. Eng. Asp.* **1993**, *78* (C), 255–270. https://doi.org/10.1016/0927-7757(93)80331-8.

(8) Zosel, A.; Schuler, B. Influence of Surfactants on the Peel Strength of Water-Based Pressure Sensitive Adhesives. *J. Adhes.* **1999**, *70* (1), 179–195. https://doi.org/10.1080/00218469908010494.

(9) Lee, W. P.; Gundabala, V. R.; Akpa, B. S.; Johns, M. L.; Jeynes, C.; Routh, A. F. Distribution of Surfactants in Latex Films: A Rutherford Backscattering Study. *Langmuir* **2006**, *22* (12), 5314–5320. https://doi.org/10.1021/la0601760.

(10) Aguirreurreta, Z.; de la Cal, J. C.; Leiza, J. R. Preparation of High Solids Content Waterborne Acrylic Coatings Using Polymerizable Surfactants to Improve Water Sensitivity. *Prog. Org. Coatings* **2017**, *112*, 200–209. https://doi.org/10.1016/j.porgcoat.2017.06.028.

(11) Aguirreurreta, Z.; Dimmer, J. A.; Willerich, I.; Leiza, J. R.; de la Cal, J. C. Improving the Properties of Water-Borne Pressure Sensitive Adhesives by Using Non-Migratory Surfactants. *Int. J. Adhes. Adhes.* **2016**, *70*, 287–296.

https://doi.org/10.1016/j.ijadhadh.2016.07.011.

(12) Guyot, A.; Tauer, K. Reactive Surfactants in Emulsion Polymerization. *Adv. Polym. Sci.* **1994**, *111*, 42–65. https://doi.org/10.1007/bfb0024126.

(13) Guyot, A. Advances in Reactive Surfactants. *Adv. Colloid Interface Sci.* **2004**, *108–109*, 3–22. https://doi.org/10.1016/j.cis.2003.10.009.

(14) Chimenti, S.; Vega, J. M.; Lecina, E. G.; Grande, H. J.; Paulis, M.; Leiza, J. R. Combined Effect of Crystalline Nanodomains and in Situ Phosphatization on the Anticorrosion Properties of Waterborne Composite Latex Films. *Ind. Eng. Chem. Res.* **2019**, *58* (46), 21022–21030. https://doi.org/10.1021/acs.iecr.9b02233.

(15) Chimenti, S.; Cerra, M.; Zanetta, T.; Leiza, J. R.; Paulis, M. Taking Advantage of Phosphate Functionalized Waterborne Acrylic Binders to Get Rid of Inhibitors in Direct-to-Metal Paints. *Polymers (Basel).* **2022**, *14* (2). https://doi.org/10.3390/polym14020316.

(16) Chimenti, S.; Vega, J. M.; García-Lecina, E.; Grande, H. J.; Paulis, M.; Leiza, J. R. In-Situ Phosphatization and Enhanced Corrosion Properties of Films Made of Phosphate Functionalized Nanoparticles. *React. Funct. Polym.* **2019**, *143* (August), 104334. https://doi.org/10.1016/j.reactfunctpolym.2019.104334.

(17) Edurne, G.; Stuhr, R.; Vega, J. M.; García-Lecina, E.; Grande, H. J.; Ramon Leiza, J.; Paulis, M. Assessing the Effect of CeO2 Nanoparticles as Corrosion Inhibitor in Hybrid Biobased Waterborne Acrylic Direct to Metal Coating Binders. *Polymers (Basel).* **2021**, *13* (6).

(18) Solvay S. A. Sipomer®, Resin Modifiers, Technical report, 2014.

Chapter 5

Corrosion protection of mild steel in acidic environment by cetrimonium cinnamate cationic surfactants

5.1 Introduction

The use of corrosion inhibitors is one of the most effective and cheap methods for mitigation of corrosion of metals and alloys[1–3]. They can be incorporated into paint coatings, added to water tanks, or continuously fed into pipelines or streams[4–6]. Conventional inhibitors are typically efficient for specific environmental conditions[7], however, variations of temperature, pH, humidity and salinity are likely to be found in industrial environments such as in the oil and chemical industry. Therefore, the development of environmental friendly compounds that could prevent the corrosion of mild steel in different conditions is desired[2]. An interesting approach is to blend inhibitions with different properties[7]. From that understanding, the group of Prof. Forsyth has studied the combination of carboxylates with rare earth metals group[8–10]. The studies revealed that these compounds act by suppressing both the anodic and cathodic reactions and showed a synergetic effect leading to a higher efficiency[7,10,11].

Recently, corrosion inhibitors comprised of cation groups and aromatic carboxylate counter-ion groups were disclosed[12]. The 4-hydroxycinnamate anion (OHcinn) was combined with a surface-active counterion, hexadecyl trimethylammonium bromide (cetrimonium trimethylammonium bromide, CTAB) that is known for its biocidal[13] and anticorrosive properties[14], in order to analyze if a synergic behavior of both properties could be achieved[15]. Results suggested that CTA-4OHcinn is able to inhibit the corrosion of steel in saline solutions of neutral pH[16]. CTA-4OHcinn was also tested as a multi-function compound for prevention of biofilm formation in marine environments, showing promising results[17].

Other studies revealed that when dissolved in solution, CTA-4OHcinn forms micelles that are susceptible to changes of morphology according to its concentration and the pH of the environment, which consequently affects the anticorrosive properties[15,16,18,19]. It was also

proposed that the alkyl chain length of the anion may modify the properties of the formed micelle[18]. Therefore, the aim of this Chapter is to investigate the corrosion protection of carboxylate anions with different alkyl chain length (trans-4-hydroxy-cinnamate, trans-4-etoxy-cinnamate, and trans-4-butoxy-cinnamate) combined with hexadecyl trimethylammonium bromide (CTAB) (Figure 5.1), in extremely acid conditions of pH 2 and 1, which could be very useful in industrial applications. The increase of the hydrophobic alkyl chain length on the cinnamate anions is expected to decrease the solubility of the final inhibitors and increase their corrosion protection ability[20,21]. The molecules were prepared by Ghorbani *et al.,* according to the methodology presented in his works[17,18].

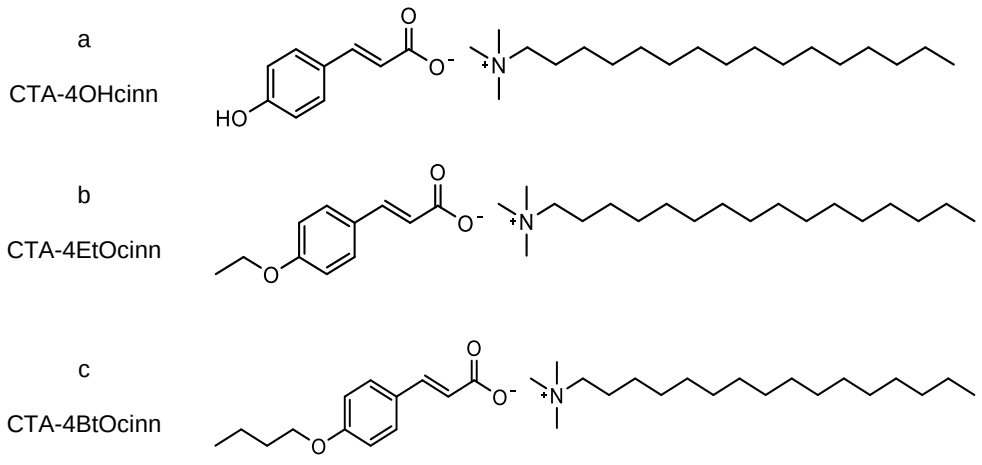

Figure 5.1. Chemical structures of inhibitors; a) Hexadecyl trimethylammonium bromide trans-4-hydroxy-cinnamate, b) Hexadecyl trimethylammonium bromide trans-4-ethoxy-cinnamate, c) Hexadecyl trimethylammonium bromide trans-4-butoxy-cinnamate.

The anticorrosive properties of the inhibitors in solution will be investigated by electrochemical analysis. As a proof of concept that those compounds could also be incorporated into coatings for industrial applications, the inhibitors were blended with an acrylic polymeric

binder obtained by dispersion polymerization. The composite coatings were analyzed by EIS under neutral and acid saline corrosive solutions. Finally, an attempt was made to use CTA-4OHcinn, the most soluble between the compounds studied, as a surfactant for carrying out emulsion polymerization reactions. The concept is to replace the traditional surfactants that are fundamental for the polymerization reaction processing but are not beneficial to the dried film, since they increase its hydropilicity[22,23], for a new surfactant that could provide anticorrosive properties to the system.

5.2 Experimental Section

5.2.1 Characterization of cetrimonium cinnamates cationic surfactants as free inhibitors

5.2.1.1 Preparation of solution containing the inhibitors

The inhibitor compounds were prepared by a researcher at IFM Deakin University, Mahdi Ghorbani, and provided with high purity for further testing, according to the methodology presented in his works[17,18]. Solutions of 0.01 M NaCl, with MiliQ water, and 0.1 mM of each one of the inhibitors were prepared as well as a control solution with no inhibitors. A solution of 0.1 mM CTAB and 0.01 M NaCl was also prepared for comparison purposes. In order to better solubilize the compounds, the solutions were heated to 40 °C and mixed with a magnetic stirrer. After cooling, the pH of the solutions were adjusted to 2 or 1 with the addition of a diluted solution of HCl. Solutions were stored at room temperature.

5.2.1.2 Preparation of Steel Coupons

Initially, cylindrical coupons of mild steel 1030 were embedded in epoxy resin, leaving an exposed circular area 0.786 cm^2 (1 cm diameter). Before each experiment, the exposed areas were polished with 240, 600, and 1200 grit silicon carbide paper using a mechanical polisher with continuous flow of distilled water. Then, the samples were dried with nitrogen drying gun and placed in a silica gel desiccator for 1 h prior to the tests.

5.2.1.3 Immersion tests, Optical and SEM analysis

Coupons were prepared according to section 5.2.1.1 and immersed in the solutions of inhibitors. After 24 hours, the coupons were kindly rinsed with MiliQ water, dried with nitrogen drying gun, and placed in silica gel desiccator. Optical images were carried out in a Leica DMi8 microscope and SEM images were performed in a JEOL IT300. Some immersion tests were also carried out for 4 days in order to visually analyze the performance of the inhibitors for a longer period of time.

5.2.1.4 Potentiodynamic polarization (PP) and electrochemical impedance spectroscopy (EIS)

Tests were performed using a low current channel of the potentiostat BIO-LOGIC VMP3 and EC Lab 11.27 software. The experiments were performed at room temperature, with a conventional three-electrode cell composed of a saturated silver/silver chloride reference electrode, a titanium mesh as the counter electrode, and AS1030 mild steel as the working electrode with an exposed area of 0.786 cm^2 (1 cm diameter).

The open circuit voltage (OCV) was monitored for 47 minutes over the frequency range from 100 kHz to 10 mHz, followed by EIS at a scan rate of 0.167 mV/s with 6 points per decade

and a sinoidal amplitude of 10 mV. Impedance responses were monitored for 24 hours, followed by a PP experiment. PP experiments were also performed after 30 minutes of immersion, for comparison purpose. All of the experiments were carried out in triplicate. The corrosion current density (I_{corr}) and corrosion potential (E_{corr}) values were extracted from the PP curves by Tafel extrapolation. The linearity of the curves was found over the range of 10-25 mV at both sides of Ecorr. The inhibitors efficiency (IE) was calculated by Equation 2.1 of Chapter 2.

5.2.2 Cryo TEM imaging of micelles

Solutions of 1 mM of the cetrimonium cinnamate inhibitors in a corrosive solutions of 0.1M NaCl were prepared for Cryo-TEM imaging. The solution was contained in a holder coated with a negatively charged carbon film. Copper grids (200-mesh) coated with holey carbon film (Quantifoil R1.2/1.3) were placed in a Pelco glow discharge unit to render them hydrophilic. A sample volume of 3.5 µL was applied onto the grids, which were then blotted against two filter papers for 3 seconds at a blot force of -3 in a Vitrobot plunge freezer system (FEI).The resulting thin sample film was vitrified in a controlled environment vitrification system at 5 °C and 100% relative humidity by plunging the sample into liquid ethane, which was maintained at its melting point (-160 °C) with liquid nitrogen. The vitrified specimens were transferred to a Gatan 626 cryoholder and observed at an operating voltage of 120 kV in a Tecnai 12 Transmission Electron Microscope (FEI) at temperatures between -170 °C and -175 °C. Images were recorded with a Gatan Eagle highresolution CCD camera (4 k x 4 k) and digitized with the Tecnai Image Acquisition (TIA) program.

5.2.3 Analysis of cetrimonium cinnamates inhibitors in polymeric coatings

5.2.3.1 Blending of inhibitors into a dispersion latex

The inhibitors were mechanically blended into the dispersion control latex prepared in Chapter 2, according to section 2.2.3. The blends have the final concentration of 3 % of inhibitor (g inhibitor / 100 g polymer).

5.2.3.2 Incorporation of CTA-4OHcinn as emulsifier in semi batch emulsion polymerization of poly(MMA/BA)

Polymerization reactions were carried out under N_2 atmosphere in a 100 mL round bottom flask. The temperature was maintained at 70 °C, and the impeller rotation speed at 250 rpm. Initially, a seed of 16% solids content with DTAB (2% wbm) was prepared by emulsion polymerization (Figure 5.2). Then, a pre-emulsion of MMA, BA, water, and a mixture of CTA-4OHcinn and DTAB was continuously fed for 2 hours in order to increase the solids content of the latex to 40 %. A post polymerization step was performed at 90 °C for one hour to eliminate traces of monomer. A control latex with no CTA-4OHcinn was also produced for comparison purposes. The recipe used for the polymerizations is presented in Table 5.1.

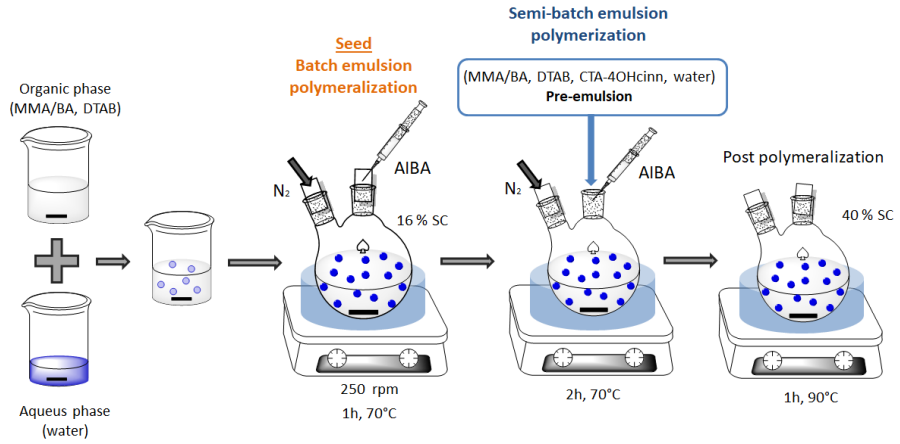

Figure 5.2: Schematic representation of semi batch emulsion polymerization of poly(MMA/BA) using CTA-4OHcinn as an emulsifier.

Table 5.1**.** Recipe used for the two stage seeded semibatch emulsion polymerization reactions.

Seed		
	Components	Mass (g)
Organic phase	MMA	1
	BA	1
	DTAB (2 %wbm)	0.04
Aqueous phase	H_2O	10
Initiator solution	AIBA	0.06
	H_2O	10
Feeding		
	Components	Mass (g)
Organic phase	MMA	13.5
	BA	13.5
	DTAB (1 % wbm)	0.27
Aqueous phase	CTA-4OHcinn (1% wbm)	0.27
	H_2O	25.5
Initiator solution	AIBA	0.12
	H_2O	2

5.3 Results and Discussion

5.3.1 Electrochemical analysis of cetrimonium cinnamate cationic surfactants as free inhibitors

Representative polarization curves obtained after 30 min and 24 hours of immersion of mild steel in solutions of 0.01 M NaCl in pH 1 and pH 2 in the absence (Control) and in the presence of free inhibitors are presented in Figure 5.2 and the data extracted from the Tafel extrapolation is shown in Table 5.2. A significant anodic shift and reduction of current density (icorr) is observed in all of the solutions after 30 minutes of immersion, when compared to the control, indicating that the inhibitors are able to suppress the process of dissolution of iron even at extremely acid conditions (Figure 5.3 a and b). At this stage, the results obtained for the solution of CTAB at pH1 is very similar to the solutions of the cetrimonium cinnamate cationic surfactants studied (Figure 5.3 b).

After 24 hours of immersion, a significant shift to the cathodic site is also observed (Figure 5.3 c and d). The data show that the corrosion protection of cetrimonium cinnamates cationic surfactants is time dependent, with better film formation over time, as they migrate from the bulk of the solution to the metallic surface. Moreover, it also indicates that the inhibitors are able to suppress both anodic and cathodic corrosion reactions (mixed inhibitors). After 30 minutes of immersion, the surface was not fully covered yet, therefore the suppression of the anodic reactions is more visible. However, after 24 hours of immersion, E_{corr} moves towards lower values meanwhile E_{pit} increases, when compared to the controls (Table 5.2). The results obtained after 24 hours also suggest that the inhibitors are more efficient at pH 1 than at pH 2. It is also observed that all of the solutions of cetrimonium cinnamate inhibitors proposed show better performance than the solution of CTAB, at 24 hours and pH1 (Figure 5.3 d), with significant lower values of i_{corr} (Table 5.2).

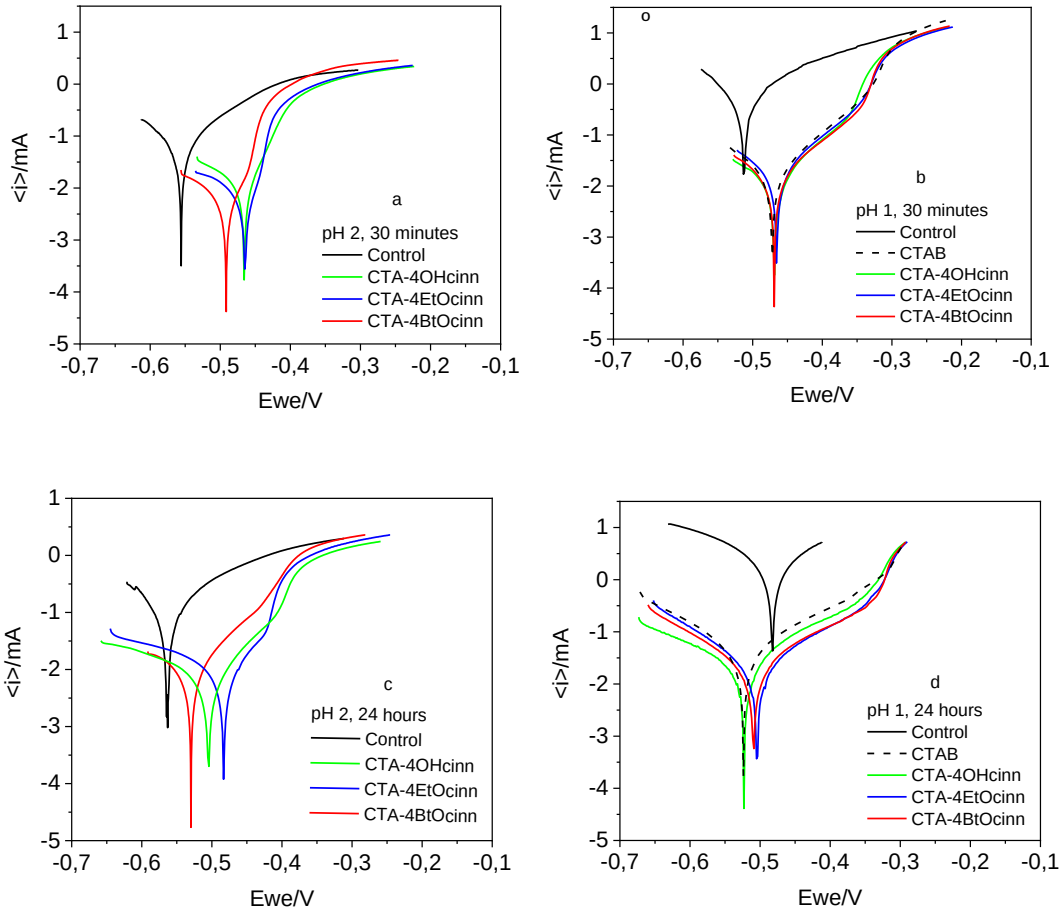

Figure 5.3. Representative polarization curves after immersion of mild steel in 0.01 M NaCl and 0.1 mM inhibitors solutions a) after 30 min, pH 2, b) after 30 minutes, pH 1, c) after 24 hours, pH 2, and d) after 24 hours, pH1.

Table 5.2. Corrosion Current Density (i_{corr}), Corrosion Potential (E_{corr}), Pitting potential (E_{pit}) and Inhibitor Efficiency (IE) extracted from the polarization curves for mild steel immersed in different solution of inhibitors.

H	Sample	Concentration (mM)	Time (h)	icorr (μA/cm2)	Ecorr (mV)	Epit (mV)	E (%)
2	Control	0	0.5	21.6 ± 1.2	-560.5 ± 6.2	-	-
		0	4	25.7 ± 3.3	-562.8 ± 7	-	-
	CTA-4OHcinn	0.1	0.5	5.4 ± 1.2	-461.3 ± 3.4	-	5
		0.1	4	1.9 ± 0.4	-504.6 ± 2.3	-364.54 ± 7.6	2.6
	CTA-4EtOcinn	0.1	.5	3.6 ± 0.7	-462.0 ± 3.5	-	83.3
		0.1	24	2.5 ± 0.4	-487.4 ± 5.8	-420.16 ± 3.3	90.3
	CTA-4BtOcinn	0.1	5	2.63 ± 0.24	-491.6 ± 1.5	-460 ± 2.4	87.8
		0.1	24	3.3 ± 0.35	-529.9 ± 2.2	-425 ± 6	87.2
1	Control	0	5	136.8 ± 20.7	-513.1 ± 2.7	-	-
		0	24	329.7	-483	-	-
	CTAB	0.1	0.5	4.7 ± 0.52	-469.65 ± 8.5	-329.8 ± 2.3	96.6
		0.1	24	13.9 ± 5.6	-530.8 ± 6.7	-334.5 ± 8.9	95.8
	CTA-4OHcinn	0.1	0.5	3.2 ± 0.7	-459.1 ± 12.6	-356.8 ± 2.9	97.6
		0.1	24	4.8 ± 0.9	-521.1 ± 3.6	-348.5 ± 8.4	98.5
	CTA-4EtOcinn	0.1	0.5	6.0 ± 0.6	-469.3 ± 6.9	-341.7 ± 0.9	95.6
		0.1	4	4.3 ± 0.4	-501.5 ± 4.0	-336.3 ± 11.1	98.7
	CTA-4BtOcinn	0.1	0.5	4.9 ± 1.6	-469.1 ± 6.1	-343.5 ± 12.3	96.4
		0.1	24	6.24 ± 2.1	-519.9 ± 13.5	-330.5 ± 6.4	98.1

Bode plots and phase angles of the samples exposed to a corrosive solution without and with inhibitors at pH 2 and pH 1 are shown in Figure 5.4 and Figure 5.5, respectively. The impedance of the samples with inhibitors are considerably higher ($10^{3.2}$ - $10^{3.5}$ Ω for pH 2, and $10^{3.1}$ - $10^{3.2}$ for pH 1) than the ones observed for the control sample (maximum of $10^{2.8}$ Ω for pH 2, and maximum of $10^{1.2}$ Ω for pH 1), which confirms the corrosion protection given by the molecules to the system in both harsh conditions. The same is observed with the phase angles, it is higher in the systems with inhibitors (maximum of approximately 50 degrees at pH 2, and 70

degrees at pH 1), than in the control systems (maximum of approximately 30 degrees, at pH 2 and 20 degrees pH 1) .

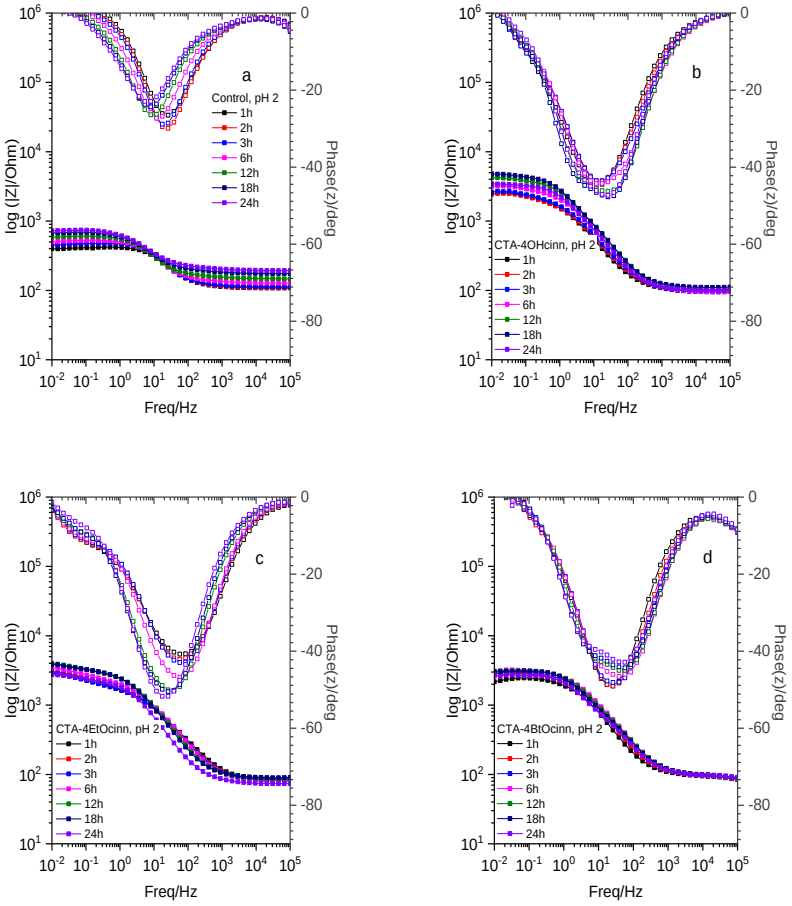

Figure 5.4. Bode plot and phase angle of inhibitors in solution at pH 2, a) Control, b) CTA-4OHcinn, c) CTA-4EtOcinn, d) CTA-4BtOcinn.

At pH 1, the highest phase angle is found in the solution of CTA-4BtOcinn that is 70 degrees (Figure 5.5 d) and the broader phase angle is found in the sample with CTA-4OHcinn

(Figure 5.5 b) which can be an indication that this inhibitors is able to form a more stable film on the metal surface. The impedance obtained for the cetrimonium cinnamate surfactants at pH1 (Figure 5.5 b), in all cases, are higher ($10^{3.1}$ - $10^{3.2}$ Ω) than the one obtained for the solution of CTAB ($10^{2.6}$ - $10^{3.1}$ Ω), confirming that the increase of efficiency when the anodic part is added to the inhibitor.

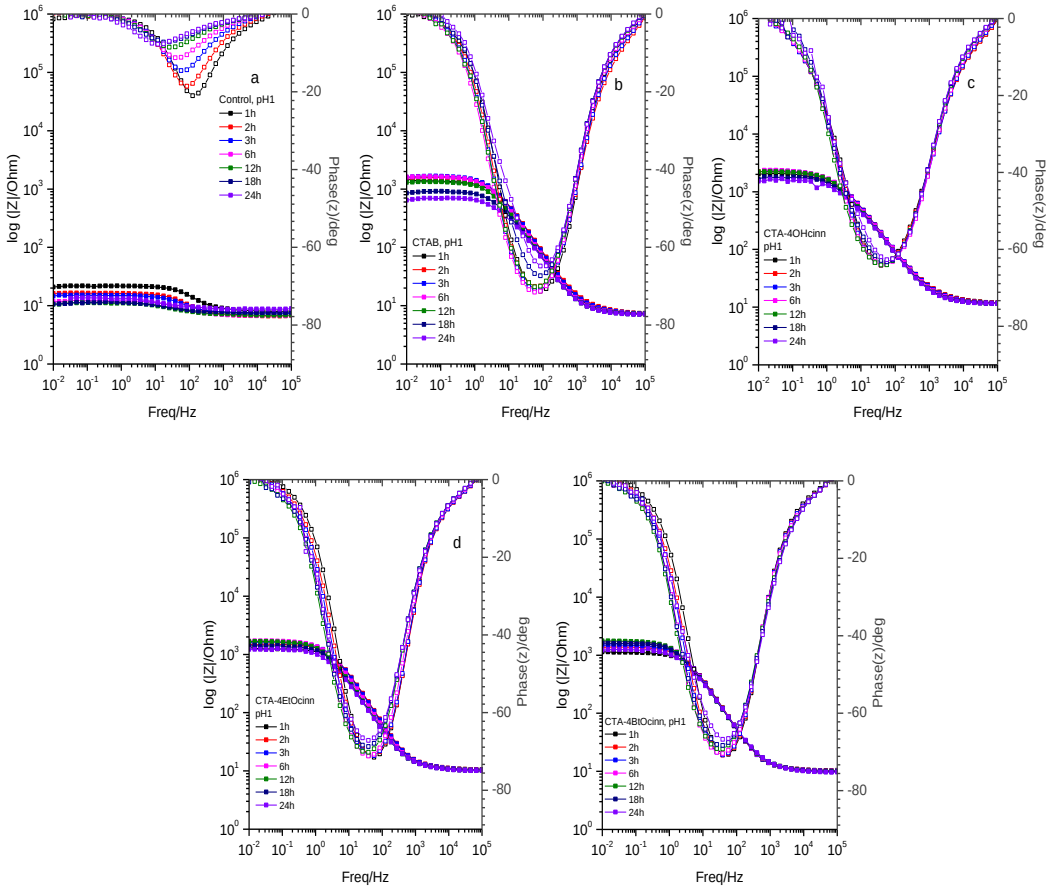

Figure 5.5. Bode plot and phase angle of inhibitors in solution at pH 1, a) Control, b) CTAB, c)CTA-4OHcinn, d) CTA-4EtOcinn, e) CTA-4BtOcinn.

5.3.2 Optical and SEM analysis of samples immersed in solutions of inhibitors

Optical and SEM images of the coupons after immersion for 24 hours in the solutions are presented in Figure 5.6. The control sample immersed in the saline solution of pH 1 (Figure 5.6 b) is significantly more corroded than the one immersed at pH 2 (Figure 5.6 a), which shows the corrosive capacity of the solution of lower pH. At pH 2, a significant amount of pitting is observed on the sample surface, while at pH 1 part of the material seems to be dissolved forming voids and holes on the surface. However, the compounds immersed in the solutions of inhibitors showed only mild corrosion, due to the protection provided by the inhibitors. The anticorrosive protection given by the inhibitors to the mild steel at pH 1 is highly efficient, especially when compared to the control sample at the same pH. It is also important to mention that the optical and SEM images obtained are consistent with the previous EIS results analyzed (Figure 5.4 and 5.5).

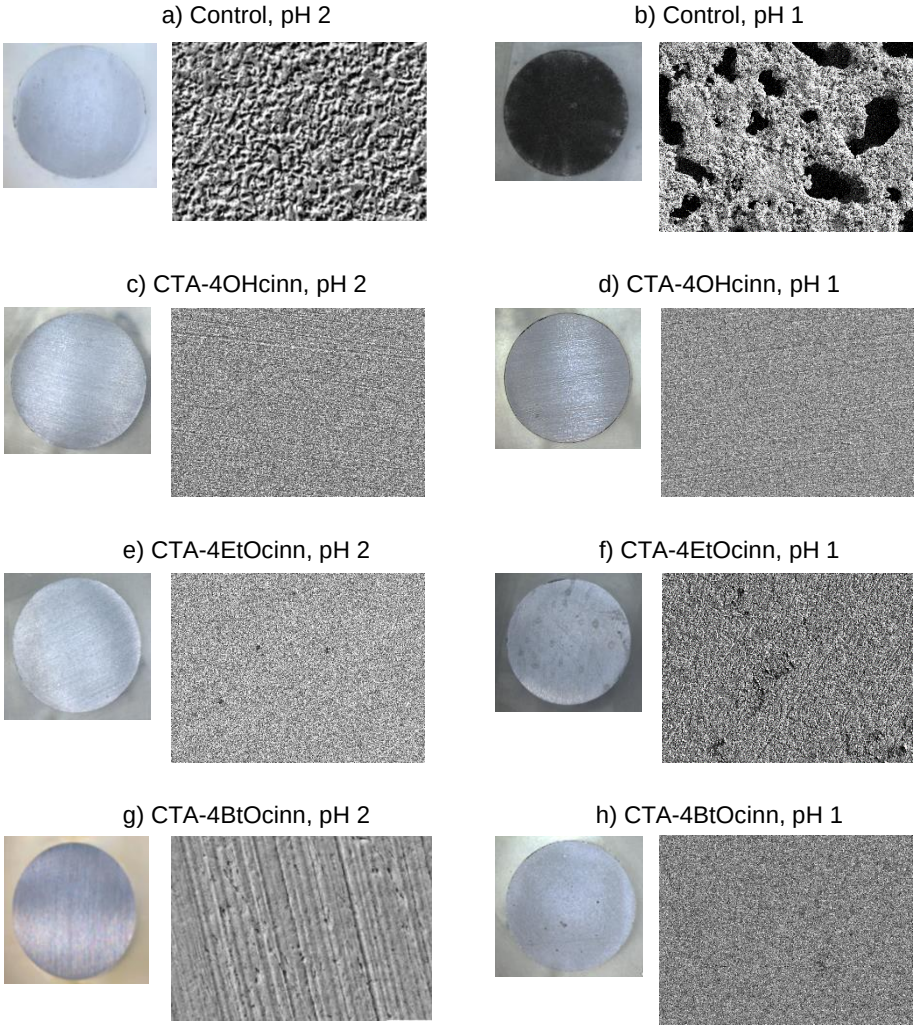

Figure 5.6. Optical images (left) and SEM images X5000 (right) of samples after 24 hours of immersion in corrosive solutions with 0.1 mM of inhibitor.

In order to better compare the efficiency of the cetrimonium cinnamate surfactant that showed the best results, CTA-4OHcinn, with the CTAB, coupons were immersed for 4 days in solutions of 0.1 mM. The surface of the sample immersed in the solution of CTAB was covered

with stains, showing visible signs of localized corrosion (Figure 5.7 a). The sample immersed in the solution of CTA-4OHcinn showed only mild signs of corrosion (Figure 5.7 b). Therefore, cetrimonium cinnamate inhibitors are more efficient in the protection of corrosion than the CTAB alone.

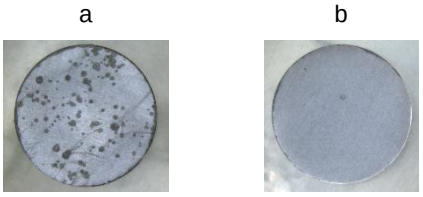

Figure 5.7. Optical images of samples immersed in a corrosive solution of 0.1mM of inhibitor, for 4 days; a) CTAB and b) CTA-4OHcinn.

5.3.3 Cryo TEM imaging of micelles

The formation of wormlike entangled micelles from CTA-4OHcinn and CTA-4EtOcinn were previously reported[18]. Therefore, Cryo TEM image were used to investigate the micelle structure of solutions of 0.1 mM of the proposed cetrimonium cinnamate at pH 1 and pH 2. The obtained images are presented in Figure 5.8, and the observed micelles are labeled by red cycles, for better visualization. Spherical micelles are observed in all of the studied inhibitors, at pH 1, and pH 2.

It is known that the shape of the formed micelles as well as the efficiency of the inhibitor may change due to the alkyl tail of the anion that composes the proposed cetrimonium cinnamate inhibitor, the concentration, the pH, and the temperature [15,18,19]. It seems that bigger micelles are present in the solution of pH 1 than in pH 2 (Figure 5.8). The biggest micelles are formed by the solution of CTA-4BtOcinn (Figure 5.8.f), probably due to the longer alkyl tail of the anion that composes the inhibitor.

	pH 2	pH 1
CTA-4OHcinn	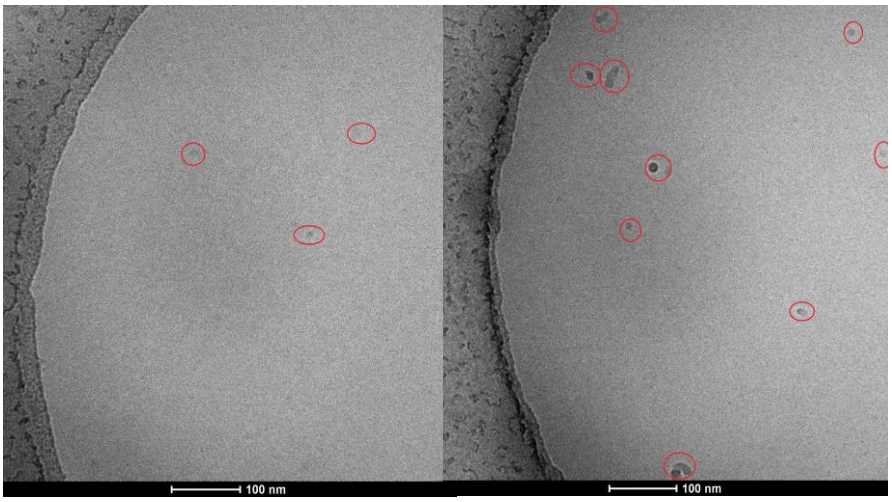	
CTA-4EtOcinn	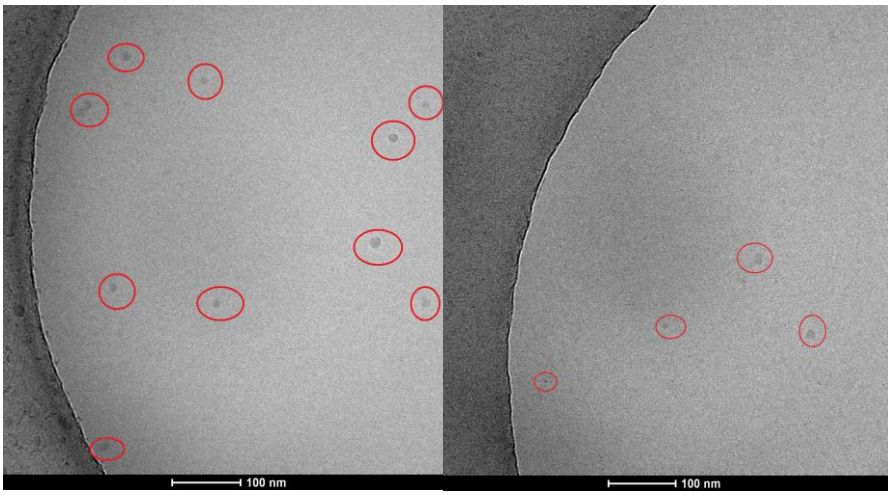	

CTA-4BtOcinn

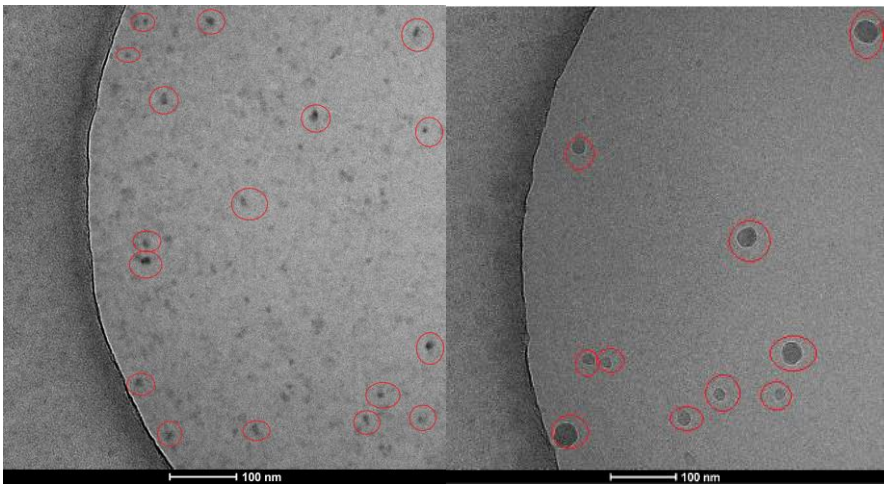

Figure 5.8. Cryo-TEM image solutions of 0.1 mM of the cetrimonium cinnamate proposed inhibitors with 0.1 mM NaCl, at pH 2 and pH 1.

Previously, it was observed that those types of inhibitors form wormlike micelles when dissolved in at neutral pHs[24]. However, at pH 2 and 1, it was observed the formation of spherical micelles (Figure 5.8). The spherical configuration may facilitate the delivery of the organic anion to the metallic surface along with the CTA^+ molecule, enabling better corrosion protection when compared to the systems at neutral pH.

5.3.4 Corrosion protection of cetrimonium cinnamate inhibitors blended in polymer coatings

As it was explained in the experimental part, initially the different cetrimonium cinnamate inhibitors where blended to acrylic binders produced by dispersion polymerization, in order to analyze their corrosion protection when incorporated to a polymeric coating. The protection provided by the control film and by the films with the inhibitor blended, after coated on steel, was

analyzed by EIS in neutral (Figure 5.9) and in acid solutions (Figure 5.10). Optical images of the sample before and after the experiment were also taken.

The Bode spectra of the control coatings in neutral pH (Figure 5.9) is characteristic of soft coatings that allow diffusion of water, and it has no phase angle peaks at high frequencies that are normally associated with a barrier coating[25]. Therefore, the control-dispersion coating offers no significant anticorrosive protection to the bare steel substrate (Figure 5.9 a). Higher impedances and phase angles are observed in the first hour of analysis of the coatings with CTA-4EtOcinn and CTA-4BtOcinn (Figure 5.9 c and d, respectively), at neutral pH, due to the anticorrosive properties of the inhibitors in the films. Nevertheless, the inhibitors seem to not be able to maintain the protection to the system after that time. Signals of rust, formed in non acidic media, can be seen in the optical images of the samples. In this system, CTA-4OHcinn seems not to be efficient, probably due to its higher solubility in water. Since the coating is highly permeable, the inhibitor may be washed out of the coating. (Figure 5.9 b).

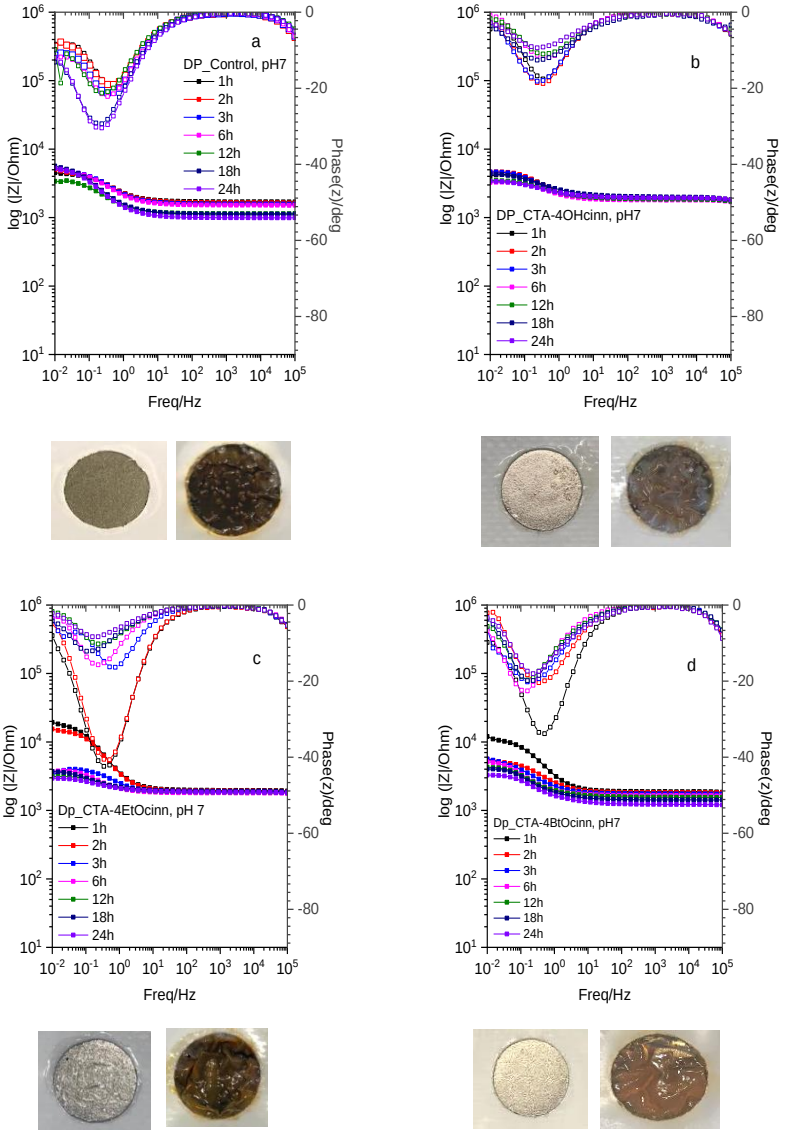

Figure 5.9. Bode plot and phase angle of coatings with inhibitors blended tested in a corrosive solution of 0.005 M NaCl and pH 7, followed by optical images of before the experiment (left) and after the experiment (right) a) Control, b) CTA- 4OHcinn, c) CTA-4EtOcinn, d) CTA-4BtOcinn

As expected, due to the higher concentration of ions in the system, impedance values are lower in the higher frequency range of the Bode plot of the samples immersed at pH 1 (Figure 5.10), when compared to the data obtained in neutral conditions. Rust is not observed in the optical images since the product of corrosion in acid media is soluble in water. In this case, the control coating seems to somehow give some protection to the surface (Figure 5.10 a and b). Higher impedances are seen in the coatings with inhibitor (Figure 5.10 b - d), when compared to the control (Figure 5.10 a). Contrary to what was seen in the system immersed at neutral pH, the inhibitors are able to give protection to the system for the whole 24 hours of experiment.

The equivalent circuit (EC) typically employed in representation of coatings (Figure 3.9, Chapter 3) was used to fit the EIS spectra of the bare steel, control coating, and coating with the inhibitors blended at pH 1, after 24 hours of experiment[1,25]. R_s represents the solution resistance, C_{coat} is the coating capacitance, R_{pore} is the resistance in the pores of the coating, C_{dl} represents the double layer capacitance at the interface and R_{ct} is the charge transfer resistance at the interface. The fitting results are shown in the Table 5.3.

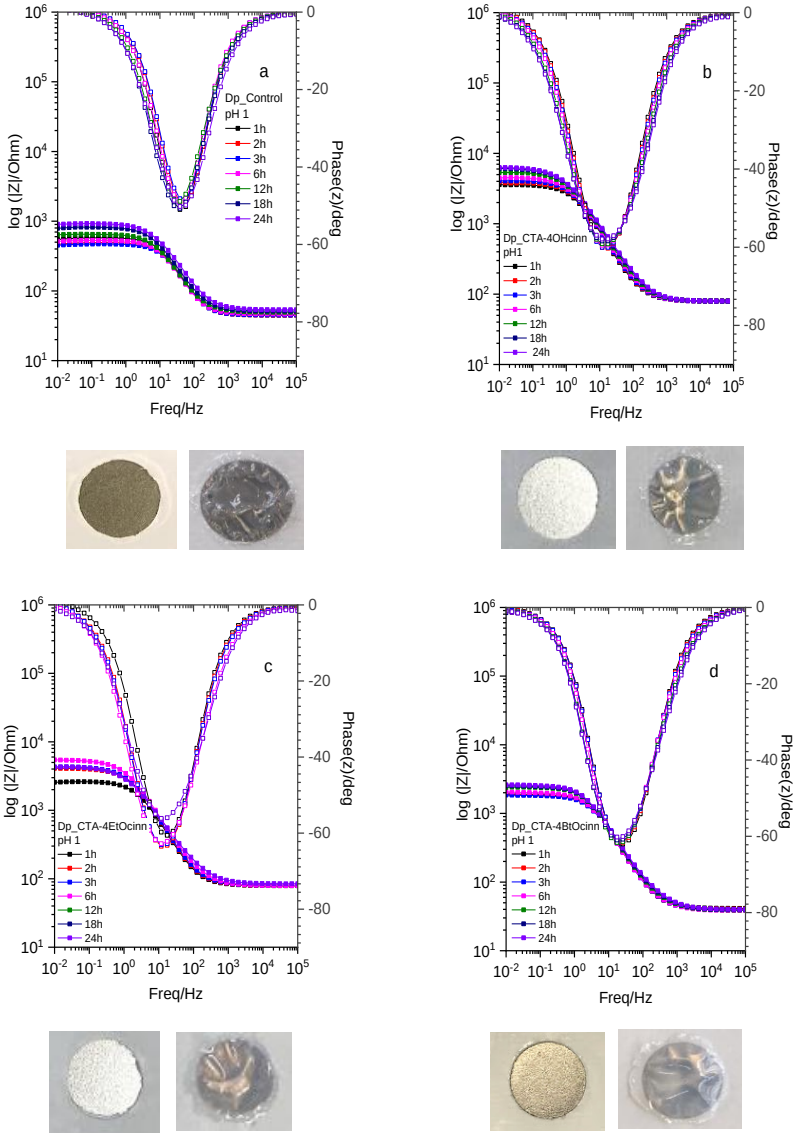

Figure 5.10. Bode plot and phase angle of coatings with inhibitors blended tested in a corrosive solution of 0.005 M NaCl and pH 1, and optical images of the sample before the experiment (left) and after the experiment (right) a) Control, b) CTA- 4OHcinn, c) CTA-4EtOcinn, d) CTA-4BtOcinn.

Table 5.3: Fitting results for dispersion coatings after 24 hours of experiment at pH 1, with inhibitors blended.

Sample	R_s (Ω)	C_{coat} ($\mu F.s^{ncoat-1}$)	n_{coat}	R_{pore} (Ω)	C_{dl} ($\mu F.s^{ndl-1}$)	n_{dl}	R_{ct} (Ω)	χ^2//Z/
Dp_Control	53.07	24.42	0.8250	0.1319	24.83	0.8250	870	0.0055
Dp_CTA-4OHcinn	77.10	40.36	0.7739	5828	11.17	0.9751	446.3	0.0069
Dp_CTA-4EtOcinn	83.53	45.81	0.7830	3102	5.657	0.3000	1172	0.0064
Dp_CTA-4BtOcinn	46.381	42.6	0.8529	1315	10.75	0.5442	1245	0.3381

The fitting results obtained for the experiments at pH 1 are in agreement with what was previously observed. The coatings with inhibitors blended show higher values of C_{coat} than the control, which could be an indication that the addition of the inhibitor into the coating may improve its barrier property. R_{pore} values are significantly higher in the coatings with inhibitors, suggesting that the inhibitors are able to provide additional protection to the system. The highest value is found in the coating with CTA-4OHcinn blended. A lower value of C_{dl} is observed in the coatings with inhibitors, which is frequently associated with less corroded surfaces[26]. The values of R_{ct} also increase with the addition of the inhibitors, indicating that the inhibitors are able to provide further protection to the surface.

5.3.5 Incorporation of CTA-4OHcinn as emulsifier in the emulsion polymerization of poly(MMA/BA)

The use of cationic emulsifier in emulsion polymerization reactions is challenging since the system is usually more prone to coagulation. Initially, an attempt to carry out the emulsion polymerization reaction of MMA/BA using CTA-4OHcinn alone as the emulsifier was performed. However, coagulum was formed during the polymerization. In a second approach CTA-4OHcinn was used in combination with a well stablished cationic surfactant (DTAB) (Table 5.1). The polymerization reaction was successfully carried out without the production of coagulum. A

control latex, without CTA-4OHcinn was also produced for comparison purposes. Conversion and particle size were measured as reported in Chapter 2 (section 2.2.6.1 and 2.2.6.2, respectively). Full conversion was reached after 3 hours of reaction (Figure 5.11 a) with a final particle size of 195 nm for the control latex and 177 nm for the latex with CTA-4OHcinn (Figure 5.11 b).

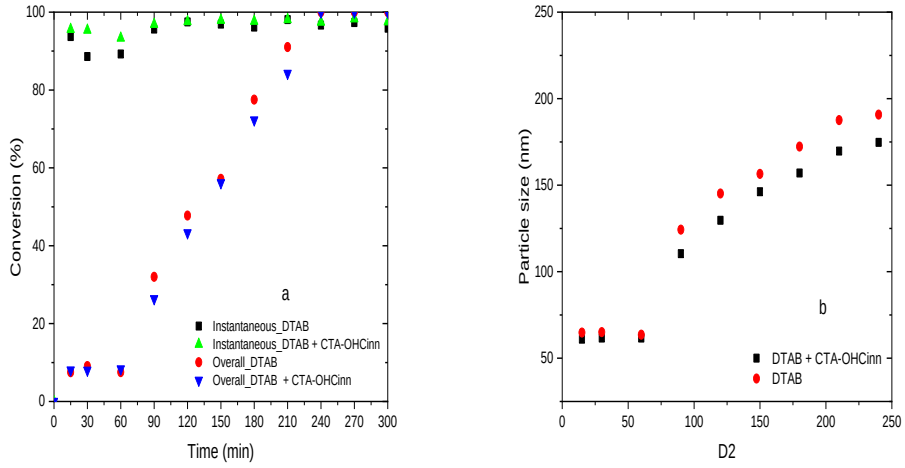

Figure 5.11. a) Kinetics of emulsion polymerization reactions with DTAB (Control) and DTAB + CTA-4OHcinn, b) evolution of particle size.

Both latexes were casted on metallic substrates, dried at room temperature, and analyzed by EIS in a corrosive media of 0.005 M NaCl and pH 7 and pH 1 in order to verify if the anticorrosive properties of CTA-OHCinn observed when it is free in solution, could improve the properties of the coating when it was incorporated as surfactant. The spectra are shown in Figure 5.12. Different process are taking place when the coatings are exposed to the corrosive media of pH 1 and pH 7, based on the phase angle spectra. The impedances obtained for DTAB (control) coating and DTAB + CTA-4OHcinn coating, at pH 7, are similar. Some noise is observed

in the phase angle spectra of the DTAB + CTA-4OHcinn coating, that could be an indication of some type of action from the inhibitor.

The impedances obtained at pH 1 for the DTAB (control) coating is also similar to the ones of the DTAB + CTA-4OHcinn coating (Figure 5.12). However, the phase angle profile of the DTAB + CTA-4OHcinn coating are broader in the low frequency range, when compared to the control, which could be an indication of a protective film formed by CTA-4OHcinn, attached to the surface. Moreover, at the high frequency range it seems that the resistive response of the DTAB + CTA-4OHcinn is faster than the control coating.

By the optical images, it is possible to observe that stains were formed through the coating, as it was dried; this is probably due to migration of surfactant. The excess of surfactant in the final polymeric film may lead to the formation of hydrophilic pathways or migration toward the film-air or the film-substrate interface[22,23], which is prejudicial to the quality of the polymeric coating. As an attempt to extract the excess of surfactant present in the final latexes, dialysis were carried out for 7 days in distilled water, however, as surfactants were extracted, particles started to coagulate, as an indication that the system requires a certain amount of surfactant to be stable. Thus, the optimal quantity of CTA-4OHcetCinn in the latex and its proportion in relation to DTAB still needs to be studied for the production of a better coating. However, the fact that a stable latex could be synthesized with CTA-OHCinn is a proof of concept that cetrimonium cinnamate cationic surfactants can be incorporation into latexes as emulsifiers.

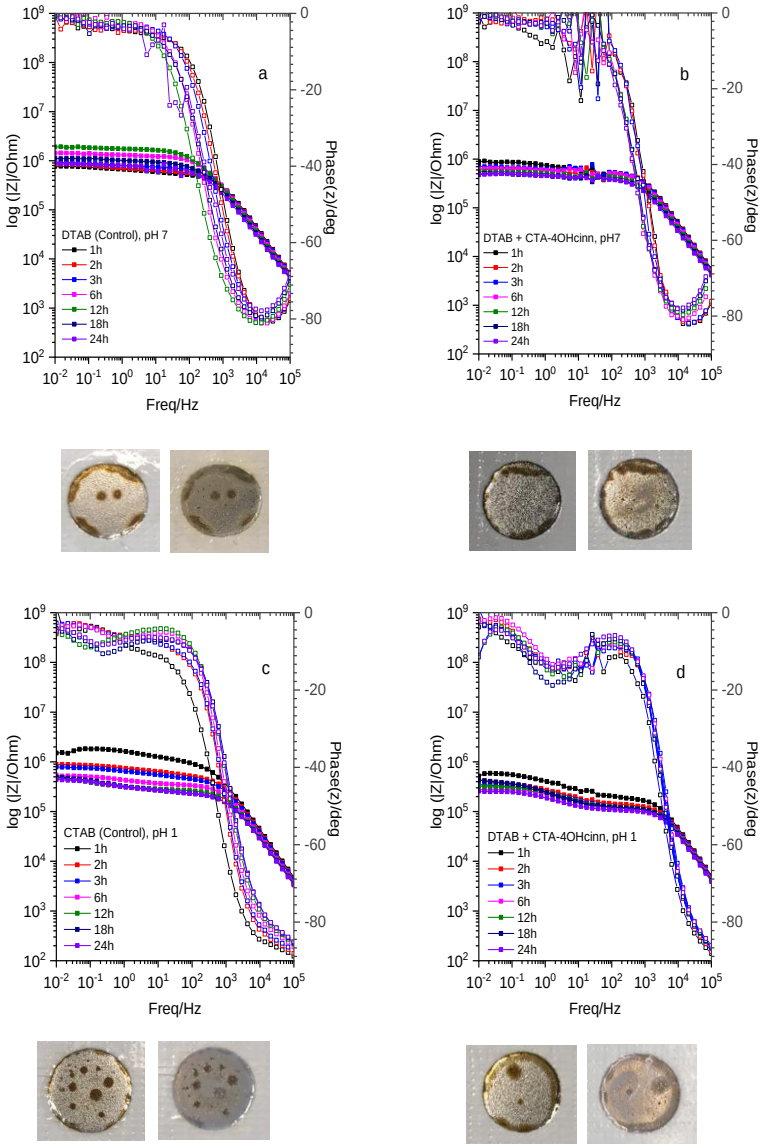

Figure 5.12. Bode plot, phase angle of coatings made by emulsion polymerization using CTA-4OHcinn as emulsifier, in a corrosive media of 0.005 M NaCl, and optical images of samples before the analysis (left), and after the analysis (right). a) Coating with DTAB (Control), pH 7, b) DTAB + CTA-4OHcinn, pH 7, c) DTAB (Control), pH 1, and d) DTAB + CTA-4OHcinn, pH1.

5.4 Conclusions

Three cetrimonium cinnamates cationic surfactants were studied as free inhibitors in solution (CTA-4OHcinn, CTA-4EtOcinn, and CTA-4BtOcinn) showing high performance in harsh environments of 0.01 NaCl with pH 2 and pH 1, that approaches real industrial applications. The efficiency of CTAB, alone, as a free inhibitor was also analyzed, for comparison proposes. Immersion tests of 4 days confirmed that the cetrimonium cinnamate CTA-4OHcinn has better performance than CTAB alone.

Results obtained from EIS tests of films formed from the blend of those cetrimonium cinnamates inhibitors into dispersion coatings in a corrosive medias of pH 7 and pH 1, strongly suggest that the studied cetrimonium cinnamates are functional for application as paint additives in real word, being especially efficient in lower pHs.

The proposed emulsion polymerization recipe with CTA-4OHcinn as an emulsifier still needs to be optimized for production of a better film. However, the fact that a stable latex could be synthesized is a proof of concept that the proposed cetrimonium cinnamates cationic surfactants could possibly be incorporation into latexes as emulsifiers, reducing the use of conventional surfactants that are not beneficial to the final coating.

5.5 References

(1) Peng, Y.; Hughes, A. E.; Deacon, G. B.; Junk, P. C.; Hinton, B. R. W.; Forsyth, M.; Mardel, J. I.; Somers, A. E. A Study of Rare-Earth 3-(4-Methylbenzoyl)-Propanoate Compounds as Corrosion Inhibitors for AS1020 Mild Steel in NaCl Solutions. *Corros. Sci.* **2018**, *145*, 199–211. https://doi.org/10.1016/j.corsci.2018.09.022.

(2) Kaur, J.; Daksh, N.; Saxena, A. Corrosion Inhibition Applications of Natural and Eco-Friendly Corrosion Inhibitors on Steel in the Acidic Environment: An Overview. *Arab. J. Sci. Eng.* **2022**, *47* (1), 57–74. https://doi.org/10.1007/s13369-021-05699-0.

(3) Finsgar, M.; Jackson, J. Application of Corrosion Inhibitors for Steels in Acidic Media for the Oil and Gas Industry: A Review. *Corros. Sci.* **2014**, *86*, 17–41. https://doi.org/10.1016/j.corsci.2014.04.044.

(4) Chong, A. L.; Mardel, J. I.; MacFarlane, D. R.; Forsyth, M.; Somers, A. E. Synergistic Corrosion Inhibition of Mild Steel in Aqueous Chloride Solutions by an Imidazolinium Carboxylate Salt. *ACS Sustain. Chem. Eng.* **2016**, *4* (3), 1746–1755. https://doi.org/10.1021/acssuschemeng.5b01725.

(5) Little, B. J.; Blackwood, D. J.; Hinks, J.; Lauro, F. M.; Marsili, E.; Okamoto, A.; Rice, S. A.; Wade, S. A.; Flemming, H. C. Microbially Influenced Corrosion—Any Progress? *Corros. Sci.* **2020**, *170* (November 2019), 108641. https://doi.org/10.1016/j.corsci.2020.108641.

(6) Lyon, S. B.; Bingham, R.; Mills, D. J. Advances in Corrosion Protection by Organic Coatings: What We Know and What We Would like to Know. *Prog. Org. Coatings* **2017**, *102*, 2–7. https://doi.org/10.1016/j.porgcoat.2016.04.030.

(7) Somers, A. E.; Deacon, G. B.; Macfarlane, D. R.; Junk, P. C.; Forsyth, M. Recent Developments in Environment-Friendly Corrosion Inhibitors for Mild Steel. *J. Indian Inst. Sci.* **2016**, *96* (4), 285–292.

(8) Forsyth, M.; Wilson, K.; Behrsing, T.; Forsyth, C.; Deacon, G. B.; Phanasgoankar, A. Effectiveness of Rare-Earth Metal Compounds as Corrosion Inhibitors for Steel. *Corrosion* **2002**, *58* (11), 953–960. https://doi.org/10.5006/1.3280785.

(9) Deacon, G. B.; Junk, P. C.; Lee, W. W.; Forsyth, M.; Wang, J. Rare Earth 3-(4′-Hydroxyphenyl)Propionate Complexes. *New J. Chem.* **2015**, *39* (10), 7688–7695. https://doi.org/10.1039/c5nj00787a.

(10) Blin, F.; Leary, S. G.; Wilson, K.; Deacon, G. B.; Junk, P. C.; Forsyth, M. Corrosion

Mitigation of Mild Steel by New Rare Earth Cinnamate Compounds. *J. Appl. Electrochem.* **2004**, *34* (6), 591–599. https://doi.org/10.1023/B:JACH.0000021932.87043.7b.

(11) Forsyth, M.; Seter, M.; Hinton, B.; Deacon, G.; Junk, P. New “Green” Corrosion Inhibitors Based on Rare Earth Compounds. *Aust. J. Chem.* **2011**, *64* (6), 812–819. https://doi.org/10.1071/CH11092.

(12) Forsyth, M.; Somers, A.; Ghorbani, M. Organic Corrosion Inhibitors. WO 2021/097532 A1, 2022.

(13) Gopi, D.; Govindaraju, K. M.; Manimozhi, S.; Ramesh, S.; Rajeswari, S. Inhibitors with Biocidal Functionalities to Mitigate Corrosion on Mild Steel in Natural Aqueous Environment. *J. Appl. Electrochem.* **2007**, *37* (6), 681–689. https://doi.org/10.1007/s10800-007-9300-x.

(14) El-Maksoud, S. A. A. The Effect of Hexadecyl Pyridinium Bromide and Hexadecyl Trimethyl Ammonium Bromide on the Behaviour of Iron and Copper in Acidic Solutions. *J. Electroanal. Chem.* **2004**, *565* (2), 321–328. https://doi.org/10.1016/j.jelechem.2003.10.026.

(15) Ghorbani, M.; Soto Puelles, J.; Forsyth, M.; Catubig, R. A.; Ackland, L.; Machuca, L.; Terryn, H.; Somers, A. E. Corrosion Inhibition of Mild Steel by Cetrimonium Trans-4-Hydroxy Cinnamate: Entrapment and Delivery of the Anion Inhibitor through Speciation and Micellar Formation. *J. Phys. Chem. Lett.* **2020**, *11* (22), 9886–9892. https://doi.org/10.1021/acs.jpclett.0c02389.

(16) Soto Puelles, J.; Ghorbani, M.; Crawford, S.; Ackland, M. L.; Chen, F.; Forsyth, M.; Somers, A. E. Modelling Cetrimonium Micelles as 4-OH Cinnamate Carriers Targeting a Hydrated Iron Oxide Surface. *J. Colloid Interface Sci.* **2022**, *610*, 785–795. https://doi.org/10.1016/j.jcis.2021.11.139.

(17) Tuck, B.; Watkin, E.; Forsyth, M.; Somers, A.; Ghorbani, M.; Machuca, L. L. Evaluation of a Novel, Multi-Functional Inhibitor Compound for Prevention of Biofilm Formation on

Carbon Steel in Marine Environments. *Sci. Rep.* **2021**, *11* (1), 1–12. https://doi.org/10.1038/s41598-021-94827-9.

(18) Ghorbani, M.; Soto Puelles, J.; Forsyth, M.; Zhu, H.; Crawford, S.; Chen, F.; Cáceres-Vélez, P. R.; Jusuf, P. R.; Somers, A. Engineering Advanced Environmentally Friendly Corrosion Inhibitors, Their Mechanisms, and Biological Effects in Live Zebrafish Embryos. *ACS Sustain. Chem. Eng.* **2022**, *10* (9), 2960–2970. https://doi.org/10.1021/acssuschemeng.1c07958.

(19) Puelles, J. S.; Ghorbani, M.; Yunis, R.; MacHuca, L. L.; Terryn, H.; Forsyth, M.; Somers, A. E. Electrochemical and Surface Characterization Study on the Corrosion Inhibition of Mild Steel 1030 by the Cationic Surfactant Cetrimonium Trans-4-Hydroxy-Cinnamate. *ACS Omega* **2021**, *6* (3), 1941–1952. https://doi.org/10.1021/acsomega.0c04733.

(20) Ali, S. A.; El-Shareef, A. M.; Al-Ghamdi, R. F.; Saeed, M. T. The Isoxazolidines: The Effects of Steric Factor and Hydrophobic Chain Length on the Corrosion Inhibition of Mild Steel in Acidic Medium. *Corros. Sci.* **2005**, *47* (11), 2659–2678. https://doi.org/10.1016/j.corsci.2004.11.007.

(21) Milošev, I.; Bakarič, T.; Zanna, S.; Seyeux, A.; Rodič, P.; Poberžnik, M.; Chiter, F.; Cornette, P.; Costa, D.; Kokalj, A.; Marcus, P. Electrochemical, Surface-Analytical, and Computational DFT Study of Alkaline Etched Aluminum Modified by Carboxylic Acids for Corrosion Protection and Hydrophobicity. *J. Electrochem. Soc.* **2019**, *166* (11), C3131–C3146. https://doi.org/10.1149/2.0181911jes.

(22) Aguirreurreta, Z. *Water-Borne Coatings and Water Pressure Sensitive Adhesives - Sensitive Adhesives Produced with Polymerizable Produced with Polymerizable Surfactants*; PhD thesis, University of the Basque Country UPV/EHU, 2016.

(23) Keddie, J. L.; Routh, A. F. *Fundamentals of Latex Film Formation: Processes and Properties*; Springer: Dortecht, The Netherland, 2010. https://doi.org/10.1007/978-90-481-2845-7.

(24) Ghorbani, M.; Quites, D.; Forsyth, M.; Somers, A. The Art of Constructing Molecular Structure of an Inhibitor Open Insights to Engineer Unprecedented Inhibition Properties in Acidic Environments. To be submitted.

(25) Murray, J. N. Electrochemical Test Methods for Evaluating Organic Coatings on Metals: An Update. Part III: Multiple Test Parameter Measurements. *Prog. Org. Coatings* **1997**, *31* (4), 375–391. https://doi.org/10.1016/S0300-9440(97)00099-4.

(26) Loveday, D.; Peterson, P.; Rodgers, B. Evaluation of Organic Coatings with Electrochemical Impedance Spectroscopy: Part 1: Fundamentals of Electrochemical Impedance Spectroscopy. *CoatingsTech* **2004**, *1* (8), 46–52.

Chapter 6

Conclusions

6 Conclusions

This PhD thesis aimed to study the anticorrosive properties of new environmental friendly cinnamate based corrosion inhibitors as free inhibitors in solution, and whenever possible perform their incorporation into waterborne polymeric latexes by different techniques such as emulsion, miniemulsion and dispersion polymerization. The effectiveness of the obtained coatings for mitigation of corrosion of mild steel surfaces was investigated by electrochemical analysis.

In **Chapter 2**, the anticorrosive property of Butylcoumaric acid (H4) in solution was confirmed by potentiodynamic polarization analysis. It was not possible to incorporate H4 in waterborne binders by emulsion polymerization due to its resistance to diffusion through the water phase. However, H4 was successfully incorporated into the waterborne polymeric binder by dispersion polymerization, batch miniemulsion, and seeded semibatch emulsion polymerization with the H4 incorporated in the seed, previously synthesized by miniemulsion polymerization. Blending H4 into the final latex, as opposed to incorporation into the separate polymer particles was possible only in the case of dispersion polymerization due to the presence of methanol in media that dissolves the inhibitor.

The coatings made by dispersion polymerization did not provide effective barrier protection to the steel substrate, but in the presence of H4, either incorporated or blended, higher impedances were reached in the first hours of experiment. These results prove the concept that the presence of H4 in a coating can provide extra protection to the system. The coating with H4 blended provided protection for 6 hours, while the one with H4 incorporated only provided it for

the first hour. This difference was related to the availability of H4 in the system, as when blended, the inhibitor has higher mobility.

The coatings obtained by batch miniemulsion polymerization with low solids content were not able to avoid flash rust when applied to steel substrates. However, this could be avoided by increasing the solids content of the latex by seeded semibatch emulsion polymerization. These high solids content latexes provided an effective barrier protection to the steel surface ($10^{5.2}$ to 10^{6} Ω and phases angles of 54 to 72 degrees) and when the inhibitor was incorporated (1.5 mg H4/g polymer), it gave extra protection to the system (≈10^{6} to $10^{6.7}$ Ω and phases angles of 65 to 80 degrees).

In **Chapter 3***,* the inhibitors metoxy p-coumaric acid (H1), trifluoromethoxy p-coumaric acid (HCF3), butoxy p-coumaric acid (H4), and p-4-ethyloxymethacrylate coumarate (HMA) were successfully incorporated into waterborne polymeric binders using batch miniemulsion polymerization at loadings of 4 mg inhibitor/g latex (1 g inhibitor/100 g monomer) and significant improvement was observed relative to an un-inhibited coating. EIS analyses were used to determine the corrosion protective properties of the films produced. Even though the control latex itself provided good barrier protection to the steel surface ($10^{5.2}$ Ω and 66 degrees), when the inhibitors were incorporated into the formulation, better performances were achieved in all cases. The coating with H4 incorporated showed impedances in the range of $10^{6.2}$ to $10^{6.3}$ Ω and phase angles of 80 - 82 degrees, considerably more stable than the ones previously obtained in Chapter 2, in which 1.5 mg H4/g polymer was incorporated by semi batch emulsion incorporation (≈10^{6} to $10^{6.7}$ Ω and phases angles of 65 to 80 degrees). This is an indication that a higher concentration of inhibitor provides better protection.

Between the intact coatings studied, the one with H1 incorporated showed the highest impedances and phase angles ($10^{6.7}$ Ω and 84 degrees, respectively), which approaches capacitive behavior. The better performance of H1 when incorporated into the coating is probably due to its higher solubility in the media, which means that the molecule is able to efficiently migrate from the bulk of the coating to the metallic surface. In order to test the active protection of the systems, electrochemical analysis was also performed on the coatings, with a controlled scratch. All inhibitors provided an improvement in pore resistance and also lower corrosion as indicated by the C_{dl} values over 24 hours. The charge transfer resistance also remained higher over the 24 hour period compared to the control coating. The best results for the scratched samples were obtained for the coating with HMA incorporated. Its impedance was maintained at ≈$10^{4.3}$ Ω for the 24 hours of experiment while for the control scratched sample the impedance dropped from ≈ $10^{4.6}$ to $10^{4.1}$ Ω. This suggests that there is a benefit in bonding an inhibiting molecule into the polymer structure during the polymerization process. Unfortunately, our preliminary attempt to combine this polymerizing approach (HMA) together with the incorporation of a non reactive, leachable molecule (H1) to achieve synergistic protection was not successful, although future work will continue to investigate the optimum methods to incorporate active inhibition along with enhanced barrier properties in these coating systems.

In **Chapter 4**, an attempt was made to further improve the barrier properties of the coating with H1 incorporated, produced in Chapter 3. The particles of the latex with H1, were functionalized by the incorporation of Sipomer® PAM200 (SIP) by semibatch emulsion polymerization. This phosphate polymerizable surfactant is promising for reducing the water sensibility of the films and, at lower drying rates, the phosphate groups interacts with the hydroxyl groups of the surface of the steel, producing a thin iron phosphate passive layer at the coating metal interface that increases its barrier property. The final latex with SIP and H1 in its

composition would ideally have higher barrier properties due to the combination of both components, by but also active protection provided by H1 in case of the presence of a defect in the coating.

The control coating with SIP showed higher performance when dried at the conditions that allows the formation of the phosphate layer (23 °C, RH = 60 %). However, the EIS spectra of the coating with SIP and H1 (Ep_H1_SIP) is less stable than the one of the control. This could be an indication that the coexistence of H1 and the phosphate function in the particles is not compatible. As both components are known for protecting the surface by being attached to it, some competition may be occurring between them. A blend of Ep_SIP and Mp_H1 latex (1:1) was also studied. However the resultant coating did not show higher impedances than previous ones, even when dried at 23 °C, RH = 60 %, indicating that the phosphate layer was not homogeneously formed in this case. It would be interesting, as future work, to use of a higher surface analysis technique such as TOF-SIMS for better understand of the distribution of Sipomer® PAM-200, and H1 on the metallic surface, under the proposed coatings (Ep_Sipomer, Ep_H1_Sipomer and the Blend Ep_Sipomer + Mp_H1), when dried at the conditions that allows the formation of the phosphate layer (23 °C, RH = 60 %).

The results obtained for the proposed 2-layer-coatings composed of a film with SIP followed by a layer with H1 incorporated, indicates that the presence of SIP in the first layer and H1 in the second layer contributes for better corrosion protection of the system in the first hours of the experiment (~ 6 hours). The same was observed for the coatings with a controlled scratch.

In **Chapter 5**, cetrimonium cinnamates cationic surfactants were studied as free inhibitors in solution showing high performance in extremely acid media of pH 2 and 1, which could be very useful in real industrial applications. The results obtained from the EIS tests of films formed from

the blend of those inhibitors into the dispersion coatings in a corrosive media of pH 1 and pH 7 are a proof of concept that they are functional for application as paint additives in real word, being especially efficient at lower pHs.

The attempt of using the inhibitor CTA-OHcinn as the only emulsifier in emulsion polymerization reactions, led to a severe coagulation of the system. A second approach was to include in the formulation a well established cationic surfactant (DTAB), and use CTA-OHcinn as a second emulsifier. In this system, the reaction was successfully carried out without the presence of coagulum. However, as the films were dried on the metallic surfaces, stains were formed through the film, probably due to migration of surfactant that is in excess. This is prejudicial to the quality of the polymeric coating since it may lead to the formation of hydrophilic pathways and therefore lower barrier properties. As an attempt to extract the excess of surfactant present in the system, dialysis of the latexes were carried out for 7 days, in distilled water. However, as the surfactants were extracted, the polymeric particles started to coagulate, indicating that the stability of the system is sensible in fact to the concentration of surfactant. This emulsion polymerization recipe still needs to be optimized for better performance. Nevertheless, the fact that a stable latex was able be synthesized is a proof of concept that cetrimonium cinnamates cationic surfactants could be incorporation into latexes as emulsifiers.

Therefore, the incorporation of the studied friendly cinnamate based corrosion inhibitors into the binders of the waterborne coatings were able to improve its corrosion protection in all cases. Higher concentration of inhibitors resulted in higher corrosion protection (Chapter 3), and the best impedances were observed in the 2-layer-coatings composed of a film with SIP followed by a layer with H1 incorporated (Chapter 4).

6.1 List of publications and conferences presentations

Parts of this thesis have been already published and other parts have been or will be submitted for publication. The list of papers and conference presentations are listed below (variations in the paper title might be possible):

Articles

"Incorporation of a coumarate based corrosion inhibitor in waterborne polymeric binders for corrosion protection applications". Diulia Quites, Jose Ramon Leiza, Daniele Mantione, Anthony Somers, Maria Forsyth, Maria Paulis. *Macromolecular Materials and Engineering*, 2022, 307. 1-13. https://doi.org/10.1002/mame.202100772.

"Comparison of corrosion inhibition ability of different coumarate based compounds incorporated into waterborne binder". Diulia Quites, Daniele Mantione, Sharon Monaci, Anthony Somers, Maria Forsyth, Maria Paulis. Submitted to ACS Applied Engineering Materials.

"The art of constructing molecular structure of an inhibitor open insights to engineer unprecedented inhibition properties in acidic environments". Diulia Quites, Mahdi Ghorbani, Jhonatan Soto Puelles, Maria Forsyth, Anthony E. Somers. To be submitted.

Poster presentation

“Incorporation of a coumaric acid based corrosion inhibitor in waterborne polymeric binders”. Diulia Quites, Jose Ramon Leiza, Maria Forsyth, Maria Paulis. The European Corrosion Congress (EUROCORR), 2020, online.

“Analysis of the efficiency of coumaric acid based corrosion inhibitors incorporated in waterborne polymeric binders”. Diulia Quites, Jose Ramon Leiza, Maria Forsyth, Maria Paulis. The European Corrosion Congress (EUROCORR), 2021, online.

“Waterborne anticorrosive coatings with a coumarate based corrosion inhibitor and phosphate functionalization”. Diulia Quites, Daniele Mantione, Anthony Somers, Maria Forsyth, Maria Paulis. Royal Australian Chemical Institute National Congress (RACI), 2022, Brisbane – Australia.

Appendix I

I.1 Materials

The monomers Methyl methacrylate (MMA), n-butyl acrylate (BA) (Quimidroga), acrylic acid (AA, Aldrich), were used as received, for the polymerization reactions. Octadecyl acrylate (OA, Aldrich), was used as a co-stabilizer.

Dodecyl diphenyl oxide disulfonate (Dowfax 2A1 45%, Dow Chemical Company), sodium dodecyl sulfate (SDS, Sigma Aldrich), Methoxypolyethylene glycol methacrylate (VISIOMER® MPEG 2005 50%, Evonik), were used as anionic emulsifiers. Phosphate esters of polypropylene glycol monomethacrylate Sipomer® PAM200, (Solvay) was used as a surfmer (Chapter 4). Dodecyltrimethylammonium bromide (DTAB, Sigma Aldrich) was used as a cationic emulsifier (Chapter 5).

Potassium persulfate (KPS, Aldrich), Azobis(isobutyronitrile) (AIBN, Fluka), 2,2′-Azobis(2-methylbutyronitrile) (AMBN, Aldrich), and 2'-Azobis(2-methylpropionamidine) dihydrochloride (AIBA, Aldrich) were used as radical initiators.

Hydroquinone (HQ, Aldrich) was used as a polymerization inhibitor for quantification of reactions conversion.

Methanol anhydrous (Sigma Aldrich) was used as a dispersant in the dispersion polymerization reactions (Chapter 2 and 5), distilled water was used in the aqueous media of the polymerization reactions and MiliQ water was used for the electrochemical tests.

Ethanol was used in some experiments to dissolve the inhibitors into the media in the solution tests.

p-coumaric acid (p-CA, Aldrich) was used for the synthesis of the inhibitors H1, H4, HCF3, HMA in Chapter 2, 3, and 4. Cetrimonium trimethylammonium bromide (CTAB, Aldrich) was blended with carboxylate counter-ions resulting in the inhibitors CTA-4BtOHcinn, CTA-4EtOHcinn, and CTA-4OHcinn, in Chapter 5. The counter-ions (4ButOHcinn, 4EtOHcinn and 4OHcinn) were also synthesized from the p-coumaric acid.

Steel substrates (medium carbon steel with 0.5 % of carbon) from URDURI ACEROS were used as metallic substrates for application of the latex and electrochemical tests of inhibitors in solution in Chapter 2, 3, and 4. In Chapter 5, mild steel AISI1030 (98.27% Fe, 0.35% C, 0.21% Si, 0.74% Mn,0.17% Cr, and others 0.26%.) was used for the electrochemical tests in solution.

High purity NaCl (Corrosalt, Ascott-Analytical) was used for preparation of corrosive solutions for the electrochemical tests.

I.2 Supporting information

- Synthesis of HMA

The synthesis of p-4-ethyloxymethacrylate p-coumaric acid (HMA) was performed in two steps (Figure S.1) by Daniele Mantione, and Sharon Monaci. In the first step (Figure S.1 a) p-coumaric acid was added in a mixture of NaOH (2.3 eq) and KI (0.13 eq)[1]. After p-coumaric acid was dissolved, 2-chloroethanol was added (1.5 eq) and the solution was stirred at 120 °C under reflux overnight. The dark brown mixture was cooled at room temperature, filtered, and washed with diethyl ether three times. The filtrate was then acidified with the addition of acidic water until the precipitation of the product. The obtained white powder, 4-(2-Hydroxyethoxy)phenyl-2-propenoic acid, was dried under vacuum. The yield of this first step is of 60%.

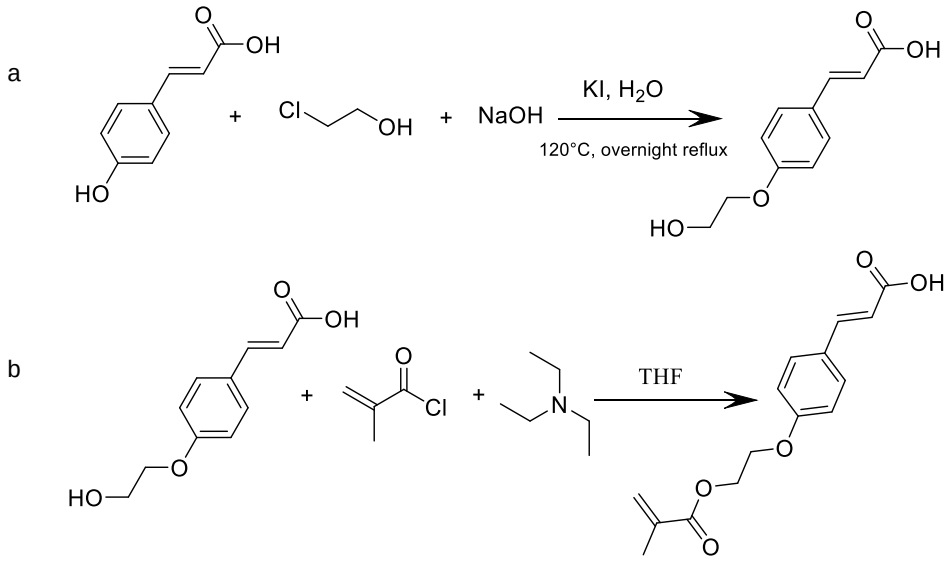

Figure S.1. Schematic route of two steps for the synthesis of p-4-ethyloxymethacrylate coumarate (HMA); a) Syhtnesis of 4-(2-Hydroxyethoxy)phenyl-2-propenoic acid from p-coumaric acid, b) Syhtnesis of HMA from 4-(2-Hydroxyethoxy)phenyl-2-propenoic acid.

In the second step (Figure S.1 b), 4-(2-Hydroxyethoxy)phenyl-2-propenoic acid was dissolved in Tetrahydrofuran (THF) and then trimethylamine (3 eq) was added. The solution was cooled to 0°C followed by the addition of methacryloyl chloride (2.4 eq). The mixture was stirred overnight, and extracted with HCl 0.001M and dichloromethane, three times. . Brine and sodium sulfate were used to remove water, and then the solvent was evaporated under reduced pressure. The product was purified with a column using a mixture of Hexane/ethylacetate 1:1 as eluent. The yield of this final step is of 40%.

I.3 List of acronyms

AA	acrylic acid
AIBA	2'-Azobis(2-methylpropionamidine) dihydrochloride
AIBN	Azobis(isobutyronitrile)
AMBN	Azobis(2-methylbutyronitrile)
BA	n-butyl acrylate
CTA-4BtOHcinn	Hexadecyl trimethylammonium bromide trans-4-butoxy-cinnamate
CTA-4EtOHcinn	Hexadecyl trimethylammonium bromide trans-4-etoxy-cinnamate
CTA-4OHcinn	Hexadecyl trimethylammonium bromide trans-4-hydroxy-cinnamate
CTAB	Cetyltrimethylammonium bromide
Def_Blend Ep_SIP + Mp_H1	Coating with a controlled scratch,obtained from a blend of the latex Ep_SIP + Mp_H1
Def_Ep_H1_SIP	Coating with a controlled scratch, obtained from a latex made by emulsion polymerization, containing H1 and Sipomer® PAM200
Def_Ep_SIP	Coating with a controlled scratch, obtained from a latex made by emulsion polymerization, containing Sipomer® PAM200
Def_Mp_1 % H1	Coating with a controlled defect, obtained from a latex made by miniemulsion polymerization, containing 1% wbm of H1

Def_Mp_1 % H4	Coating with a controlled defect, obtained from a latex made by miniemulsion polymerization, containing 1% wbm of H1
Def_Mp_1 % HCF3	Coating with a controlled defect, obtained from a latex made by miniemulsion polymerization, containing 1% wbm of HCF3
Def_Mp_1 % HMA	Coating with a controlled defect, obtained from a latex made by miniemulsion polymerization, containing 1% wbm of HMA
Def_2L - Ep_SIP / Mp_Control	2 layer-coating with a controlled scratch, the first layer was prepared with the latex EP_SIP and the second one with Mp_Control.
Def_2L - Ep_H1_SIP / Mp_H1	2 layer-coating with a controlled scratch, the first layer was prepared with the latex EP_SIP and the second one with Mp_H1
DLS	dynamic light scattering
Dp_Control	Latex made by dispersión polymerization
DTAB	Dodecyltrimethylammonium bromide
EDX	Energy Dispersive X-ray spectroscopy
EIS	Electrochemical impedance spectroscopy
EP_H1_SIP	Coating/Latex made by emulsion polymerization, containing H1 and Sipomer® PAM200
Ep_SIP	Coating/Latex made by emulsion polymerization, containing Sipomer® PAM200
H1	metoxy p-coumaric acid

H4	butoxy p-coumaric acid
HCF3	trifluoromethoxy p-coumaric acid
HMA	p-4-ethyloxymethacrylate coumarate
HQ	Hydroquinone
KPS	Potassium persulfate
MMA	Methyl methacrylate
Mp_1% H1	Coating/Latex made by miniemulsion polymerization, containing 1% wbm of H1
Mp_1% H4	Coating/Latex made by miniemulsion polymerization, containing 1% wbm of H4
Mp_1% HCF3	Coating/Latex made by minuemulsion polymerization, containing 1% wbm of HCF3
Mp_1% HMA	Coating/Latex made by minuemulsion polymerization, with 1% wbm of HMA
Mp_Control	Coating/Latex made by minuemulsion polymerization, without inhibitor
p-CA	p-coumaric acid (trans-4-hydroxycinnamate)
poly(MMA/BA)	copolymer of PMMA and PBA
PP	potentiodynamic polarization

SDS	sodium dodecyl sulfate
SEM	Scanning Electron Microscopy
SIP	Sipomer® PAM200
2L - Ep_SIP / Mp_Control	2 layer-coating, the first layer was prepared with the latex EP_SIP and the second one with Mp_Control.
2L - Ep_H1_SIP / Mp_H1	2 layer-coating, the first layer was prepared with the latex EP_SIP and the second one with Mp_H1
% wbmb	weight based monomer porcentage

Resumen y conclusiones

Esta tesis doctoral ha tenido como objetivo el estudio de las propiedades anticorrosivas de nuevos inhibidores de corrosión, basados en cinamato, libres en solución y siempre que fuera posible incorporados en látexes poliméricos mediante diferentes técnicas como polimerización en emulsión, miniemulsión y dispersión. Las eficacias de los recubrimientos obtenidos para mitigar la corrosión de las superficies de acero se investigaron mediante análisis electroquímicos.

En el **Capítulo 2** se confirmó la propiedad anticorrosiva del ácido butilcumárico (H4), en solución, mediante análisis de polarización potencio dinámica. No fue posible incorporar H4 en látex en base de agua por polimerización en emulsión, debido a su resistencia a la difusión a través de la fase acuosa. Sin embargo, el H4 fue incorporado con éxito mediante polimerización por dispersión, miniemulsión discontinua y polimerización en emulsión semicontinua sembrada con el H4 incorporado en la siembra, sintetizado previamente mediante polimerización en miniemulsión. La mezcla de H4 en el látex final, a diferencia de la incorporación en las partículas de polímero durante la polimerización, solo fue posible en el caso de polimerización en dispersión debido a la presencia de metanol, que disuelve el inhibidor, en la fase continua.

Los recubrimientos hechos por polimerización en dispersión no proporcionaron una protección de barrera efectiva al sustrato de acero, pero en presencia de H4, ya sea incorporado o mezclado, se alcanzaron impedancias más altas en las primeras horas del experimento. Estos resultados prueban el concepto de que la presencia de H4 en un recubrimiento puede proveer protección adicional al sistema. El recubrimiento con H4 mezclado proporcionó protección por 6 horas, mientras que el que tenía H4 incorporado solo la proporcionó en la primera hora. Esta

diferencia se relacionó con la disponibilidad de H4 en el sistema, ya que cuando se mezcla, el inhibidor tiene mayor movilidad.

Los recubrimientos obtenidos por polimerización en miniemulsión discontinua con bajo contenido de sólidos no lograron evitar la oxidación instantánea cuando se aplicaron sobre los aceros. Sin embargo, esto se solucionó aumentando el contenido de sólidos del látex mediante polimerización en emulsión semicontinua sembrada. Estos látex con alto contenido de sólidos proporcionaron una protección de barrera eficaz a la superficie del acero ($10^{5.2}$ a 10^{6} Ω y ángulos de fase de 54 a 72 grados) y cuando se incorporó el inhibidor (1,5 mg H4/g de látex), esto proporcionó protección adicional al sistema (≈10^{6} a $10^{6.7}$ Ω y ángulos de fase de 65 a 80 grados).

En el **Capítulo 3**, ácido metoxi p-cumárico (H1), ácido trifluorometoxi p-cumárico (HCF3), ácido butoxi p-cumárico (H4) y cumarato de p-4-etiloximetacrilato (HMA) fueron incorporados en látex por medio da polimerización en miniemulsión, con cargas de 4 mg de inhibidor/g de látex (1 g de inhibidor/100 g de monómero) y se observó una mejora significativa en relación al revestimiento sin inhibidor. Se utilizaron análisis EIS para determinar las propiedades protectoras contra la corrosión de los filmes producidos. Aunque el látex control proporcionó una buena protección de barrera a la superficie del acero ($10^{5.2}$ Ω y 66 grados), cuando se incorporaron los inhibidores a la formulación, se lograron mejores desempeños en todos los casos. El recubrimiento con H4 incorporado mostró impedancias en el rango de $10^{6.2}$ a $10^{6.3}$ Ω y ángulos de fase de 80 – 82 grados, considerablemente más estables que los obtenidos previamente en los que se incorporó 1.5 mg H4/g de látex por polimerización en emulsión semicontinua (≈10^{6} a $10^{6.7}$ Ω y ángulos de fase de 65 a 80 grados). Esta es una indicación de que una mayor concentración de inhibidor proporciona una mejor protección.

Entre los recubrimientos intactos estudiados, el que tenía H1 incorporado mostró las mayores impedancias y ángulos de fase ($10^{6.7}$ Ω y 84 grados, respectivamente), lo que se aproxima al comportamiento capacitivo. El mejor rendimiento fue observado en el que tenía H1 incorporado, probablemente debido a su mayor solubilidad en el medio, lo que significa que la molécula puede migrar eficientemente desde el recubrimiento hacia la superficie metálica. Para probar la protección activa de los sistemas, también se realizó un análisis electroquímico de los recubrimientos, con un rayado controlado. Todos los inhibidores proporcionaron una mejora en la resistencia de los poros y también menor corrosión, como lo indican los valores de C_{dl}, durante 24 horas. La resistencia a la transferencia de carga también se mantuvo más alta durante el período de 24 horas en comparación con el recubrimiento sin inhibidor. Los mejores resultados en los recubrimientos con el defecto se obtuvieron para el recubrimiento con HMA incorporado. Su impedancia se mantuvo en ≈$10^{4.3}$ Ω durante las 24 horas del experimento, mientras que para la muestra de control con el defecto, la impedancia se redujo de ≈ $10^{4.6}$ a $10^{4.1}$ Ω. Esto sugiere que existe beneficio en incorporar las moléculas de inhibidores a la estructura del polímero, durante el proceso de polimerización. Desafortunadamente, nuestro intento preliminar de incorporar HMA y H1 en un mismo látex para obtener una protección pasiva y activa no tuvo éxito. Se propone continuar investigando los métodos óptimos para incorporar la inhibición activa junto con propiedades de barrera mejoradas en estos sistemas de revestimiento.

En el **Capítulo 4**, se intentó mejorar aún más las propiedades de barrera del recubrimiento con H1 incorporado, producido en el Capítulo 3. Las partículas del látex con H1, fueron funcionalizadas mediante la incorporación de Sipomer® PAM200 (SIP) por polimerización en emulsión semicontinua. SIP es prometedor para reducir la sensibilidad al agua de los filmes y los grupos fosfato interactúan con los grupos hidroxilo de la superficie del acero, produciendo una capa pasiva de fosfato de hierro delgada en la interfase entre el metal y el

recubrimiento, lo que aumenta la propiedad de barrera del sistema. El látex final con SIP y H1 en su composición idealmente tendría mayores propiedades de barrera debido a la combinación de ambos componentes pero también protección activa proporcionada por H1 en caso de presencia de un defecto en el recubrimiento.

El recubrimiento de control con SIP muestra un mayor rendimiento cuando se seca en las condiciones que permiten la formación de la capa de fosfato (23 °C, HR = 60 %). El espectro EIS del recubrimiento con SIP y H1 (Ep_H1_SIP) es menos estable que el del control. Esto podría ser una indicación de que la coexistencia de H1 y la función fosfato en las partículas no son compatibles. Ambos componentes son conocidos por proteger la superficie al estar adheridos a ella, por lo que es posible que se produzca cierta competencia entre ellos. También se estudió la mezcla de látex Ep_SIP y Mp_H1 (1:1). Sin embargo, el recubrimiento resultante no presentó mayores impedancias que los anteriores, aún cuando se secó a 23 °C, HR = 60 %, lo que indica que la capa de fosfato no fue formada homogéneamente en la superficie del acero. Sería interesante, como trabajo futuro, el uso de una técnica de análisis de superficie superior como TOF-SIMS para comprender mejor la distribución de Sipomer® PAM-200 y H1 en la superficie metálica, bajo los recubrimientos propuestos (Ep_Sipomer, Ep_H1_Sipomer y el Blend Ep_Sipomer + Mp_H1), cuando se secan en las condiciones que permiten la formación de la capa de fosfato (23 °C, HR = 60 %).

Los resultados obtenidos para los recubrimientos de 2 capas propuestos compuestos por una película con SIP seguida de una capa con H1 incorporado, indican que la presencia de SIP en la primera capa y H1 en la segunda capa contribuyen a una mejor protección contra la corrosión del sistema en las primeras horas del experimento. (~ 6 horas). Lo mismo se observó para los recubrimientos con defecto controlado.

En el **Capítulo 5** se estudiaron los tensioactivos catiónicos de cinamatos de cetrimonio como inhibidores libres en solución mostrando un alto rendimiento en medios extremadamente ácidos de pH 2 y 1, lo que podría ser de gran utilidad en aplicaciones industriales reales. Los resultados de EIS obtenidos de los filmes formados a partir de la mezcla de esos inhibidores en los recubrimientos de dispersión en un medio corrosivo de pH 1 y pH 7, son una prueba de concepto de que son funcionales para la aplicación como aditivos de pintura en la vida real, siendo especialmente eficientes a pHs más bajos.

El intento de utilizar el inhibidor CTA-OHcinn como único emulsificante en las reacciones de polimerización en emulsión, condujo a una severa coagulación del sistema. Un segundo enfoque fue incluir en la formulación un tensioactivo catiónico estable (DTAB) y utilizar CTA-OHcinn como segundo emulsificante. En este sistema, la reacción se llevó a cabo con éxito sin la presencia de coágulos. Sin embargo, cuando las películas se secaron sobre las superficies metálicas, se formaron manchas sobre la superficie, probablemente debido a la migración del tensioactivo en exceso. Por lo tanto, esto es perjudicial para la calidad del recubrimiento polimérico, ya que puede conducir a la formación de rutas hidrofílicas y propiedades de barrera más bajas. En un intento por extraer el exceso de tensioactivo presente en el sistema, se llevó a cabo la diálisis de los látex durante 7 días, en agua. Sin embargo, a medida que se extraían los tensioactivos, las partículas poliméricas comenzaron a coagularse, lo que indica que la estabilidad del sistema es sensible a la concentración del tensioactivo. Esta receta de polimerización en emulsión aún debe optimizarse para un mejor rendimiento. Sin embargo, el hecho de que se haya podido sintetizar un látex estable es una prueba de concepto de que los tensioactivos catiónicos cinamatos de cetrimonio podrían incorporarse a los látex como emulsificantes.

Por lo tanto, la incorporación de los inhibidores de corrosión a base de cinamato en los látex pudo mejorar su protección contra la corrosión en todos los casos. La mayor concentración de inhibidores resultó en una mayor protección contra la corrosión (Capítulo 3), y las mejores impedancias se observaron en los recubrimientos de 2 capas compuestos por una película con SIP seguida de una capa con H1 incorporado (Capítulo 4).